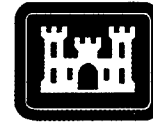


ERDC/CHL TR-00-21

Coastal and Hydraulics Laboratory

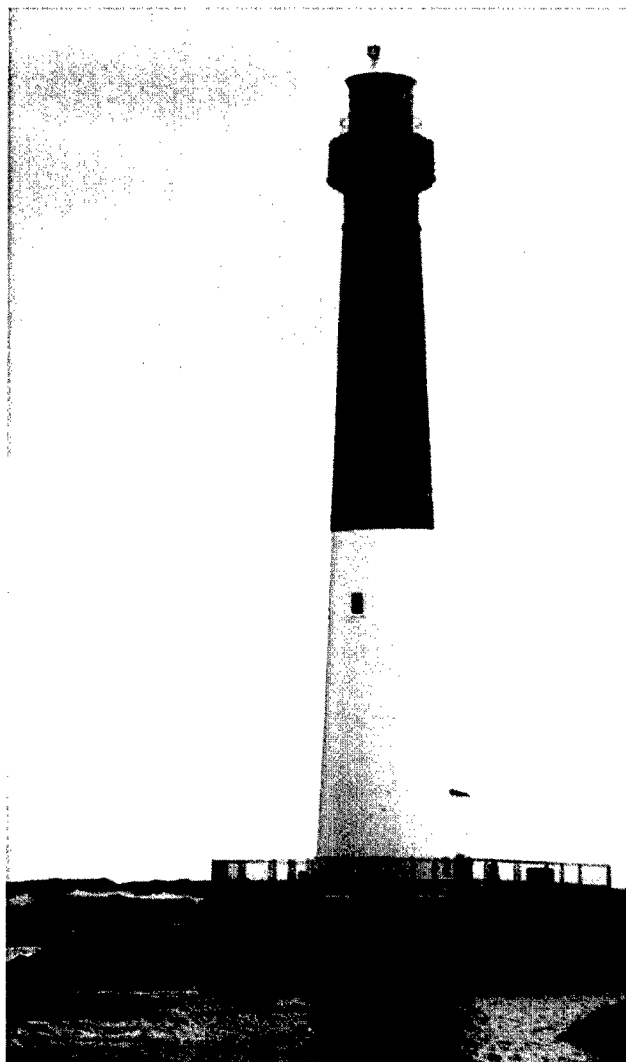


**US Army Corps
of Engineers®**
Engineer Research and
Development Center

Wave Climate and Littoral Sediment Transport Potential, Long Beach Island, New Jersey

Mary A. Cialone and Edward F. Thompson

September 2000



The contents of this report are not to be used for advertising, publication, or promotional purposes. Citation of trade names does not constitute an official endorsement or approval of the use of such commercial products.

The findings of this report are not to be construed as an official Department of the Army position, unless so designated by other authorized documents.



PRINTED ON RECYCLED PAPER

Wave Climate and Littoral Sediment Transport Potential, Long Beach Island, New Jersey

by Mary A. Cialone, Edward F. Thompson
Coastal and Hydraulics Laboratory
U.S. Army Engineer Research and Development Center
3909 Halls Ferry Road
Vicksburg, MS 39180-6199

Final report

Approved for public release; distribution is unlimited

Prepared for U.S. Army Engineer District, Philadelphia
Wanamaker Building, 100 Penn Square East
Philadelphia, PA 19107-3390

Engineer Research and Development Center Cataloging-in-Publication Data

Cialone, Mary A.

Wave climate and littoral sediment transport potential, Long Beach Island, New Jersey / by Mary A.

Cialone, Edward F. Thompson ; prepared for U.S. Army Engineer District, Philadelphia.

75 p. : ill. ; 28 cm. -- (ERDC/CHL ; TR-00-21)

Includes bibliographic references.

1. Sediment transport -- New Jersey -- Long Beach Island. 2. Ocean waves -- Mathematical models.

3. Beach nourishment. I. Thompson, Edward F. II. United States. Army. Corps of Engineers. Philadelphia District. III. Engineer Research and Development Center (U.S.) IV. Coastal and Hydraulics Laboratory (U.S.)

V. Title. VI. Series: ERDC/CHL TR ; 00-21.

TA7 E8 no.ERDC/CHL TR-00-21

Contents

Preface	vii
1—Introduction	1
Background	1
Needs and Objectives	2
Study Approach	3
2—Offshore Wave Climate	5
WIS Hindcasts	5
NDBC Buoy and DWG Measurements	8
OCTI Hindcast	10
3—Modeling Approach	11
Wave Model and Grids	11
Wave model	11
Grids	11
Incident wave conditions	12
STWAVE output	15
Wave transformation examples	16
Littoral Transport	16
Calculation of breaking wave conditions	21
Calculation of longshore transport rates	21
4—Littoral Transport Potential	24
Grid 1 Net Potential Transport	24
Grid 1 Erosion and Accretion	26
Grid 1 Renourishment Requirements	33
Grid 1 Shoreline Retreat Rate	33
Grid 2 Erosion and Accretion	37
Grid 2 Renourishment Requirements	40
Grid 2 Shoreline Retreat Rate	40
5—Conclusions	44
References	48

Appendix A: WIS Offshore Wave Climate	A1
Appendix B: OCTI Offshore Wave Climate	B1
Appendix C: Wave Model Description	C1
SF 298	

List of Figures

Figure 1. Study area location map	1
Figure 2. Regional bathymetry	3
Figure 3. WIS stations and grid limits	6
Figure 4. Wave statistics for WIS sta AU2070	7
Figure 5. Wave statistics for WIS sta AU2070-component 1	7
Figure 6. Wave statistics for WIS sta AU2070-component 2	8
Figure 7. Wave statistics for NDBC buoy 44025	9
Figure 8. Wave statistics for DWG at Barnegat Inlet	9
Figure 9. Wave statistics for OCTI sta (i=35, j=30)	10
Figure 10. Grid 1 existing condition bathymetry	13
Figure 11. Grid 2 existing condition bathymetry	13
Figure 12. Grid 1 borrow area bathymetry	14
Figure 13. Grid 2 borrow area bathymetry	14
Figure 14. Grid 1 waves from 67 deg, H= 3m, T=10 sec-without project condition	17
Figure 15. Grid 1 waves from 67 deg, H= 3m, T=10 sec-with project condition	17
Figure 16. Grid 1 waves from 180 deg, H= 3m, T=10 sec-without project condition	18
Figure 17. Grid 1 waves from 180 deg, H= 3m, T=10 sec-with project condition	18
Figure 18. Grid 2 waves from 67 deg, H= 3m, T=10 sec-without project condition	19
Figure 19. Grid 2 waves from 67 deg, H= 3m, T=10 sec-with project condition	19

Figure 20.	Grid 2 waves from 180 deg, H= 3m, T=10 sec-without project condition	20
Figure 21.	Grid 2 waves from 180 deg, H= 3m, T=10 sec-with project condition	20
Figure 22.	Location of Grid 1 nearshore reference line	22
Figure 23.	Location of Grid 2 nearshore reference line	22
Figure 24.	Net potential transport for Long Beach Island using WIS wave climatology	25
Figure 25.	Net potential transport for Long Beach Island using OCTI wave climatology	25
Figure 26.	Methods of computing erosion/accretion volumes	29
Figure 27.	Erosion and accretion for Long Beach Island reaches with WIS climatology	31
Figure 28.	Erosion and accretion for Long Beach Island reaches with OCTI climatology	31
Figure 29.	Renourishment requirements with WIS climatology	34
Figure 30.	Renourishment requirements with OCTI climatology	34
Figure 31.	Shoreline retreat with WIS climatology	36
Figure 32.	Shoreline retreat with OCTI climatology	36
Figure 33.	Net potential transport for Grid 2 using WIS wave climatology	37
Figure 34.	Net potential transport for Grid 2 using OCTI wave climatology	38
Figure 35.	Erosion and accretion for Grid 2 using WIS wave climatology	39
Figure 36.	Erosion and accretion for Grid 2 using OCTI wave climatology	39
Figure 37.	Renourishment requirements with WIS climatology	41
Figure 38.	Renourishment requirements with OCTI climatology	41
Figure 39.	Shoreline retreat for Grid 2 using WIS wave climatology	42
Figure 40.	Shoreline retreat for Grid 2 using OCTI wave climatology	43

List of Tables

Table 1.	Specifications for STWAVE Grids from SMS	12
Table 2.	Wave Conditions Simulated with STWAVE	15
Table 3.	Long Beach Island Shoreline Reaches for Grid 1	27
Table 4.	Net Longshore Transport Potential for Long Beach Island	28
Table 5.	Erosion and Accretion Potential for Long Beach Island (WIS)	30
Table 6.	Erosion and Accretion Potential for Long Beach Island (OCTI)	30
Table 7.	Shoreline Retreat Rate for Long Beach Island (WIS) . . .	35
Table 8.	Shoreline Retreat Rate for Long Beach Island (OCTI) . .	35
Table 9.	Grid 2 Shoreline Reaches	38
Table 10.	Net Longshore Transport Potential for Grid 2	38
Table 11.	Erosion and Accretion Potential for Grid 2 (WIS)	40
Table 12.	Erosion and Accretion Potential for Grid 2 (OCTI)	40
Table 13.	Shoreline Retreat Rate for Grid 2 (WIS)	42
Table 14.	Shoreline Retreat Rate for Grid 2 (OCTI)	42

Preface

This study was authorized by the U.S. Army Engineer District, Philadelphia (NAP), and was conducted by personnel of the Coastal Processes Branch (CPB), Coastal Sediments and Engineering Division (CSED), Coastal Hydrodynamics Branch (CHB), Navigation and Harbors Division (NHD), and the Coastal and Hydraulics Laboratory (CHL) of the U.S. Army Engineer Research and Development Center (ERDC). The study was conducted during the period October 1998 through April 1999. Mr. John McCormick, NAP, oversaw progress of the study.

Ms. Mary A. Cialone, CPB, was the ERDC point of contact for the study. This report was prepared by Ms. Cialone and Dr. Edward F. Thompson, CHB. Mr. Mark B. Gravens, CPB, provided valuable consultation. Direct supervision was provided by Mr. Bruce A. Ebersole, Chief, CPB. General supervision was provided by Mr. Thomas Richardson, Acting Director of CHL, Mr. Charles C. Calhoun, Jr., former Assistant Director, CHL, and Dr. James R. Houston, former Director, CHL.

At the time of publication of this report, Dr. James R. Houston was Director of ERDC and COL James S. Weller, EN, was Commander.

The contents of this report are not to be used for advertising, publication, or promotional purposes. Citation of trade names does not constitute an official endorsement or approval of the use of such commercial products.

1 Introduction

Background

Long Beach Island is located on the southern portion of the barrier islands of New Jersey, just south of where the general shoreline orientation changes from north-northeast to a northeast direction (Figure 1). The 32-km-long barrier island separates the Atlantic Ocean from three shallow bays extending along the western side of the island. The northernmost bay

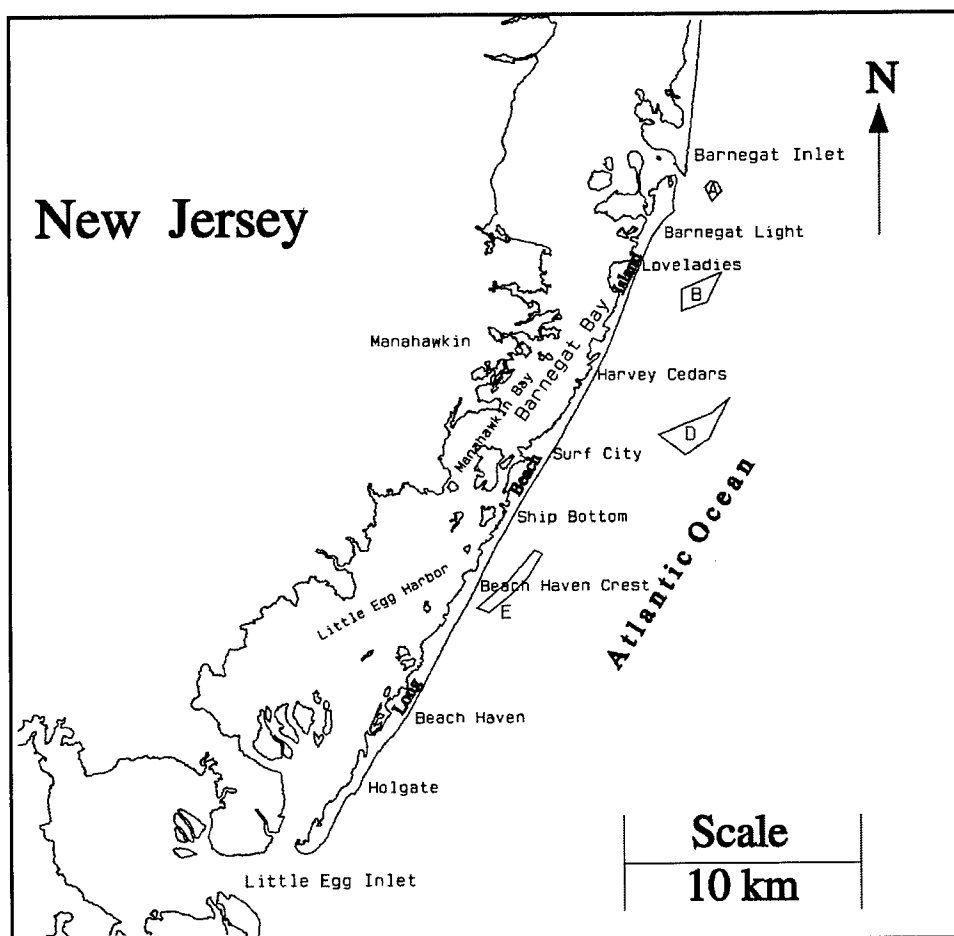


Figure 1. Study area location map

is Barnegat Bay; the centrally-located bay is Manahawkin Bay; and the southernmost bay is Little Egg Harbor. Long Beach Island is bounded on the north by Barnegat Inlet and on the south by Little Egg Inlet. Tides are semidiurnal with a neap range of 0.9 m and a spring range of 1.5 m. A generally accepted estimate of net sediment transport along Long Beach Island is approximately 75,000-150,000 m³/year towards the south. However estimates range from 40,000 to 4,000,000 m³/year (U.S. Army Engineer District, Philadelphia, 1999).

The oceanfront along Long Beach Island is developed entirely for residential use. The bay side of the island has residential development, commercial marinas, and numerous boat ramps. A 9.7-km-long causeway provides the only vehicular access to Long Beach Island. Beach erosion along the Long Beach Island oceanfront communities of Harvey Cedars, Loveladies, and Brant Beach has required recent placement of material. Some material has been trucked in from inland sources, some borrow material has come from maintenance dredging of Barnegat Inlet, and some material has come from offshore borrow areas. The offshore bathymetry includes finger-like shoal features which extend out from the shoreline in a northeasterly direction (Figure 2).

The present study was conducted to assist the Philadelphia District in evaluating the impacts of borrowing sediment from four borrow sites on nearshore wave climate, longshore transport potential, beach nourishment requirements, and shoreline change rates. Approximately 6.7×10^6 m³ of sediment proposed for the present study is to be excavated from the potential borrow sites and placed along a 27-km stretch of Long Beach Island from Loveladies to Holgate for initial construction. Approximately 1.5×10^6 m³ of material is needed for periodic nourishment every 7 years over the 50-year project life.

Needs and Objectives

As part of a beach nourishment feasibility study for Long Beach Island, NJ, a study of the impacts of borrowing material from nearshore and offshore regions on the regional coastal processes was required. Four potential borrow sites for the Long Beach Island nourishment project were identified (Figure 1): Area A—the ebb shoal at Barnegat Inlet; Area B—nearshore shoal off of Loveladies; Area D—offshore borrow area; and Area E—nearshore shoal off of Brant Beach/Beach Haven Crest. Note that these borrow sites are in three different coastal environments. Specific analyses to determine the impacts of borrowing material from these sites are: to examine the relative changes in wave climate due to bathymetric changes created at the borrow sites; to determine the changes in potential longshore transport rates; to examine the impacts on nourishment requirements for proposed beachfill areas; and to look at the relative impacts on shoreline change rates. Therefore, the objective of this study

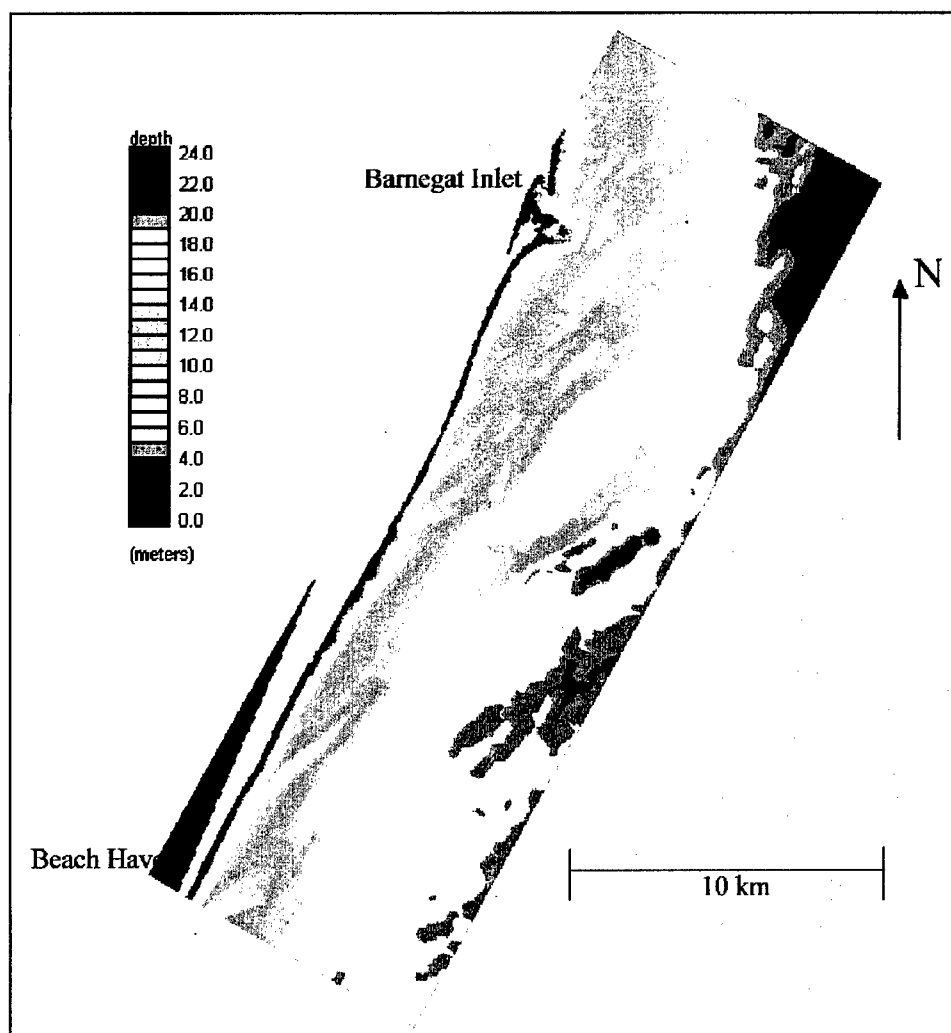


Figure 2. Regional bathymetry

was to perform these analyses and determine the relative impacts of the four borrow sites on these processes.

Study Approach

The study described in this report was performed by the U.S. Army Engineer Research and Development Center (ERDC), Coastal and Hydraulics Laboratory (CHL). The approach consisted of the following components:

- a. Evaluate offshore wave climate.
- b. Use a numerical model to transform offshore wave climate to near-shore areas, for existing and proposed bathymetric configurations.

- c. Estimate littoral transport potential along the coast, both for the existing and proposed bathymetric configurations.
- d. Estimate nourishment requirements for segments of Long Beach Island defined by the Philadelphia District for existing and proposed bathymetric configurations.
- e. Estimate shoreline change rates for existing and proposed bathymetric configurations for segments of Long Beach Island defined by the Philadelphia District.

Offshore wind wave and swell climate was investigated with the Wave Information Study (WIS) numerical hindcast information covering the 20-year time period 1976-1995 and with the Offshore and Coastal Technologies, Inc.—East Coast (OCTI) numerical hindcast covering the 10-year time period 1987-1996. Buoy measurements and a directional wave gauge near Barnegat Inlet were used to help validate the hindcasts. The offshore wave climate evaluation is presented in Chapter 2.

A numerical wave model was used to transform offshore waves to the nearshore zone. The numerical model used for the studies, STWAVE (Steady-State Spectral Wave), is a standard tool for shallow water wave transformation. Development of the two numerical model grids (one for the entire study region and a more refined grid for the Barnegat Inlet area), model output stations, longshore sediment transport calculation procedures, and other aspects of the modeling approach are described in Chapter 3. In addition to existing bathymetry, the proposed borrow area bathymetry configuration was used in numerical simulations.

Study results are presented in Chapter 4. Littoral transport results needed for assessing impacts on beach nourishment rates and shoreline change rates along Long Beach Islands are presented. Beach nourishment rates and shoreline change rates are also presented.

Conclusions and recommendations are given in Chapter 5. This chapter is followed by references and appendices with detailed information supporting the main report.

This study only involved use of wave transformation model results to estimate potential sediment transport rates, renourishment requirements, and expected shoreline change rates. A thorough analysis of historical shoreline changes and inferred volumetric changes should also be done to gain additional information about sand transport processes in the region.

2 Offshore Wave Climate

Evaluation of the incident wave climate is a critical first step in nearshore wave climate and littoral transport studies. Ideally, a long-term, high-quality hindcast is available with at least a few years of concurrent deepwater directional wave measurements in the same area to validate the hindcast. This study used a relatively recent 20-year hindcast and a recent 10-year hindcast. Nearby directional measurements (at Barnegat Inlet) were available for only a 1-year period. Previous studies of this general area have used a variety of sources for wave information, including nondirectional gauges mounted on the "Steel Pier" at Atlantic City, shipboard wave observations, and Coast Guard station observations (General Design Memorandum 1984).

WIS Hindcasts

The ERDC Wave Information Studies (WIS) has developed wave information along U.S. coasts by computer simulation of past wind and wave conditions. This type of simulation is termed hindcasting. The present hindcast information base consists of two 20-year blocks. WIS produced the first block, covering years 1956-75, in the early 1980s (Corson et al. 1982). The second block, covering years 1976-95, was produced in the mid 1990s (Brooks and Brandon 1995). The more recent hindcast is considered to be more reliable since it was produced using an improved wave hindcast model, and results were evaluated against an extensive array of wave measurements which were not available during the initial study. Also, the 1976-95 hindcasts include tropical storms whereas the previous hindcasts do not.

The 1976-95 WIS parameters are available at 3-hr intervals over the 20-year period. At each 3-hr interval, a number of wave parameters are given. Parameters typically used to represent waves are significant wave height, H_s , peak spectral period, T_p , and peak direction, θ_p . WIS parameters of importance to this study include overall H_s , T_p , and θ_p , and, when more than one wave component is present (such as a locally-generated sea and a swell coming from a distant storm), H_s , T_p , and θ_p values for primary and secondary wave components.

Hindcast information for the period 1976-1995 from two nearby WIS stations AU2069 (WIS 69) and AU2070 (WIS 70), was used to examine offshore wave climate. Sta AU2070 is located 8 km off Barnegat Inlet at 39.75N, 74.0W, and AU2069 is located approximately 20 km south of Barnegat Inlet at 39.5N, 74.0W (Figure 3). Results from the two stations were similar, and hindcast sta AU2070 was selected for use in the analysis (Figure 4) because of its closer proximity to the project study grid boundary. A percent occurrence table of significant wave height, peak period, and peak direction was constructed for sta AU2070 (Appendix A). At sta AU2070, waves typically approach the study area from between 67.5 and 180.0 deg azimuth. Wave heights are most likely in the 0.5 to 1.0-m range with a mean of 0.9 m. The maximum hindcast wave height was 8.4 m. The highest percentage of wave periods is 5.0 to 9.0 sec, with a mean wave period of 6.4 sec.

For littoral transport studies, the primary and secondary wave components were taken separately. Breaking wave height and direction are critical to longshore sediment transport. Hence, it was useful to retain information about both components of the offshore wave climate. A wave height threshold of 0.3 m was used to eliminate waves that would not likely cause transport. The primary component distribution for sta AU2070

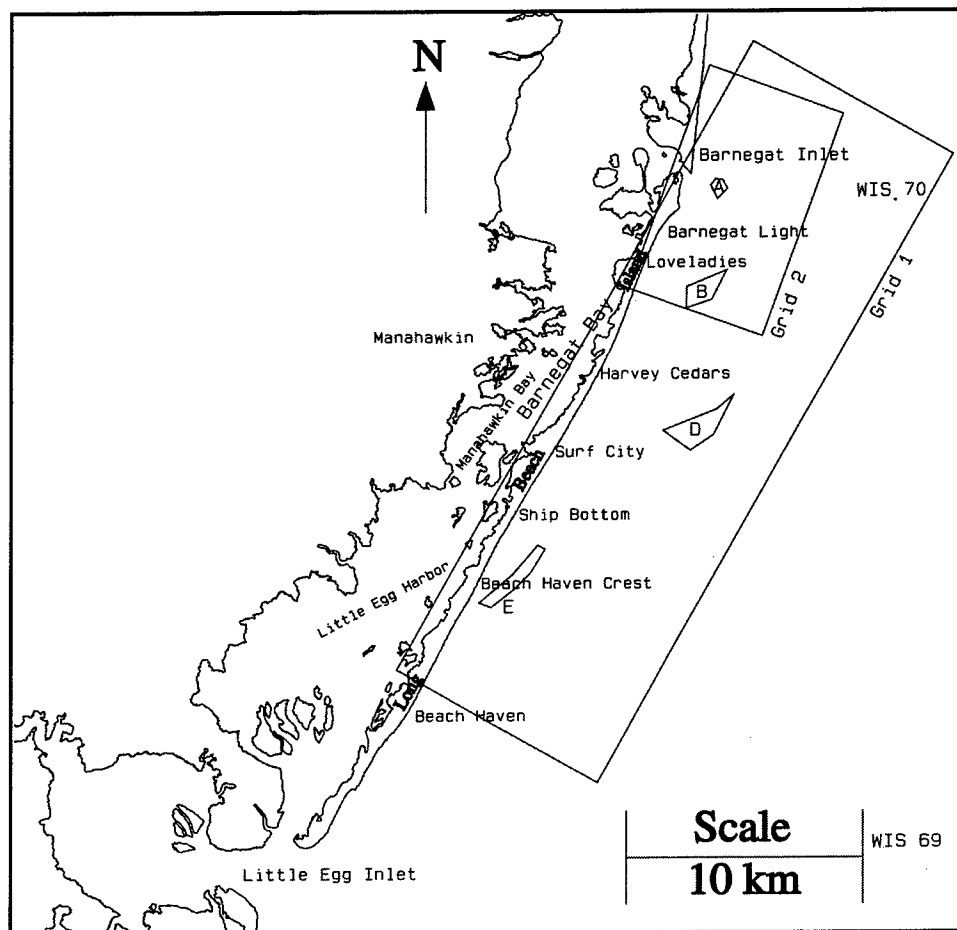


Figure 3. WIS stations and grid limits

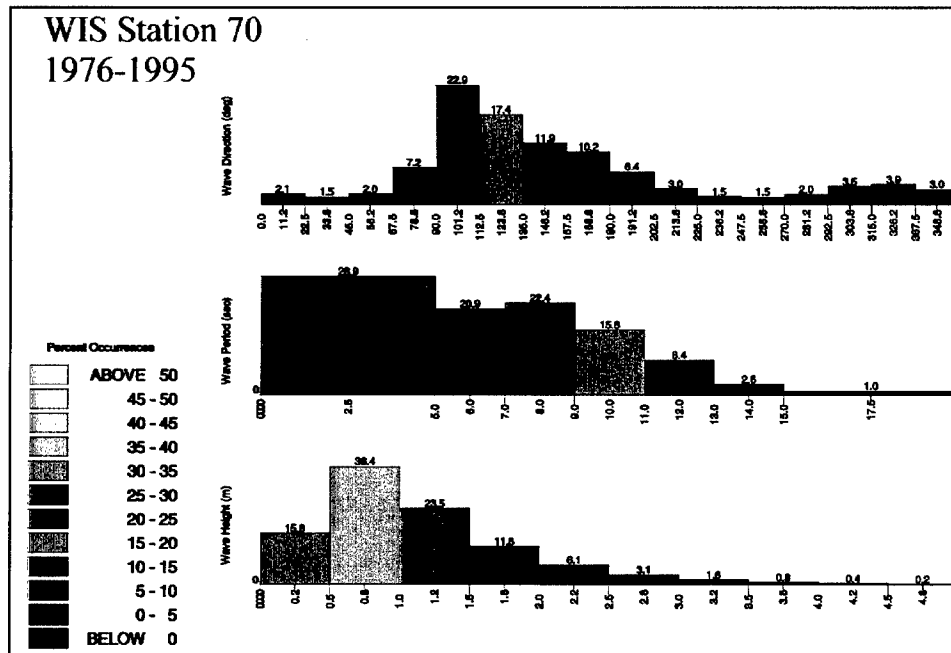


Figure 4. Wave statistics for WIS sta AU2070

(Figure 5) is similar to Figure 4. The secondary component distribution shows an increased frequency of offshore-traveling wave conditions (Figure 6). As will be shown in the model simulations, waves from 67.5 to 180 deg were used in model simulations. Therefore a large percentage of the secondary component waves were eliminated because they would not impact the coast. Even though wave heights are relatively low, the secondary components were included for littoral transport studies.

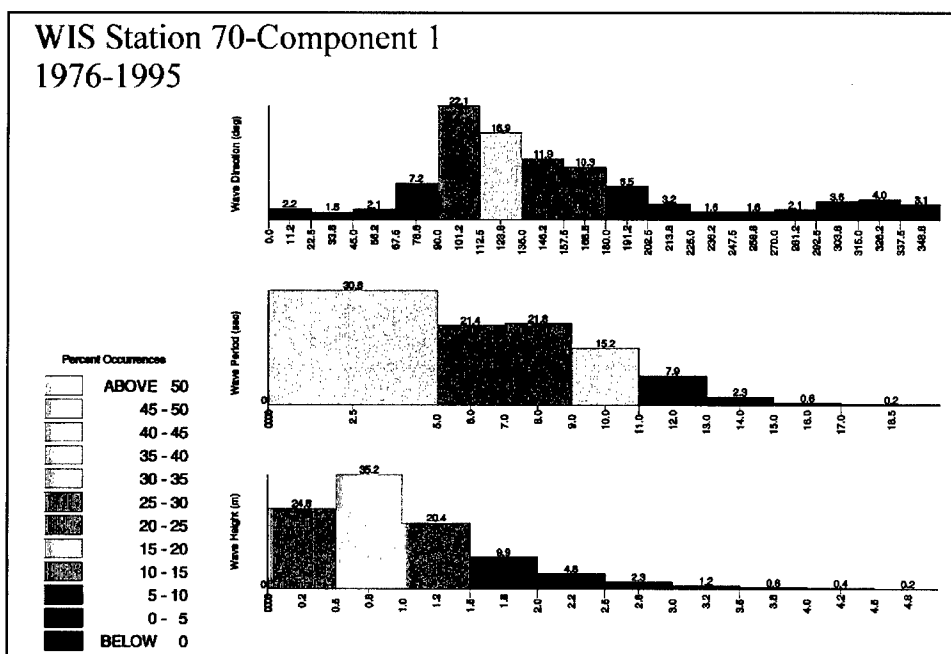


Figure 5. Wave statistics for WIS sta AU2070-component 1

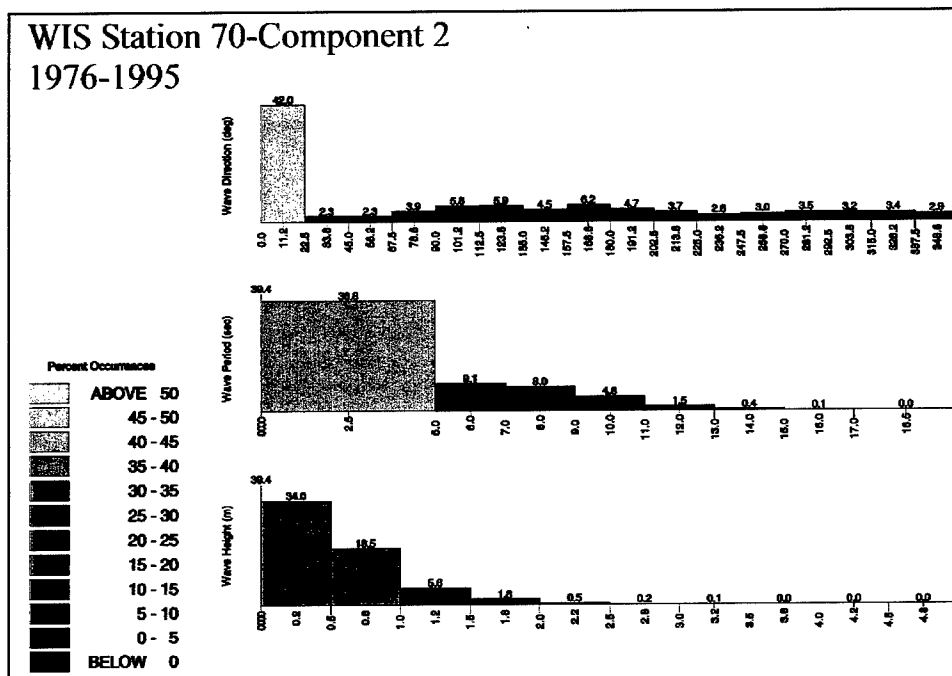


Figure 6. Wave statistics for WIS sta AU2070-component 2

NDBC Buoy 44025 and DWG Measurements

The offshore directional wave measurement station nearest the study area is National Data Buoy Center (NDBC) buoy 44025, located at 40.25 N, 73.17 W. Water depth at the buoy is 40 m. Directional wave data were available for 6 years, from November 1991 to November 1997. Data were collected hourly for 1,024 sec at a rate of 1 Hz. Although NDBC buoy 44025 is distant from the study area, it provides a valuable indication of the WIS wave climate quality. Wave statistics for buoy 44025 (Figure 7) and for the nearest WIS station (AU2070) (Figure 4) indicate similar wave direction, wave period, and wave height climates. The distribution for WIS sta AU2070 is quite consistent with buoy 44025. Overall, the study area offshore wave climate as represented by WIS sta AU2070 appears acceptable.

In May 1994, a directional wave gauge (DWG) was deployed 1,300 m off the Barnegat Inlet south jetty tip in approximately 12 m of water for a one-year period. The average significant wave height, $H_{s_{avg}}$, for that time period was 0.7-0.8 m, the average peak period, T_{avg} , was 8.9 sec, and the maximum significant wave height, $H_{s_{max}}$, was 3.8 m. The wave statistics for this shorter time period show less directional spread, a longer average wave period, and a somewhat smaller distribution of wave heights than the WIS AU2070 hindcast and NDBC buoy 44025 data (Figure 8).

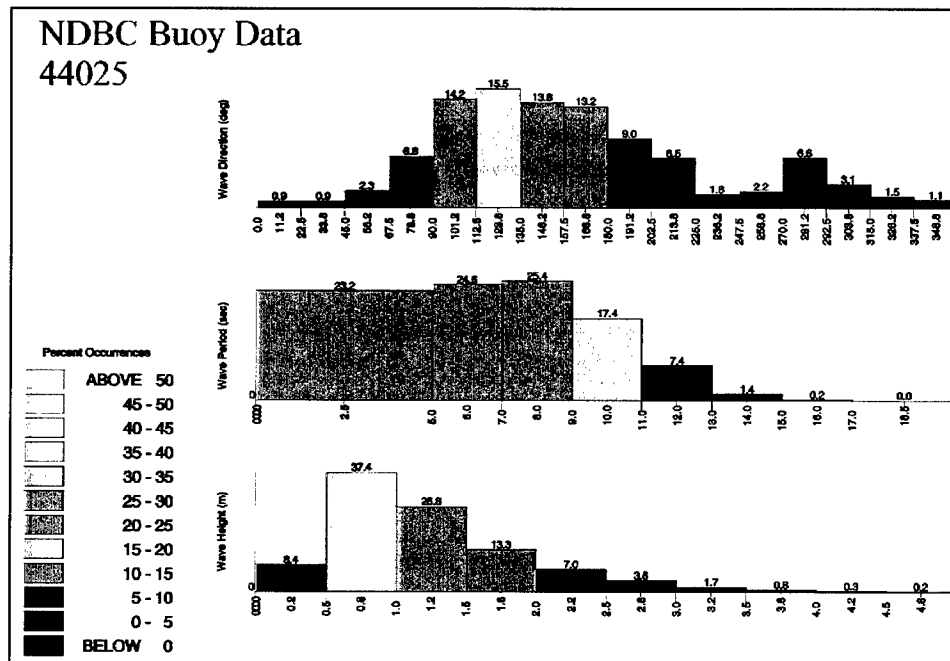


Figure 7. Wave statistics for NDBC buoy 44025

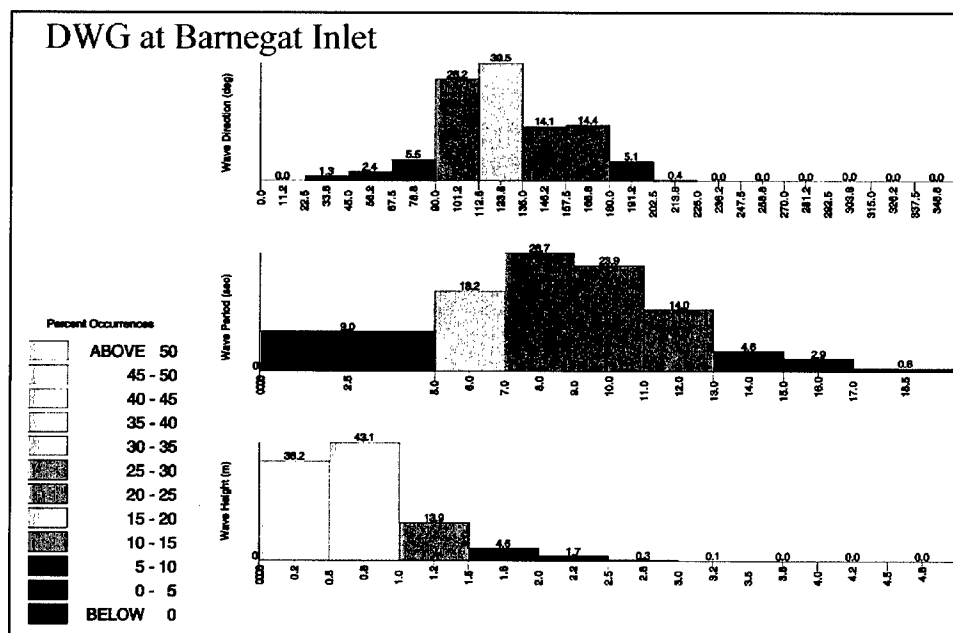


Figure 8. Wave statistics for DWG at Barnegat Inlet

OCTI Hindcast

OCTI performed a hindcast for the Philadelphia District which was also analyzed for possible use as a source for wave statistics to use in the potential littoral transport computations. OCTI sta I=35, J=30 located at 39.5833N, 74.1666W was selected due to its proximity to the grid offshore boundary. Water depth at the hindcast station was 19 m. A percent occurrence table of significant wave height, peak period, and direction were constructed for the hindcast station (Appendix B). At the hindcast station, waves approach the study area from a broader range of directions with the highest percentages being the nearly shore-normal angles between 157.5 and 202.5 deg azimuth (Figure 9). Wave heights are statistically most likely in the 0.5 to 1.0-m range with a mean of 0.9 m. The maximum hindcast wave height was 5.9 m. The highest percentage of wave periods is 0.0 to 5.0 sec, with a mean wave period of 5.4 sec. These data do not correspond to the buoy data as well as the WIS data, but both the WIS and the OCTI data sets were retained for use in computing littoral sediment transport as requested by the Philadelphia District.

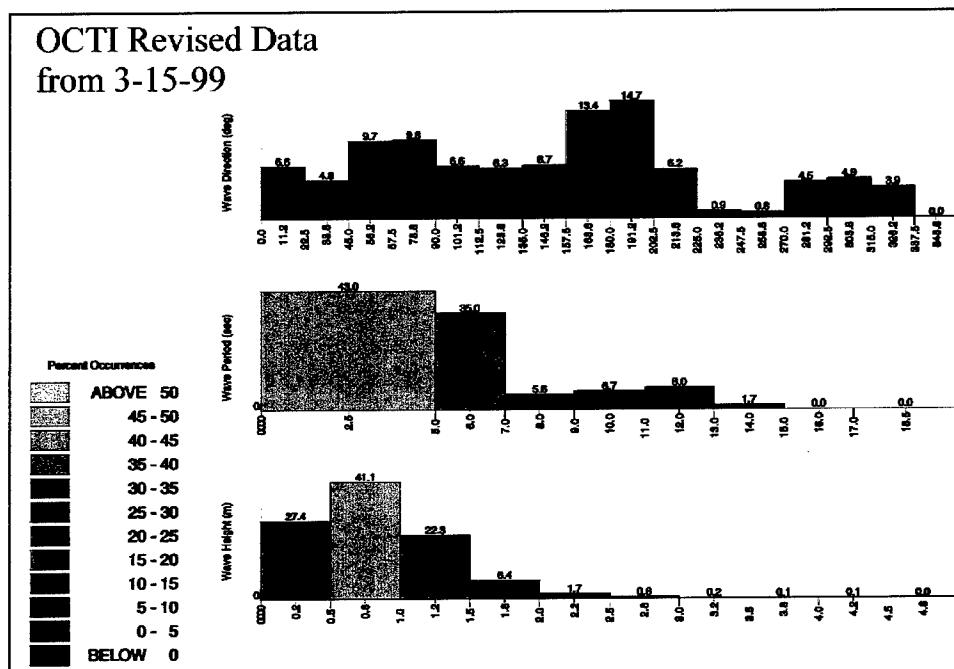


Figure 9. Wave statistics for OCTI sta (i=35 j=30)

3 Modeling Approach

Wave Model and Grids

Wave model

The spectral wind-wave growth and propagation model STWAVE (Smith, Resio, and Zundel 1999) was chosen for wave transformation modeling in this study (Appendix C). The spectral representation was expected to be advantageous for transforming waves over the complex bathymetry of the borrow areas and the finger-like shoals which exist offshore of Long Beach Island. As described in Appendix C, model input requirements include a bathymetric grid, water level, and a two-dimensional wave spectrum at the offshore boundary. Details of these data requirements, as they apply to this study, are given in the following sections.

Grids

An STWAVE grid was developed to include coastal bathymetry extending from sta AU2070 west to the Long Beach Island shoreline and from north of Barnegat Inlet to Beach Haven (Figure 3). The grid encompassed all four potential borrow areas outlined in Chapter 1. Wave transformation between offshore and the Long Beach Island shoreline was modeled with this 100-m resolution grid referred to as Grid 1. A finer grid, with 50-m resolution, was developed for the Borrow Area A Barnegat Inlet area (Figure 3) and is referred to as Grid 2. This grid was needed for investigation of sediment transport potential along beaches to the south of Barnegat Inlet, outside the immediate influence of Borrow Area A. Specifications for the two grids are given in Table 1.

Table 1
Specifications for STWAVE Grids from SMS

Parameter	Grid 1 ¹	Grid 2
Cell size, m	100	50
Oxigin, x (state plane), m	195,282.57	190,639.71
Origin, y (state plane), m	103,801.49	105,515.86
x-axis length, m	9,750	6,000
y-axis length, m	30,500	10,000
Counterclockwise rotation of x-axis from east, deg	150.5	160
No. of I's (columns)	97	120
No. of J's (rows)	305	200
¹ Used for existing conditions and borrow area bathymetry.		

Bathymetry data were taken from several sources provided by the Philadelphia District. As provided, the data were all referenced to mean high water (mhw). (Adjustment of the model to another datum can be easily accomplished within the STWAVE model framework.) Data sources included 1936 and 1954 National Ocean Survey (NOS) surveys, 1996 OCTI surveys of two nearshore regions, 1996 profile data collected along Long Beach Island for the feasibility study, and 1996 profile data north and south of Barnegat Inlet, and a 1997 ebb shoal survey collected as part of the Monitoring Completed Navigation Projects program for Barnegat Inlet. These data were combined into one data set and converted to metric units using Spectra Precision Software TerraModel. For the many places with data overlap, the most recent data superseded any older data. Data outside the STWAVE grid boundaries were eliminated to reduce the size of the data set. Contour maps for the existing condition bathymetric configuration for the two grids are given in Figures 10-11.

STWAVE is available in the PC-based Surface Water Modeling System (SMS) (Brigham Young University 1995). Hence, SMS was used for grid building and output visualization in this study. The digital bathymetry provided by the Philadelphia District was input into SMS to build the uniform rectangular grids required by STWAVE. Grids in SMS were built in the New Jersey State Plane coordinate system (metric). Grid specifications are given in Table 1. In addition, borrow areas were numerically "dredged" using SMS grid modification capabilities. Contour maps for the borrow area bathymetric configuration for the two grids are given in Figures 12-13.

Incident wave conditions

STWAVE input requirements include wave conditions defined at the offshore grid boundary. The first step in generating input wave conditions was to examine the percent occurrence tables computed from the WIS parameters at sta AU2070 and OCTI sta i35j30 (as described in Chapter 2 and

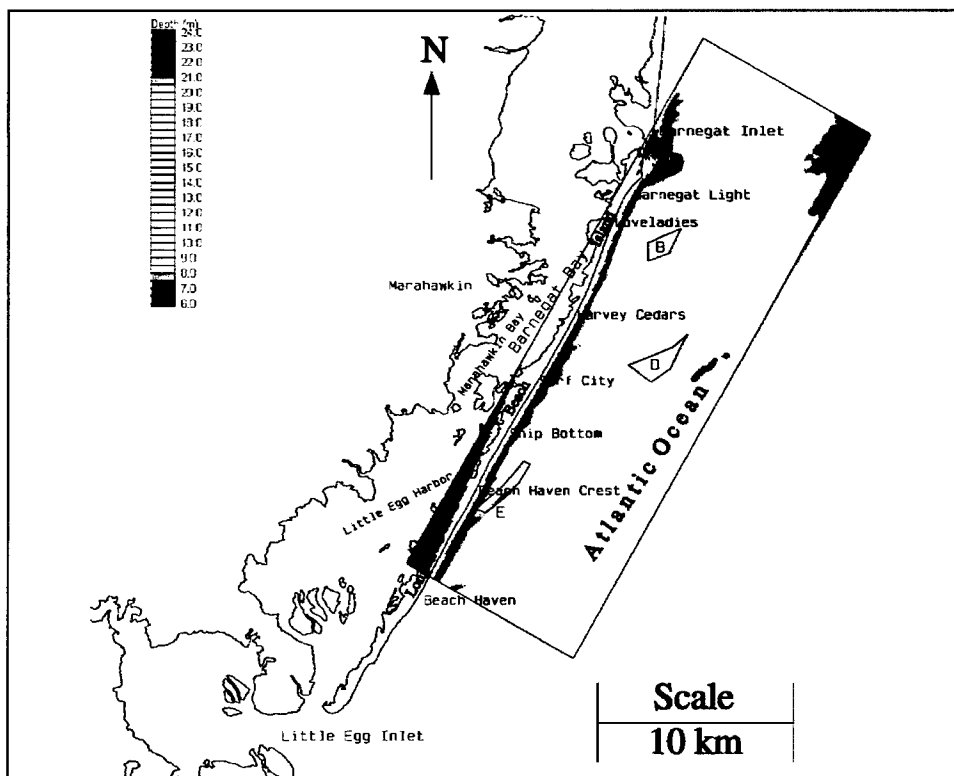


Figure 10. Grid 1 existing condition bathymetry

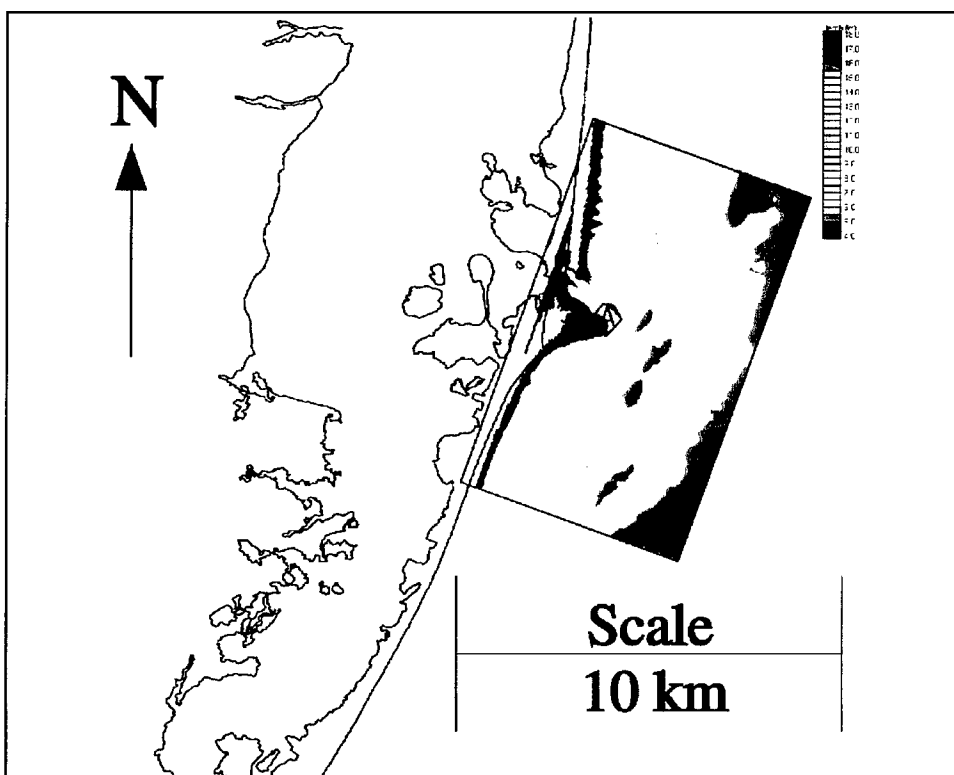


Figure 11. Grid 2 existing condition bathymetry

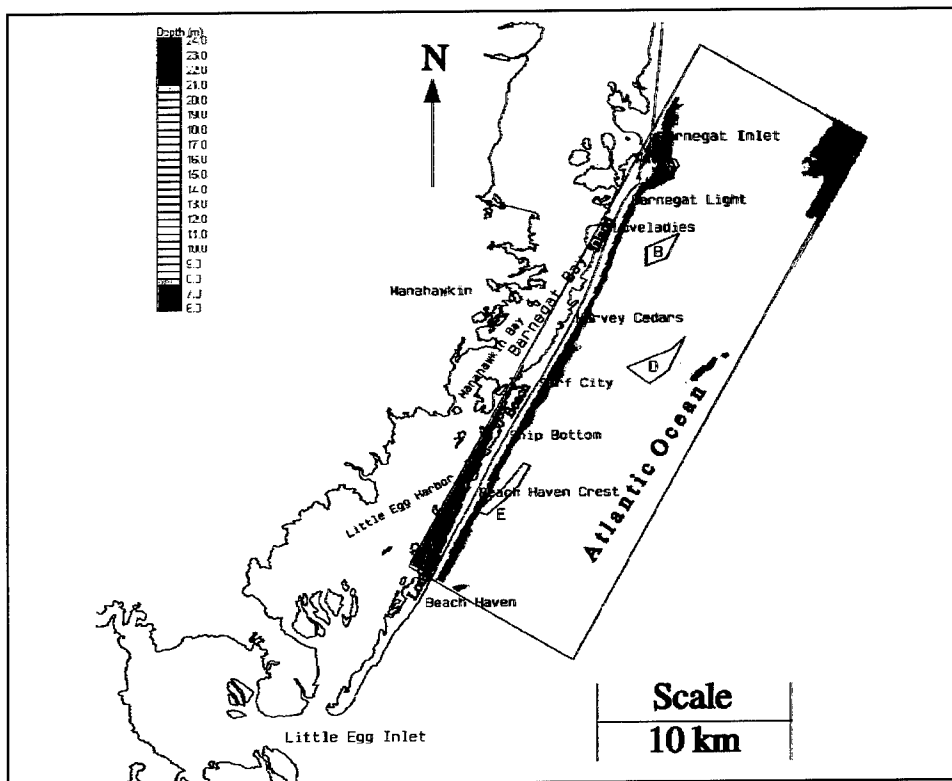


Figure 12. Grid 1 borrow area bathymetry

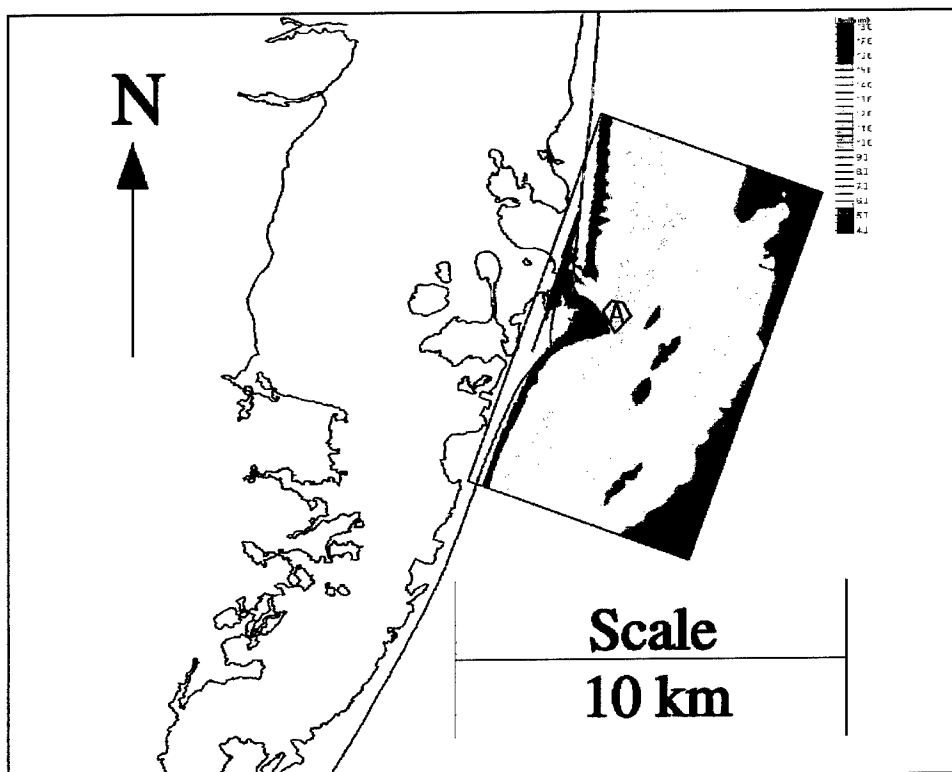


Figure 13. Grid 2 borrow area bathymetry

given in Appendices A and B). From these data, intervals selected for the wave parameters were 0.5 m for wave height, 2 sec for peak period, and 22.5 deg for direction. Wave height ranges .25-.75, .75-1.25, 1.26-1.75, etc.; period ranges 3-5 sec, 5-7 sec, 7-9 sec, etc., and direction ranges 56.25-78.75, 78.75-101.25, etc., were simulated with the parameters described in Table 2. An STWAVE simulation was run for each combination shown in Table 2, for a total of 756 wave conditions simulated.

Table 2
Wave Conditions Simulated with STWAVE

Wave Height, m	Wave Period, sec	Wave Direction, deg N
0.5	4	67.5
1.0	6	90.0
1.5	8	112.5
2.0	10	135.0
2.5	12	157.5
3.0	14	180.0
3.5	16	
4.0	18	
4.5	20	
5.0		
5.5		
6.0		
6.5		
7.0		

For each STWAVE input height/period/direction combination, the ACES 2.0 software was used to generate a directional wave spectrum in a water depth appropriate to the corresponding Grid 1 seaward boundary (20 m). Spectral frequencies ranged from 0.04 Hz to 0.33 Hz at 0.01 Hz intervals. Spectral direction components covered ± 85 deg from normal incidence to the grid, in 5-deg increments. A single water level was used in all simulations, representing mean sea level (0.61 m below the mhw datum).

For Grid 2 simulations, wave spectra from Grid 1 were saved at five points corresponding to the Grid 2 offshore boundary. The spectra were averaged for each case to give a representative incident spectrum for the Grid 2 boundary. Boundary points which were not consistent with the more representative boundary points were omitted from averaging.

STWAVE output

The main output from STWAVE simulations consists of arrays of significant wave height, peak period, and peak direction over the entire grid for each incident wave condition. These relatively large files are useful for

visualizing wave transformation over the entire grid. The height/period/direction information at selected stations in the grid is another, much more condensed output which was useful for the littoral transport computations required in this study. Station output at grid cells along a nearshore reference line was generated for each STWAVE simulation, as discussed in the following sections. Station output can be generated during the STWAVE runs or it can be extracted from the main output arrays as a post-processing step.

Wave transformation examples

Figures 14 and 15 illustrate the Grid 1 wave transformation patterns for the existing condition bathymetric configuration and borrow area bathymetric configuration, respectively. These patterns are for one incident wave case (waves approaching from the most northerly angle band 67.5 deg). In this case, a 3-m wave height and longer than average (10-sec) peak period were selected to illustrate wave transformation over the four borrow areas. Note the changes in wave height in the vicinity of the borrow areas induced by the changes in bathymetric configuration from Figure 14 to Figure 15.

Similarly, Figures 16 and 17 show computed Grid 1 wave transformation patterns for the existing condition bathymetric configuration and borrow area bathymetric configuration, respectively, for the case with the same offshore wave height and peak period, but approaching from a southerly direction (180 deg). In these cases, wave heights are more noticeably reduced as waves propagate from the offshore boundary into the nearshore area. The wave height reduction in shallow water is mainly caused by the effects of refraction and nonlinear wave-wave interaction introduced in the STWAVE model. The wave-wave interaction induces significant loss of wave energy in the high frequency range through energy transferring from spectral peak to high frequency components.

Figures 18 through 21 show wave transformation patterns for Grid 2 for the same incident wave conditions previously described. Changes in the vicinity of Borrow Area A are observed.

Littoral Transport

The approach to estimating littoral transport was to use STWAVE to transform each incident wave condition to near-breaking; transform the near-breaking wave to a point at which breaking begins, using the assumption of locally straight, parallel bottom contours; and compute potential longshore transport rate from that breaking wave height and angle. With consideration of the WIS and OCTI percent occurrence tables, the potential transport rate due to each incident wave condition was then converted to an annual potential transport volume of sediment. Finally, potential transport

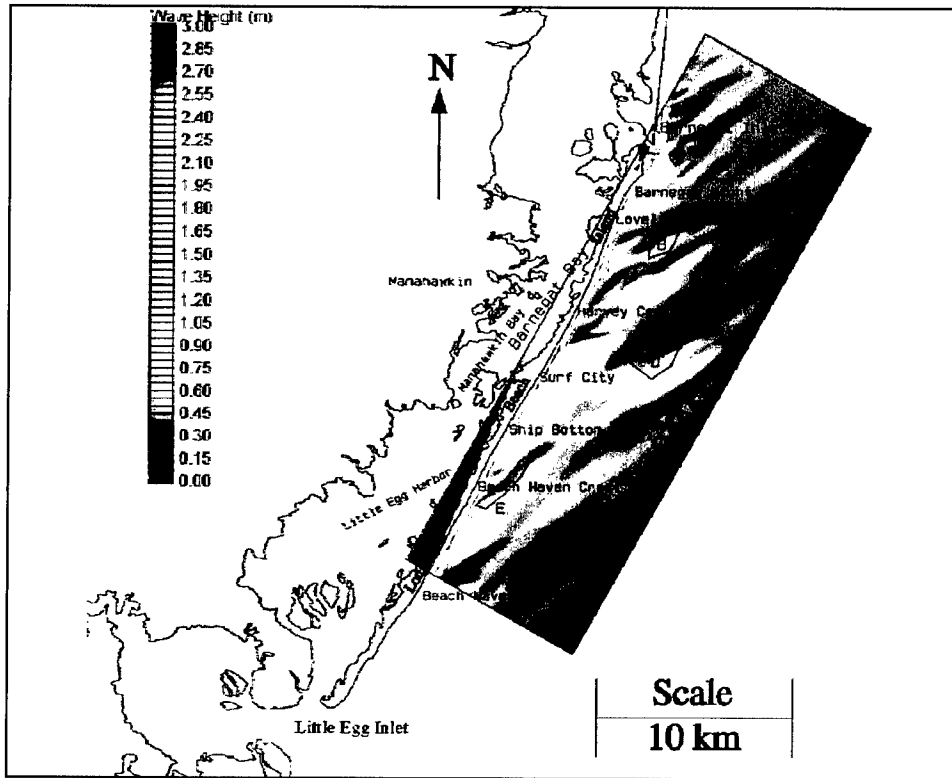


Figure 14. Grid 1 waves from 67 deg, $H = 3$ m, $T = 10$ sec — without project condition

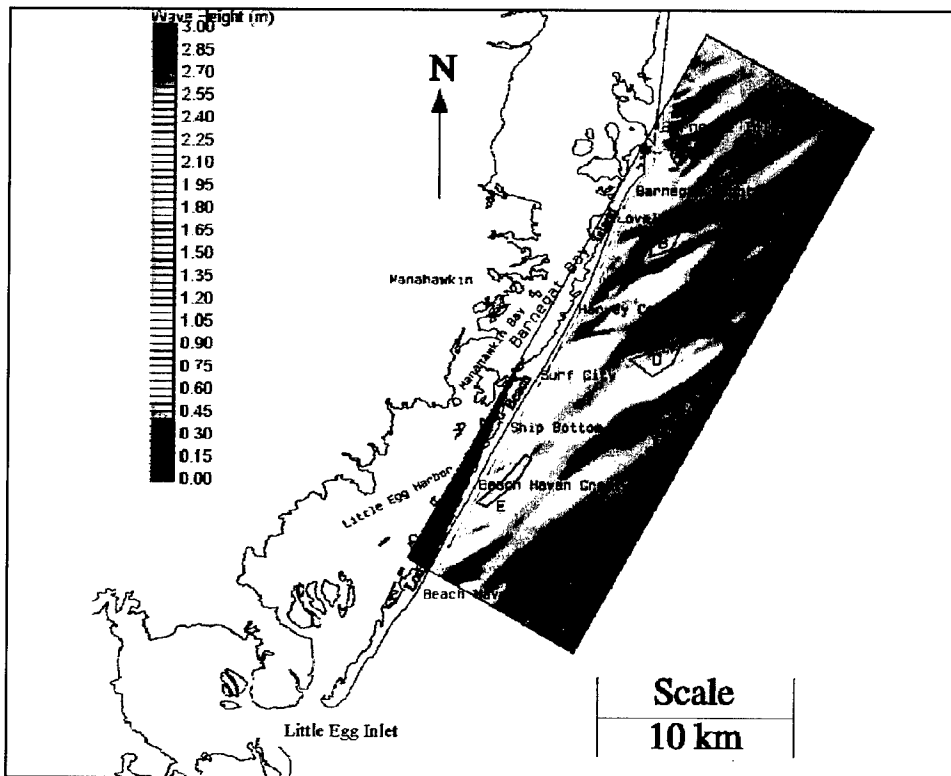


Figure 15. Grid 1 waves from 67 deg, $H = 3$ m, $T = 10$ sec — with project condition

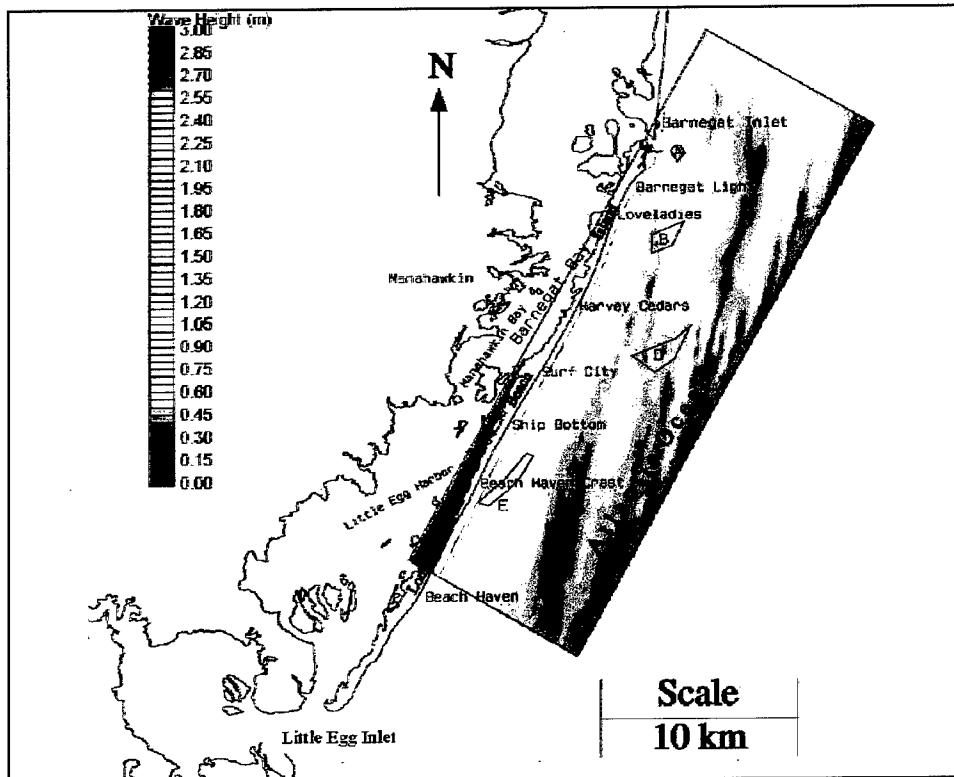


Figure 16. Grid 1 waves from 180 deg, $H = 3$ m, $T = 10$ sec — without project condition

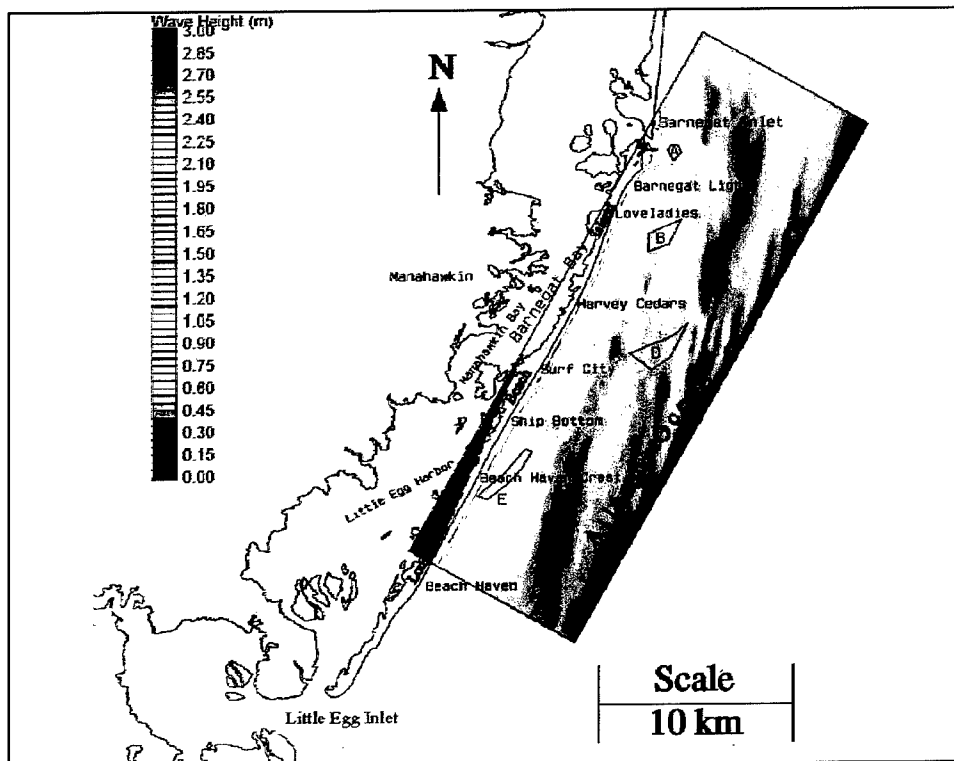


Figure 17. Grid 1 waves from 180 deg, $H = 3$ m, $T = 10$ sec — with project condition

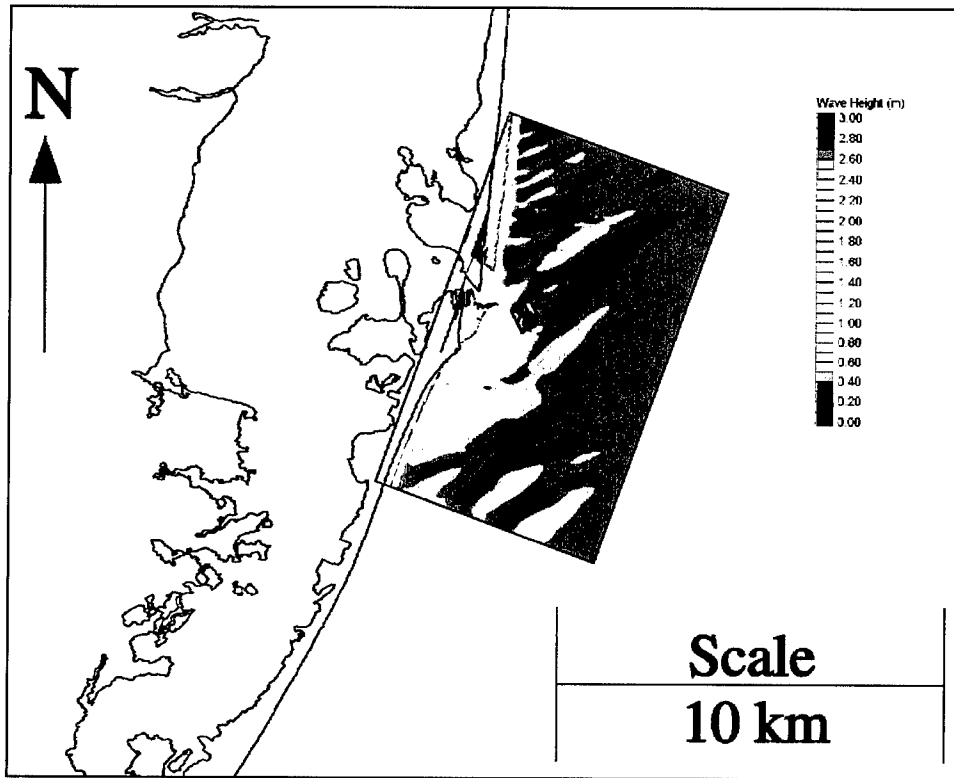


Figure 18. Grid 2 waves from 67 deg, H = 3 m, T = 10 sec — without project condition

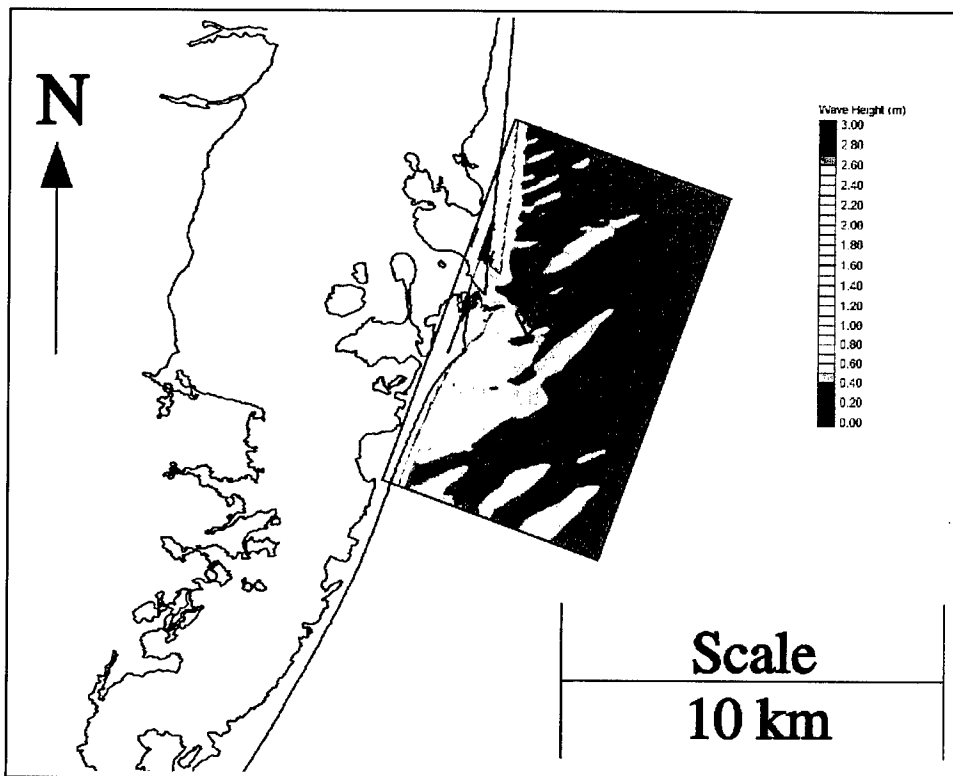


Figure 19. Grid 2 waves from 67 deg, H = 3 m, T = 10 sec — with project condition

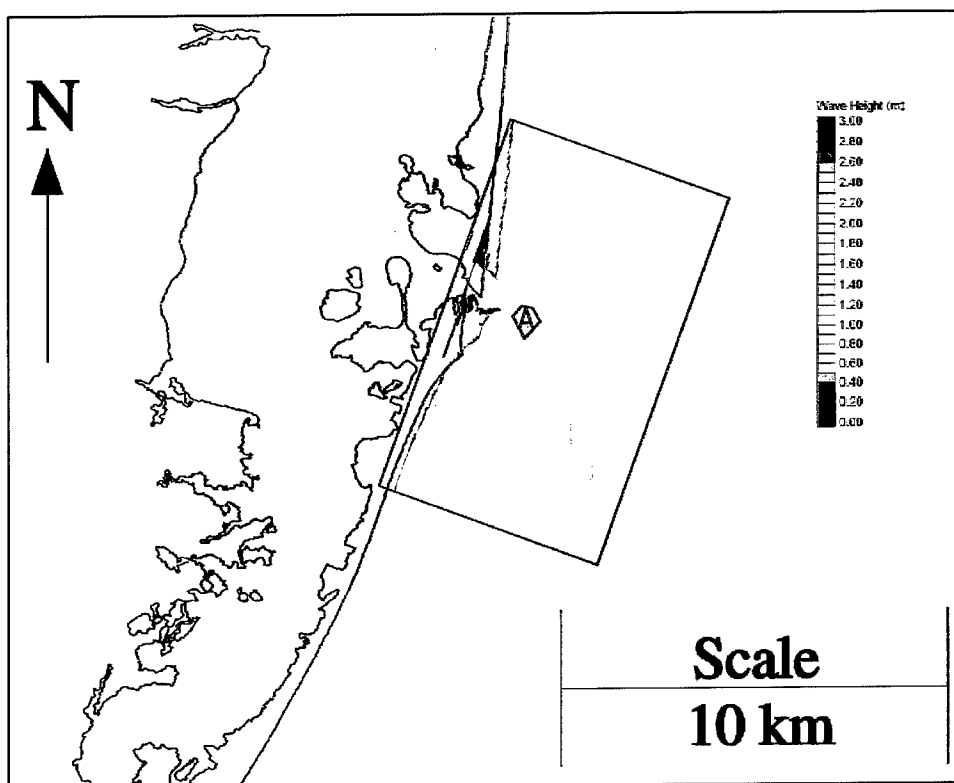


Figure 20. Grid 2 waves from 180 deg, $H = 3$ m, $T = 10$ sec — without project condition

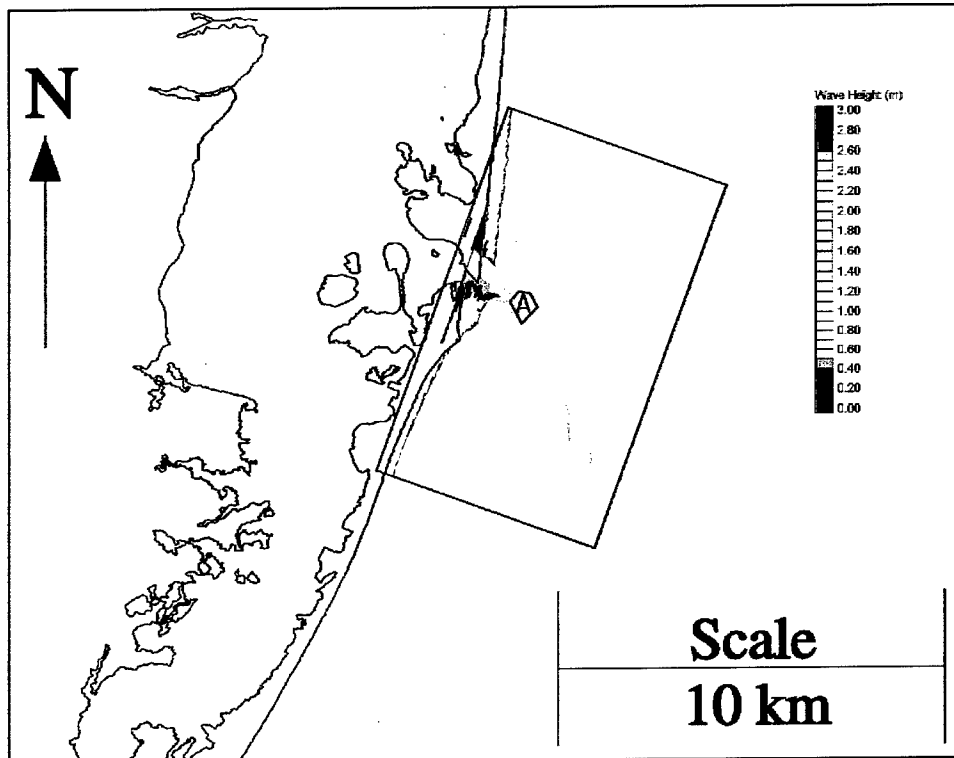


Figure 21. Grid 2 waves from 180 deg, $H = 3$ m, $T = 10$ sec — with project condition

contributions from all incident wave conditions were added to give estimates of annual northward, southward, net, and gross longshore transport.

Calculation of breaking wave conditions

Stations for saving STWAVE wave parameters to be used in littoral transport estimation were selected with two primary objectives. First, the stations should be shoreward of all significant effects of irregular bathymetry, so that STWAVE will have included these effects in wave transformation. Second, stations should be seaward of the nearshore surf zone, so that STWAVE has not yet invoked breaking limits on wave height and the breaking wave height and angle needed for calculating longshore transport rates can be accurately estimated.

A nearshore station was selected for every alongshore grid cell of the project study grids. Nearshore stations for Grid 1 and Grid 2 are illustrated in Figures 22 and 23. Stations in Grid 1 were placed around the 6-m contour, where bottom contours were reasonably parallel to the shoreline. Near Barnegat Inlet, the ebb shoal extends offshore, causing wave breaking there rather than on the nearshore beach slope. These breaking waves are not directly driving littoral transport at the beach. Hence, nearshore stations in shoal areas were placed regardless of water depth to follow a smooth line of stations reasonably parallel to the beach or along expected paths of longshore transport around small inlets. These stations are expected to be representative of the breaking wave conditions actually driving nearshore littoral transport across shoal areas and along the adjacent beaches.

A shoreline angle was specified for each nearshore station to establish the orientation of the straight, parallel bottom contours to be used in calculating wave breaking conditions. Shoreline angles were computed from a recent digitized shoreline provided by the Philadelphia District.

A computer program adapted from the Generalized Model for Simulating Shoreline Change (GENESIS) shoreline modeling system program Nearshore Transport Program (NSTRAN) (Gravens, Kraus, and Hansen 1991) was used to iteratively calculate breaking wave heights and angles. Inputs to the program included nearshore station output from STWAVE and shoreline angles. The breaking criterion is $H_s = 0.78 d$, where d = water depth.

Calculation of longshore transport rates

The program calculates potential longshore transport rates as:

$$Q = K H_{bs}^{\frac{5}{2}} \sin(2 \alpha_b) \quad (1)$$

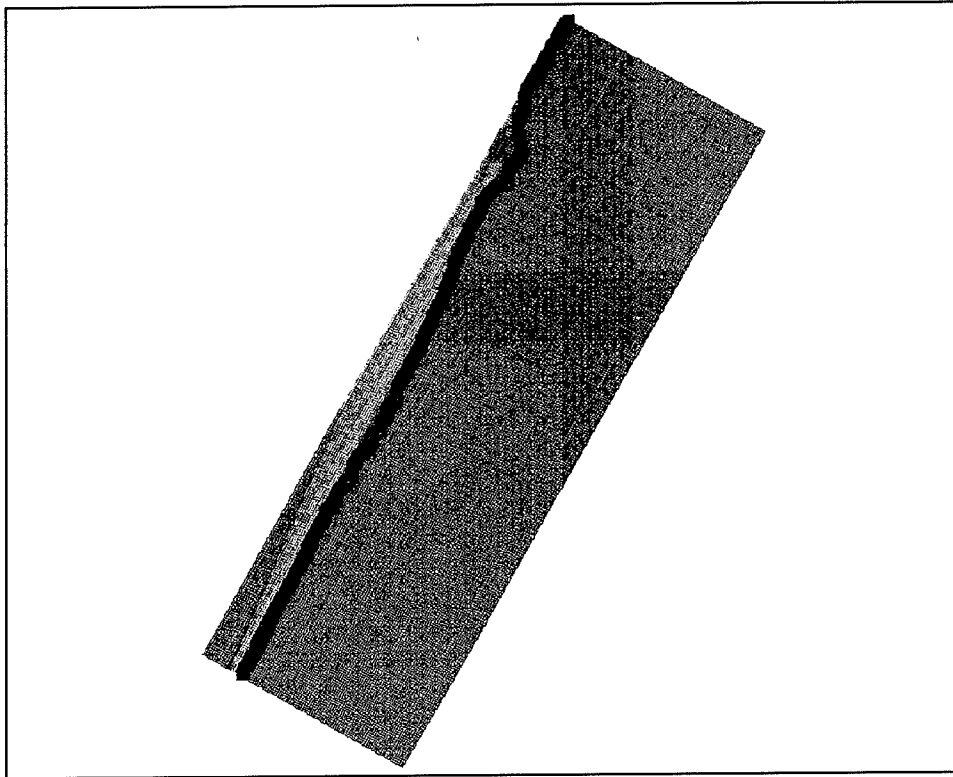


Figure 22. Location of Grid 1 nearshore reference line

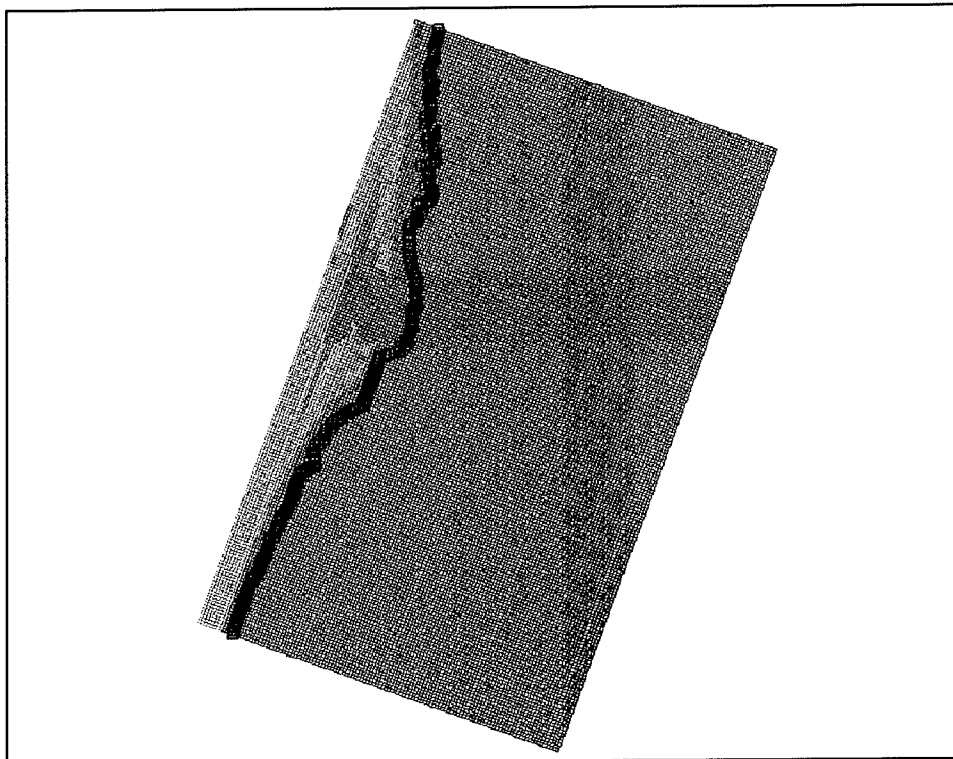


Figure 23. Location of Grid 2 nearshore reference line

where

Q = potential longshore transport rate

K = constant

H_{bs} = significant wave height at breaking

α_b = breaking wave angle relative to bottom contours

When H_{bs} is in meters and Q in m^3/day , the generally accepted value of K is $K = 5100$ (Equation 6-7b of USACE 1992). Program calculations were done in metric units with Q expressed in m^3/sec . The corresponding constant is $K = 0.0590$.

When Equation 1 is applied to the study area, longshore transport rates computed by WIS are unreasonably large. As in previous model studies, a calibration of the constant K was needed. Previous estimates of net and gross longshore transport rate along Long Beach Island provided a reasonable basis for calibration (General Design Memorandum 1984; USAED, Philadelphia 1999). The value of K in Equation 1 was reduced from 0.059 to 0.023 after calibration. The same calibration value of K was found in a concurrent STWAVE study of Cape Fear River Entrance and Smith Island to Ocean Isle Beach, North Carolina (Thompson, Lin, and Jones 1999). Transport computed with the OCTI data set did not require a reduction in the K coefficient and 0.059 was used.

A Q was calculated with Equation 1 for each wave condition. Using percent occurrences from WIS, Q was converted to an annual longshore transport volume in m^3/year . Following standard convention, longshore transport toward the right of an observer on the beach facing the ocean is positive (southward transport in this study), and transport toward the left is negative (northward transport in this study).

Contributions from all wave conditions were added together to give total annual northward and southward potential longshore transport volumes, which can be expressed as annual transport rates. Net potential longshore transport rates are determined as the difference between magnitude of the northward and southward rates. Gross potential longshore transport rates are the combined magnitudes of northward and southward transport rates.

This study used both primary and secondary WIS wave components, as represented in wave climate percent occurrence tables. This approach is expected to give a better estimate of net transport rates than if only overall WIS parameters were used. However, using the individual components tends to increase transport rates because both wave components contribute rather than just a combined event. The impact on longshore transport rates is expected to be small, but it is advisable to consider net transport rate as the most accurate littoral transport parameter in this study.

4 Littoral Transport Potential

Grid 1 Net Potential Transport

The net potential transport computed for this study is strictly controlled by the calibration coefficient K as described in the previous section. The selection of this coefficient is therefore critical. It was the intent of this study to compute "reasonable" transport values along Long Beach Island, with the ultimate goal being the comparison of these values for with- and without-project conditions. A reasonable transport value for Long Beach Island is on the order of 75,000 to 150,000 m^3/year .

Calibrated net potential longshore transport rates for Long Beach Island using the WIS and OCTI wave climatology are given in Figures 24 and 25, respectively. Alongshore cell numbers shown on the x-axis refers to the Grid 1 cell number, with Cell 1 located at the northern grid limit and Cell 300 located near the southern grid limit. Townships are given at their general location for reference. It is important to remember that these are "potential" transport rates and they do not consider the availability of sediment or the influence of coastal structures on sand transport rates. It is interesting to note the nodal zone in the vicinity of Barnegat Inlet, where the general shoreline orientation of New Jersey changes. The potential net transport shows a notable change from net northerly transport to net southerly transport in this region. The predominant shoreline orientation changes dramatically at Barnegat Inlet. The position of Long Island, NY affects the wave climate which in turn affects transport rates. The sheltering effect created by Long Island, NY limits waves from the north impinging on northern New Jersey. South of Barnegat Inlet, the sheltering effect is not as apparent and net transport along Long Beach Island, NJ is generally to the south. There is a local reversal (transport to the north) near Barnegat Inlet (Cell 134-135), probably due to the effects of the inlet and its shoal system on the downdrift beaches.

Using OCTI and WIS hindcast wave climatology for this study, net potential transport north of Barnegat Inlet is approximately 400,000-500,000 m^3/year to the north. Net potential transport across Barnegat Inlet is approximately 500,000-600,000 m^3/year to the south. Using the 1976-1995 WIS hindcast for sta 70 and the GENESIS support program

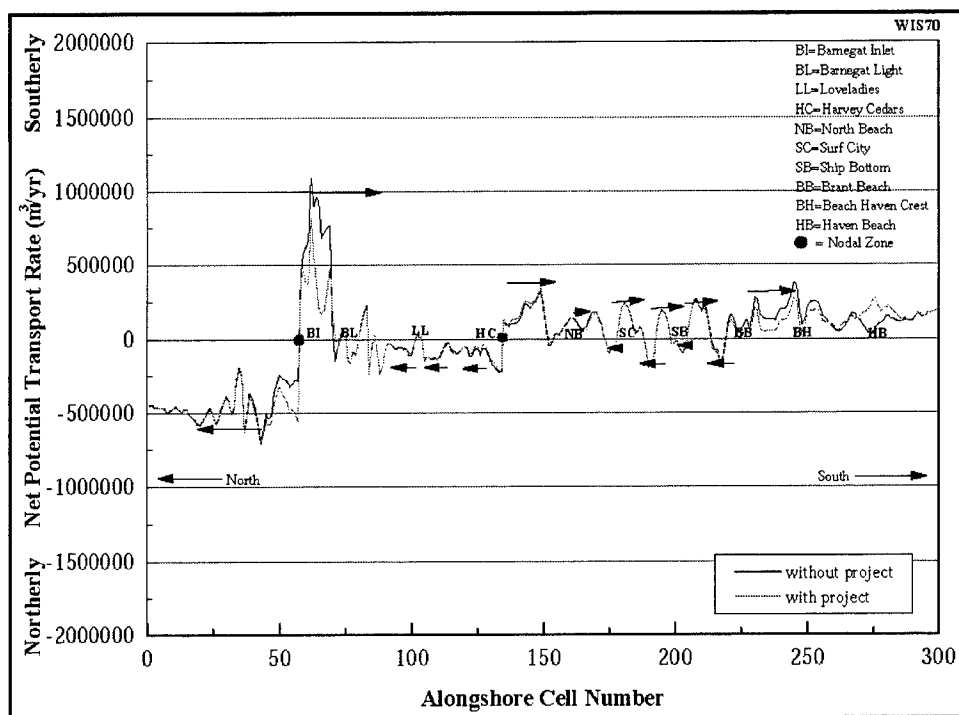


Figure 24. Net potential transport for Long Beach Island using WIS wave climatology

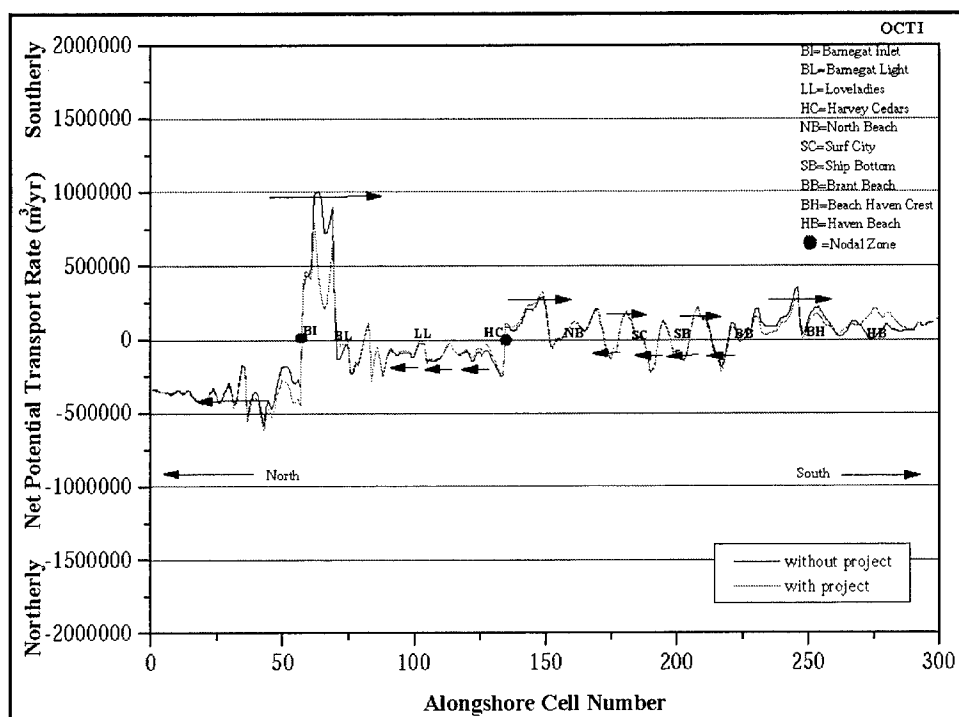


Figure 25. Net potential transport for Long Beach Island using OCTI wave climatology

SEDTRAN (Gravens, Kraus, and Hanson 1991), the net potential transport rate near Barnegat Inlet is estimated to be 530,000 m³/year to the south, assuming a local shoreline orientation of 29 deg east of north. In 1954, the Corps estimated that the net littoral transport in the Barnegat Inlet area was 190,000 m³/year to the south (U.S. Army Engineer District, New York, 1954). Other Corps estimates of net longshore transport at Barnegat Inlet range from 80,000 m³/year to the north to 280,000 m³/year to the south (U.S. Army Engineer District, Philadelphia, 1995). The average of grid Cells 135 through 305 was used to estimate the net potential transport along Long Beach Island for this study. Using OCTI hindcast wave climatology, the net potential transport for Long Beach Island was approximately 76,000 m³/year to the south and using the WIS hindcast wave climatology, the net potential transport was approximately 114,000 m³/year to the south. The Philadelphia District estimates of net longshore transport for Long Beach Island using an earlier OCTI hindcast and SEDTRAN are approximately 70,000 to 140,000 m³/year. Prior Philadelphia District estimates of net longshore transport for Long Beach Island based on 1838-1953 data and 1974 data indicate a much lower value (approximately 40,000 m³/year) (U.S. Army Engineer District, Philadelphia, 1995).

It is evident that there is great variability in longshore transport estimates due to the quality of the input data as well as the level of sophistication used in the analysis. A reasonable transport value for Long Beach Island is on the order of 75,000 to 150,000 m³/year.

By comparing the with- and without-project conditions it is observed that there are changes in the net transport potential induced by the project. The greatest changes are in the vicinity of Borrow Area A (affecting Cells 50-70) and Borrow Area E (affecting Cells 230-280).

Grid 1 Erosion and Accretion

The northerly (defined as negative) and southerly (defined as positive) longshore potential transport rates computed for Long Beach Island were used to estimate areas of erosion and accretion. Shoreline reaches defined by the Philadelphia District for Grid 1 were used in these computations with slight adjustments to the suggested Reach 3-5 boundaries (Table 3).

Table 3
Long Beach Island Shoreline Reaches for Grid 1

Reach	Grid Cells	Township
1	62-81	Barnegat Light
2	82-94	Loveladies North
3	95-119	Loveladies South
4	120-130	Harvey Cedars North
5	131-144	Harvey Cedars South
6	145-174	North Beach
7	175-194	Surf City
8	195-210	Ship Bottom
9	211-238	Brant Beach
10	239-266	Beach Haven Crest to Beach Haven Park
11	267-286	Haven Beach to Beach Haven Gardens
12	287-305	Spray Beach to Beach Haven Boro North

Longshore transport values for cells in each reach were summed and an average northerly and southerly longshore transport value was determined for each reach (Table 4). Three methods of computing erosion or accretion $X_{(i)}$ for a given Reach i were defined as follows: In Method 1 (Figure 26), the average north and south transport values for a given reach were applied at the cell faces (the boundaries of the reach):

$$X_{(i)} = LT_{S(i-1)} - LT_{S(i)} + LT_{N(i)} - LT_{N(i+1)} \quad (2a)$$

where $LT_{S(i)}$ is the southerly longshore transport value for a given Reach i and $LT_{N(i)}$ is the northerly longshore transport value for a given Reach i . $LT_{S(i)}$ is applied at the right face of Reach i and $LT_{N(i)}$ is applied at the left face of Reach i . In Method 2 (Figure 26), transport values for adjacent reaches were averaged to determine transport values at the cell faces:

$$X_{(i)} = LT_{S(i-1/2)} - LT_{S(i+1/2)} + LT_{N(i+1/2)} - LT_{N(i-1/2)} \quad (2b)$$

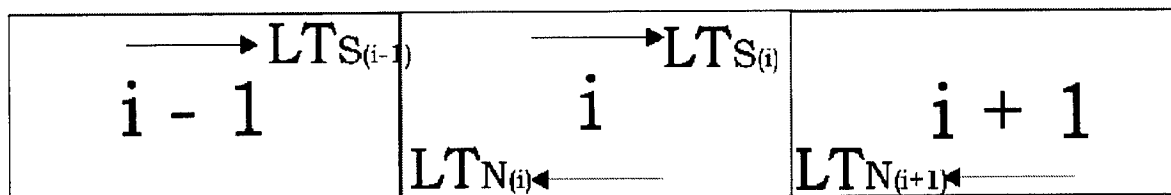
Distances to the cell face from $(i-1)$, (i) , and $(i+1)$ were incorporated into the calculations to weight the transport rates used in the averaging. In Method 3 (Figure 26), the transport rates at the cell faces were determined by averaging 25 cells around the reach boundaries. Equation 2b applies to this method also. The number of cells used in the averaging corresponds to the average length of the reaches.

These procedures were repeated for each reach. A boundary reach, Reach 0, across Barnegat Inlet (Cells 58-61) was used to provide an adjacent cell for Reach 1. It was assumed that the southerly transport rate at the inlet would lose 175,000-225,000 m^3 of sediment to the inlet and/or ebb shoal based on recent inlet dredging records. Northerly-directed transport

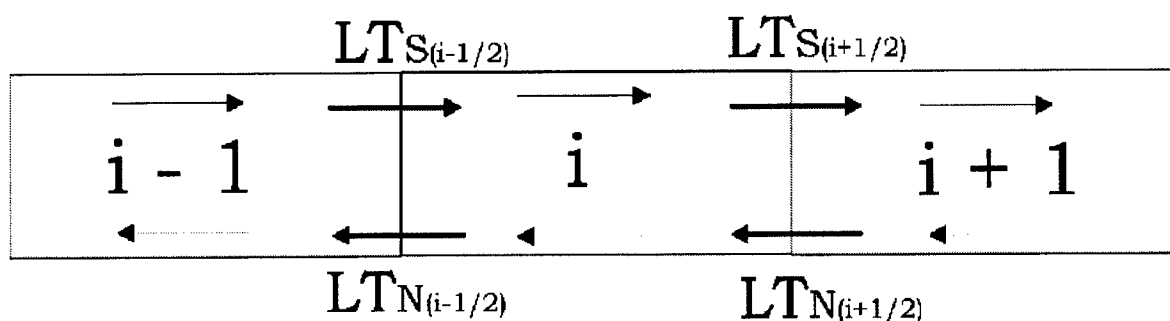
Table 4 Net Longshore Transport Potential for Long Beach Island				
Reach	Southerly and (Northerly) Longshore Transport WIS Without-Project m³/year	Southerly and (Northerly) Longshore Transport WIS With-Project m³/year	Southerly and (Northerly) Longshore Transport OCTI Without-Project m³/year	Southerly and (Northerly) Longshore Transport OCTI With-Project m³/year
0	403,300	289,400	363,000	392,000
1	453,500 (-136,300)	282,600 (-136,900)	589,000 (-241,800)	386,900 (-231,500)
2	204,300 (-254,300)	199,400 (-251,400)	265,600 (-368,100)	264,400 (-357,700)
3	179,900 (-257,500)	179,800 (-256,900)	267,400 (-359,300)	273,400 (-355,900)
4	197,900 (-288,500)	203,800 (-277,400)	293,100 (-395,900)	310,100 (-384,300)
5	292,300 (-254,500)	305,600 (-247,200)	379,700 (-361,300)	398,200 (-357,000)
6	323,400 (-213,400)	327,500 (-216,700)	422,400 (-325,900)	434,500 (-331,600)
7	226,800 (-192,900)	233,800 (-195,500)	293,500 (-301,700)	307,400 (-310,400)
8	262,000 (-177,700)	273,800 (-191,600)	316,300 (-286,600)	334,600 (-308,000)
9	272,600 (-184,500)	254,100 (-213,000)	336,700 (-288,500)	332,200 (-318,900)
10	349,300 (-176,400)	300,400 (-170,500)	419,000 (-282,600)	381,200 (-270,300)
11	293,300 (-184,400)	348,000 (-165,100)	360,400 (-298,300)	416,800 (-278,800)
12	339,300 (-166,100)	341,700 (-166,100)	402,800 (-283,700)	407,700 (-283,700)
13	(-157,500)	(-157,500)	(-277,600)	(-277,600)
Note: Southerly transport is given first followed by northerly transport given in parentheses.				

into Reach 12 from the southern boundary of the grid was estimated by averaging the northerly transport rates from the five cells closest to the grid boundary. This estimate is reasonable because the northerly-directed transport is fairly constant in this region (Table 4). This analysis assumes no losses or gains due to cross-shore transport processes.

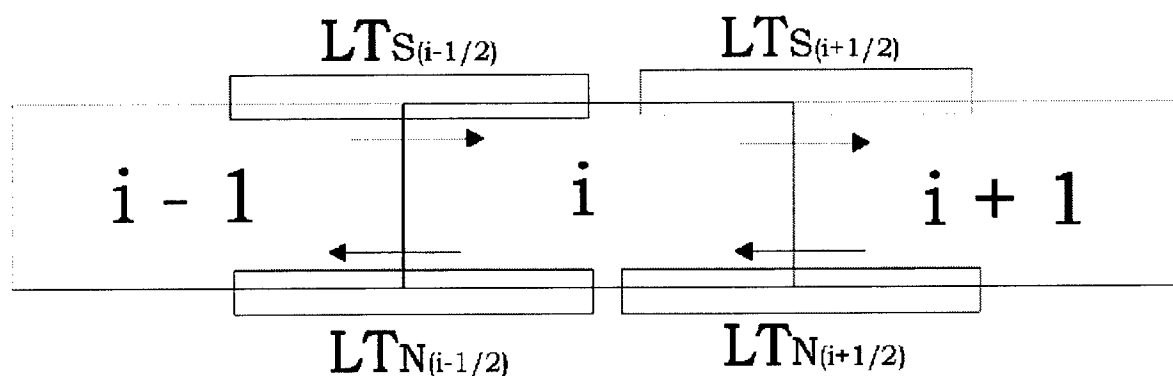
The three methods of computing erosion and accretion, and an average value are given in Tables 5 and 6 for each bathymetric configuration (with- and without-project) and each wave data set (WIS and OCTI), providing a range of results. Discussion and comparisons will focus on the average conditions as well as the range of responses. Since the overall trends for the three methods are similar, Figures 27 and 28 show only Method 1 erosion and accretion quantities for WIS and OCTI, respectively.



(a) Method 1



(b) Method 2



(c) Method 3

Figure 26. Methods of computing erosion/accretion volumes

Table 5
Erosion and Accretion Potential for Long Beach Island (WIS)

Reach	Erosion/Accretion without Project, m ³ /year				Erosion/Accretion with Project, m ³ /year			
	1	2	3	Avg	1	2	3	Avg
1	67,800	248,200	354,200	223,400	121,300	153,900	192,300	155,800
2	252,300	154,100	44,600	150,400	88,600	86,500	40,800	72,000
3	55,500	27,200	38,700	40,500	40,200	14,100	36,200	30,200
4	-52,000	-52,500	-51,100	-51,900	-54,200	-59,200	-63,100	-58,800
5	-135,600	-94,900	-132,400	-121,000	-132,400	-90,600	-134,400	-119,100
6	-51,500	-3,600	700	-18,100	-43,000	7,800	24,900	-3,400
7	81,300	2,400	60,300	48,000	89,800	4,600	52,200	48,900
8	-28,300	-23,800	-22,100	-24,700	-18,600	-4,600	-5,300	-9,500
9	-18,800	-44,800	-131,500	-65,000	-22,800	-18,300	-72,000	-37,700
10	-68,700	-5,000	76,400	900	-51,700	-75,300	-36,300	-54,400
11	37,700	-6,300	-19,900	3,900	-46,600	-18,300	-29,900	-31,600
12	-54,600	-84,900	-101,700	-80,400	-2,200	-47,900	-52,600	-34,200

Table 6
Erosion and Accretion Potential for Long Beach Island (OCTI)

Reach	Erosion/Accretion without Project, m ³ /year				Erosion/Accretion with Project, m ³ /year			
	1	2	3	Avg	1	2	3	Avg
1	400	185,400	297,400	161,100	181,300	239,900	285,700	235,600
2	264,600	153,800	37,900	152,100	120,800	94,300	42,400	85,800
3	34,700	600	7,500	14,300	19,300	-12,900	2,300	2,900
4	-60,200	-50,000	-43,200	-51,100	-64,000	-53,300	-50,700	-56,000
5	-122,100	-92,700	-131,900	-115,600	-113,500	-84,200	-130,600	-109,400
6	-66,800	9,600	8,100	-16,400	-57,600	21,500	31,800	-1,400
7	113,700	20,800	86,400	73,600	124,700	25,900	83,100	77,900
8	-20,900	-23,600	-26,800	-23,800	-16,300	-8,300	-10,100	-11,500
9	-26,300	-55,900	-129,500	-70,600	-46,200	-40,300	-101,300	-62,600
10	-66,600	-800	58,200	-3,000	-40,400	-64,600	-19,700	-41,600
11	44,000	1,800	8,000	17,900	-30,700	-4,100	-11,600	-15,500
12	-48,500	-98,000	-121,100	-89,200	3,000	-59,700	-67,200	-41,300

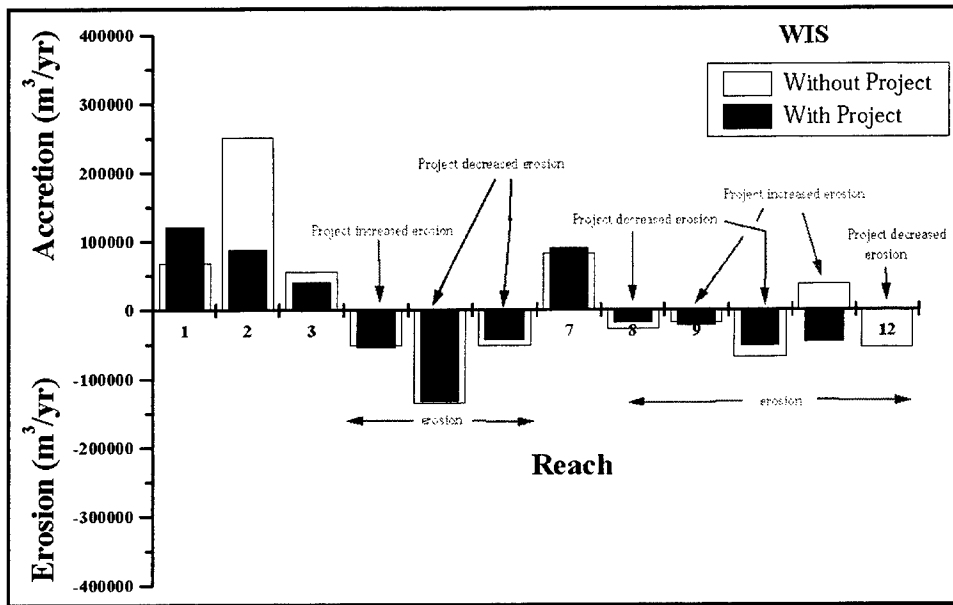


Figure 27. Erosion and accretion for Long Beach Island reaches with WIS climatology

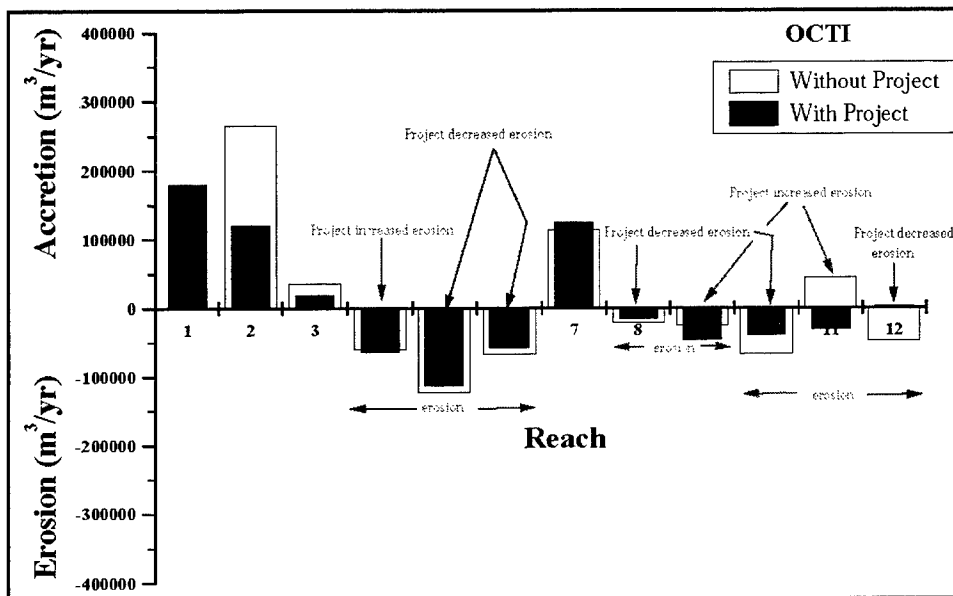


Figure 28. Erosion and accretion for Long Beach Island reaches with OCTI climatology

The three computation methods and WIS and OCTI data show the same trends of erosion and accretion. Reaches 1 and 2 are highly accretional and Reach 3 is accretional. For the with-project condition, these areas show less accretion (except Reach 1, Method 1-WIS; Reach 1, Methods 1 and 2-OCTI; and Reach 2, Method 3,-OCTI). Since the reaches would remain accretional, this is not considered an adverse impact of the project. Reaches 4 through 6, and 8 through 12 have erosion potential for with- and/or without-project construction. Considering the length of each reach, Reaches 4 and 5 (both corresponding to Harvey Cedars) appear to have the greatest potential for erosion. The project mitigates erosion in Reaches 5 and 6, but slightly increases the erosion potential in Reach 4. Reaches 8 through 10 and 12 show some erosion potential. The with-project condition decreases erosion in Reaches 8, 9 (except Method 1), and 12, but increases erosion potential in Reaches 10 (except Method 1) and 11. It should be noted that the degree of adverse impacts in Reach 4, and Reaches 10 and 11 are different. The with-project condition causes more erosion potential in these reaches, however, considering the amount of increased erosion (volume) and the length of each reach, the impact to Reaches 10 and 11 is 2-3 times greater than the impact to Reach 4. Reach 4 is a highly erosive area and will change slightly with the project in place. Reaches 10 and 11 show large increases in the erosion volumes directly due to the project (Borrow Area E).

Another observation is that the range of results varies from reach to reach. Reaches 1 and 2 have the greatest variability in response, depending on which calculation method is used. The most consistent response is observed in Reaches 3, 4, 5, and 8. Neglecting Reaches 1 and 2, volumes can be considered to be within $\pm 30,000 \text{ m}^3$ of the average erosion/accretion volumes. From these statements one can identify Reaches 1, 2, and 7 as accretional and Reaches 4, 5, 8, 9, and 12 as erosional. Reach 3 shows fairly consistent responses from method to method, but the OCTI data set indicates less accretion than the WIS data set. Considering the standard deviation of $\pm 30,000 \text{ m}^3$, this reach could be erosional or accretional. Due to the variability of results in Reaches 6, 10, and 11 and the average standard deviation of $\pm 30,000 \text{ m}^3$, it is more difficult to classify these regions as erosional or accretional. However, it can be reiterated that a comparison of with- and without-project conditions in these reaches shows a slight gain of material in Reach 6, and a large decrease in volumes (strong negative impact) in Reaches 10 and 11 because of the project (Borrow Area E).

Note that these erosion and accretion values are based on potential transport rates. Actual erosion and accretion may be limited by the presence of coastal structures and/or other engineering activities. It is recommended that historical accretion and erosion analysis (based on an analyses of historical shoreline position data) be done for comparison with these project results, i.e., compare potential erosion/accretion with observed erosion/accretion.

Grid 1 Renourishment Requirements

Areas with potential for erosion for with- and/or without-project conditions were considered areas needing periodic renourishment. Reaches 5, 9, and 12 require 65,000 to 121,000 m³/year. Reaches 9 and 12 cover longer stretches of shoreline and are therefore less of an erosional problem than Reach 5, as will be shown in the following section (Figures 29 and 30—Method 1 only). Reaches 4, 10, and 11 would require additional placement of material with the project in place. Reaches 5, 6, 8, 9, and 12 would require less material with the project in place. Computation with the OCTI and WIS data show the same trends. However, the OCTI computations predict greater renourishment requirements in Reaches 9, 10, and 12 and smaller renourishment requirements in Reaches 4, 5, 6, and 8 as compared to the WIS computations. It should be reiterated that coastal structures or engineering activities could influence the renourishment requirements. It is recommended that analysis of historical shoreline changes be made to assess renourishment requirements.

Grid 1 Shoreline Retreat Rate

The potential for shoreline erosion was computed from the erosion rates as follows. Equation 6-19 from HQUSACE (1992) estimates the rate of shoreline change:

$$\frac{\Delta x}{\Delta t} - \frac{1}{(D_b + D_c)} \left[\frac{\Delta Q_l}{\Delta y} \pm q \right] = 0 \quad (3)$$

where Δx is the cross-shore displacement of the profile, Δt is the time period, D_b is the berm crest elevation, D_c is the depth of closure, ΔQ_l is the longshore transport rate, Δy is the reach length, and q is a line source or sink of sediment along the reach. Basically this means that if we neglect source or sink terms, the entire quantity of material required for renourishment is assumed to cause the beach profile to shift landward uniformly. The quantity of material divided by the length of shoreline and height of the active profile ($D_b + D_c$) leaves the distance of shoreline retreat in a given time period, in this case, 1 year. As requested by the Philadelphia District, the active profile height assumed for Long Beach Island was 11.2 m. Each nourishment quantity was divided by the reach length and active profile height to determine the shoreline retreat rate (Tables 7 and 8; Figures 31 and 32 (Method 1 only)).

Tables 7 and 8 show that the greatest potential for shoreline retreat is in Harvey Cedars (Reaches 4 and 5) where the predictions show a shoreline retreat rate of 4-8 m/year. This area has historically had beach erosion problems and has had recent nourishment projects to maintain the beaches. The

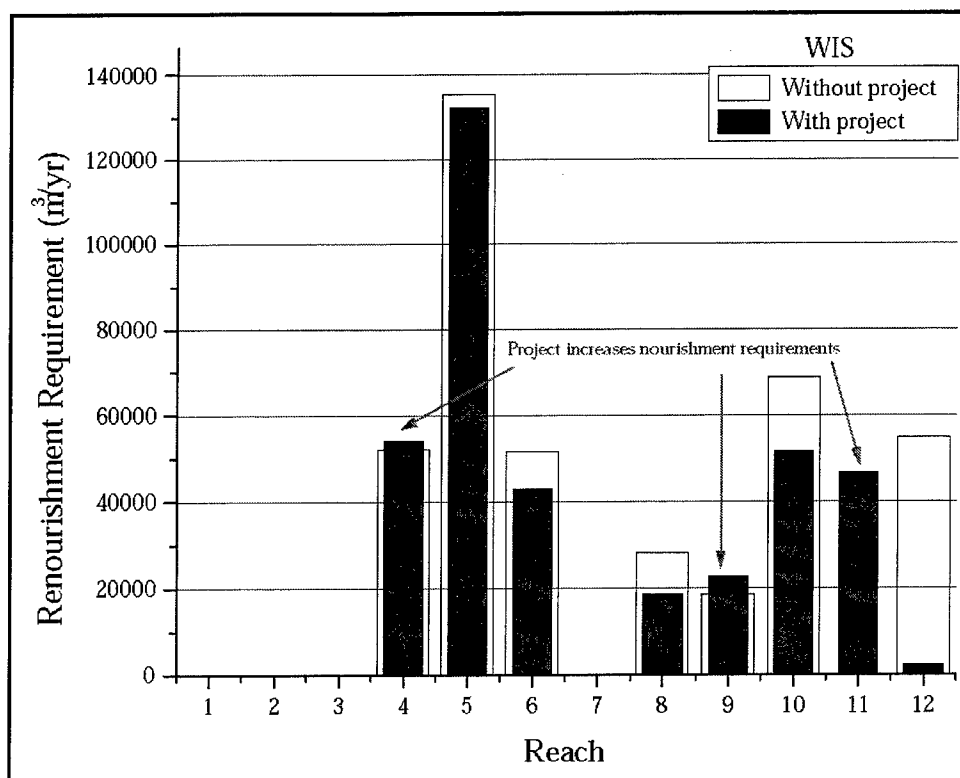


Figure 29. Renourishment requirements with WIS climatology

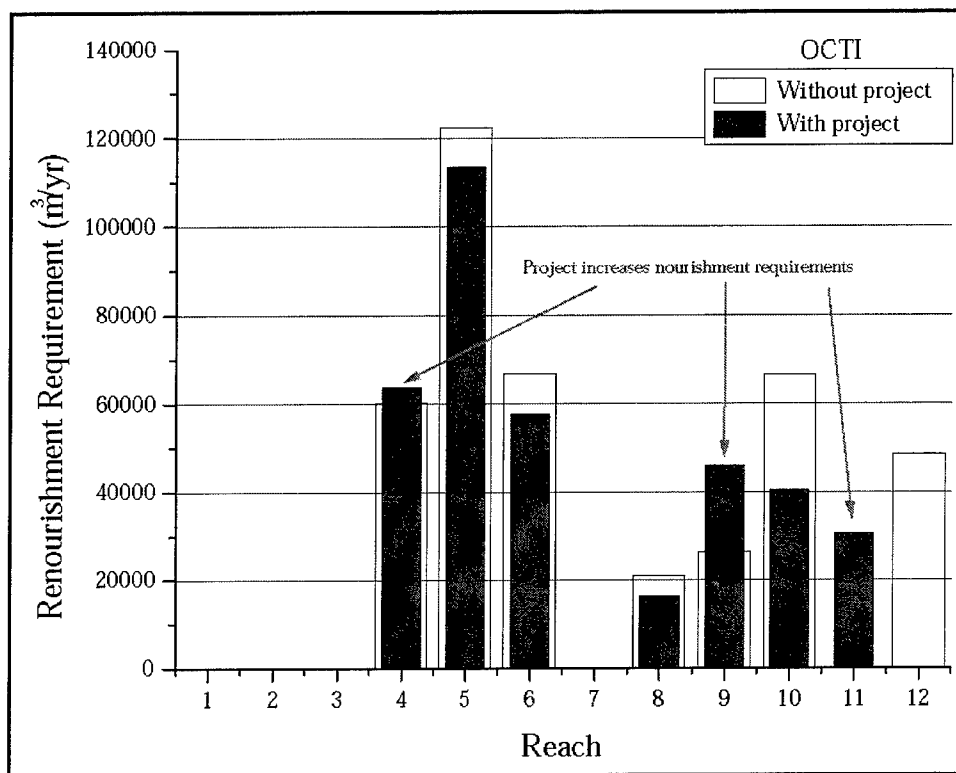


Figure 30. Renourishment requirements with OCTI climatology

Table 7
Shoreline Retreat Rate for Long Beach Island (WIS)

Reach	Shoreline Retreat without Project, m/year				Shoreline Retreat with Project, m/year			
	1	2	3	Avg	1	2	3	Avg
1	–	–	–	–	–	–	–	–
2	–	–	–	–	–	–	–	–
3	–	–	–	–	–	–	–	–
4	4.2	4.3	4.1	4.2	4.4	4.8	5.1	4.8
5	8.6	6.1	8.4	7.7	8.4	5.8	8.6	7.6
6	1.5	0.1	–	0.5	1.3	–	–	0.4
7	–	–	–	–	–	–	–	–
8	1.6	1.3	1.2	1.4	1.0	0.3	0.3	0.5
9	0.6	1.4	4.2	2.1	0.7	0.6	2.3	1.2
10	2.2	0.2	–	0.8	1.6	2.4	1.2	1.7
11	–	0.3	0.9	0.4	2.1	0.8	1.3	1.4
12	2.6	4.0	4.8	3.8	0.1	2.3	2.5	1.6

Table 8
Shoreline Retreat Rate for Long Beach Island (OCTI)

Reach	Shoreline Retreat without Project, m/year				Shoreline Retreat with Project, m/year			
	1	2	3	Avg	1	2	3	Avg
1	–	–	–	–	–	–	–	–
2	–	–	–	–	–	–	–	–
3	–	–	–	–	–	0.5	–	0.2
4	4.9	4.1	3.5	4.2	5.2	4.3	4.1	4.5
5	7.8	5.9	8.4	7.4	7.2	5.4	8.3	7.0
6	2.0	–	–	0.7	1.7	–	–	0.6
7	–	–	–	–	–	–	–	–
8	1.2	1.3	1.5	1.3	0.9	0.5	0.6	0.6
9	0.8	1.8	4.1	2.2	1.5	1.3	3.2	2.0
10	2.1	–	–	0.7	1.3	2.1	0.6	1.3
11	–	–	–	–	1.4	0.2	0.5	0.7
12	2.3	4.6	5.7	4.2	–	2.8	3.2	2.0

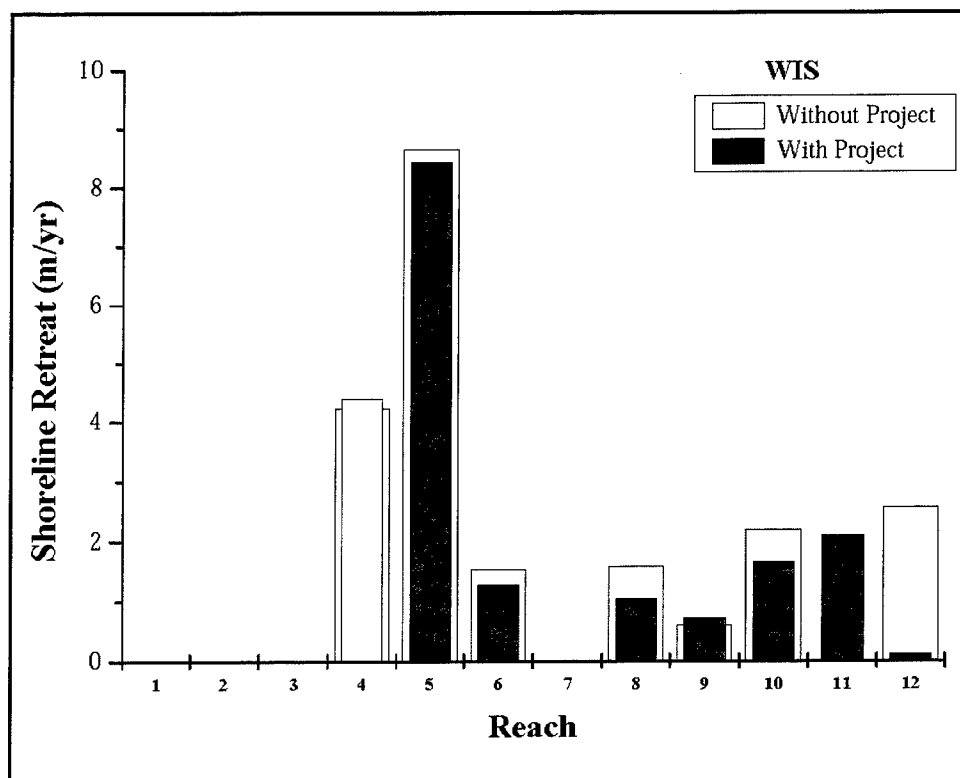


Figure 31. Shoreline retreat with WIS climatology

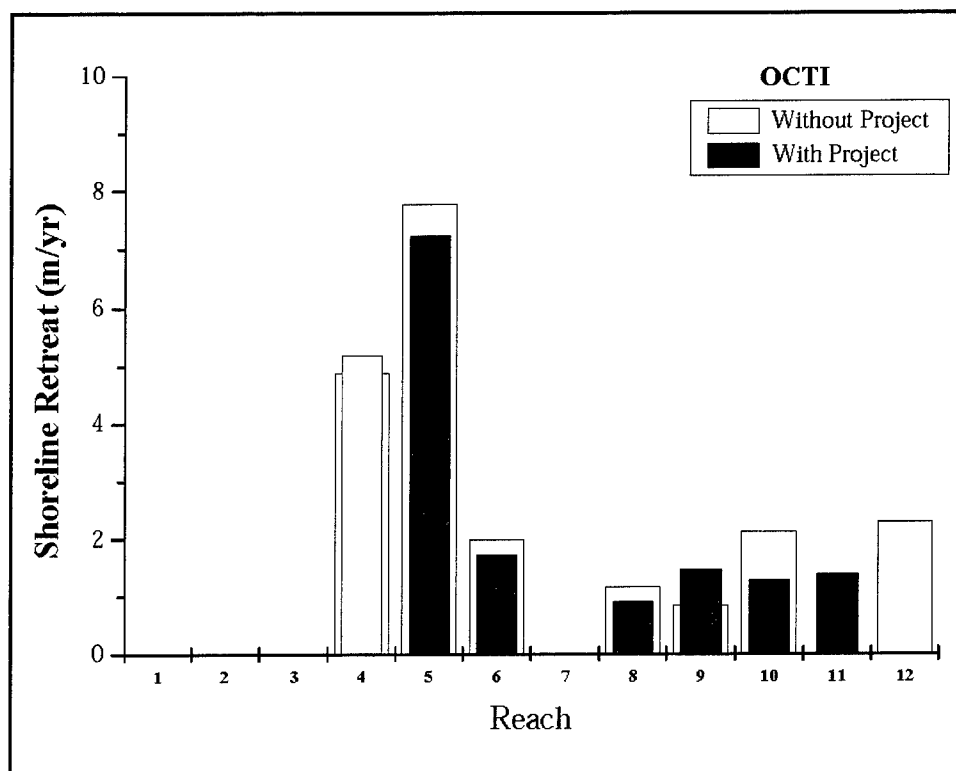


Figure 32. Shoreline retreat with OCTI climatology

predictions show a shoreline retreat rate of 1-4 m/year in Ship Bottom (Reach 8), Brant Beach (Reach 9), and Spray Beach (Reach 12). The with-project conditions tend to balance out the erosion in Harvey Cedars resulting in the southern portion eroding slightly less, and the northern portion eroding slightly more. The with-project conditions decrease the shoreline retreat rate in Reaches 6, 8, 9, and 12. The with-project conditions increase the shoreline retreat rate in Reaches 10 and 11. The largest potential negative impact of the project is in Reach 11, with the shoreline retreat rate increasing by 1 to 1.5 m/year (0.4 m/year to 1.4 m/year (WIS), and accreting 0.8 m/year to eroding 0.7 m/year (OCTI)). Note that the presence of functioning coastal structures may prevent these rates from being realized.

Grid 2 Erosion and Accretion

The net longshore transport potential computed for the Grid 2 Borrow Area A region using the WIS and OCTI data sets are given in Figures 33 and 34, respectively. Shoreline reaches defined by the Philadelphia District for Grid 2 were modified for use in these computations (Table 9). The original Philadelphia District reaches were combined to depict the general trend of transport. Longshore transport values for cells in each reach were summed and an average northerly and southerly longshore transport value was determined for each reach (Table 10). Southerly and northerly longshore transport potential was used to estimate areas of erosion and accretion using the three methods outlined for Grid 1.

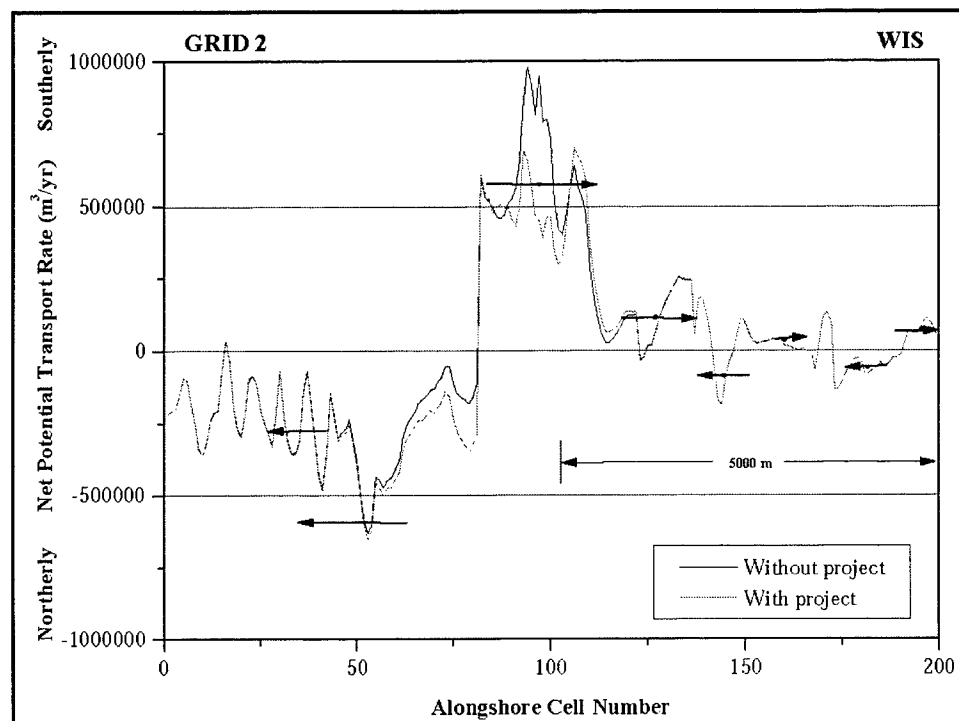


Figure 33. Net potential transport for Grid 2 using WIS wave climatology

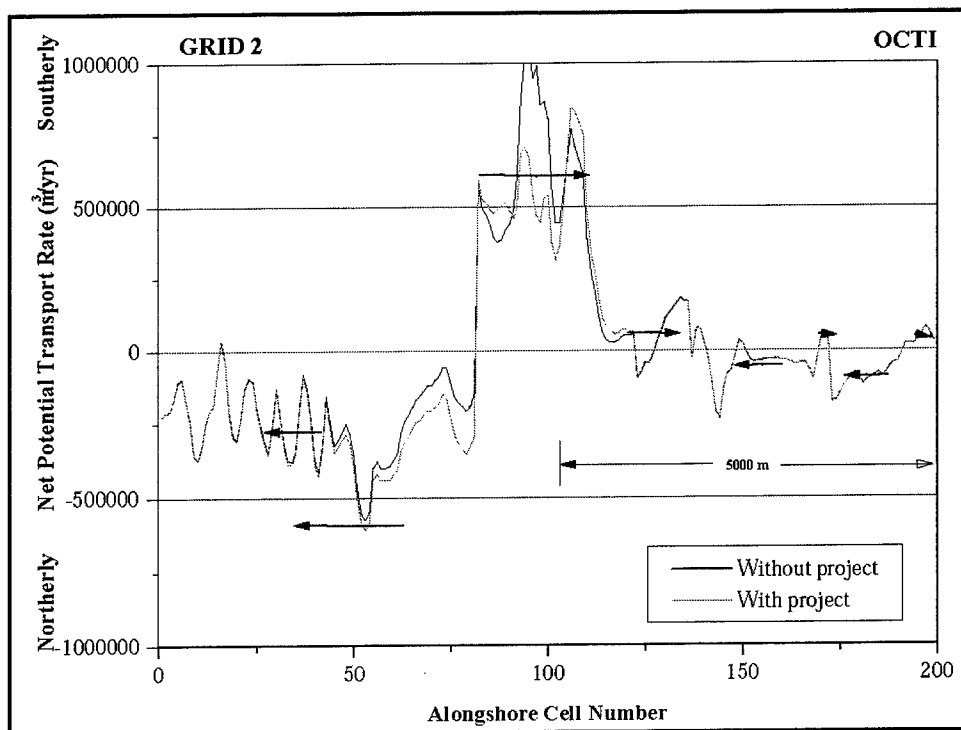


Figure 34. Net potential transport for Grid 2 using OCTI wave climatology

Table 9
Grid 2 Shoreline Reaches

Reach	Grid Cells	Township
1	110-136	Barneгат Light
2	137-144	Barneгат Light
3	145-168	Barneгат Light/Loveladies
4	169-190	Loveladies

Table 10
Net Longshore Transport Potential for Grid 2

Reach	Southerly and (Northerly) Longshore Transport WIS without Project, m ³ /year	Southerly and (Northerly) Longshore Transport WIS with Project, m ³ /year	Southerly and (Northerly) Longshore Transport OCTI without Project m ³ /year	Southerly and (Northerly) Longshore Transport OCTI with Project, m ³ /year
0	413,400	314,500	491,700	403,100
1	227,000 (-107,600)	241,000 (-102,800)	280,900 (-197,800)	296,500 (-191,400)
2	225,300 (-202,900)	226,800 (-202,800)	256,600 (-308,700)	258,600 (-308,700)
3	219,800 (-201,100)	220,500 (-201,100)	266,500 (-307,300)	267,800 (-307,300)
4	193,300 (-225,500)	193,600 (-225,500)	243,600 (-319,300)	244,200 (-319,300)
5	(-174,100)	(-174,100)	(-273,600)	(-273,600)

Note: Southerly transport is given first followed by northerly transport given in parentheses.

A boundary reach across Barnegat Inlet (Cells 82-109) was used to provide an adjacent cell for Reach 1. It was assumed that the southerly transport rate at the inlet would lose 175,000-225,000 m³ of sediment to the inlet and/or ebb shoal based on recent inlet dredging records. Northerly transport into Reach 4 from the south was provided by averaging Cells 191-200. This analysis assumes no losses or gains from cross-shore transport.

The WIS and OCTI data show the same trends of erosion and accretion (Figures 35 and 36—Method 1 only, Tables 11 and 12). Reach 4, corresponding to an 1,100-m portion of Loveladies, has erosion potential for with- and without-project conditions. The with-project conditions show

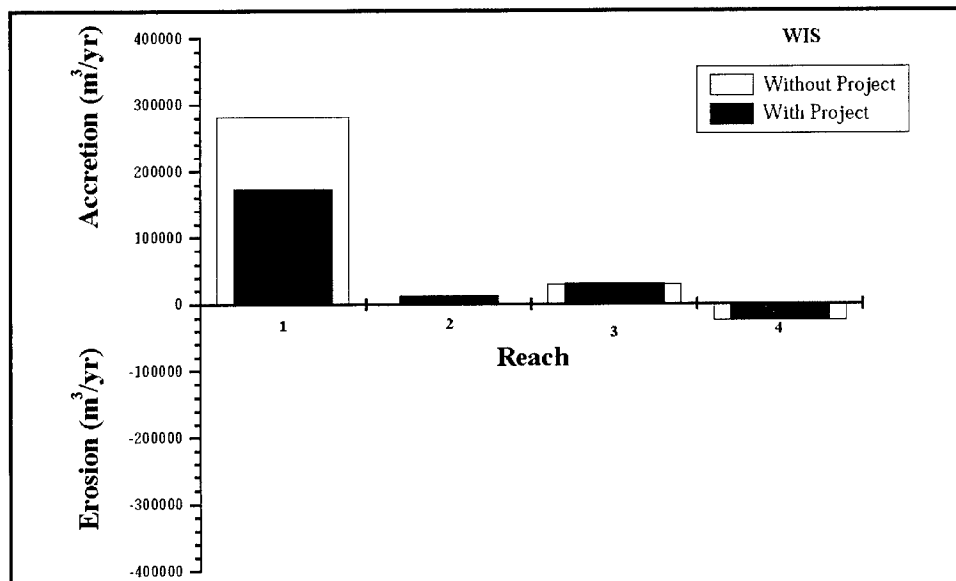


Figure 35. Erosion and accretion for Grid 2 using WIS wave climatology

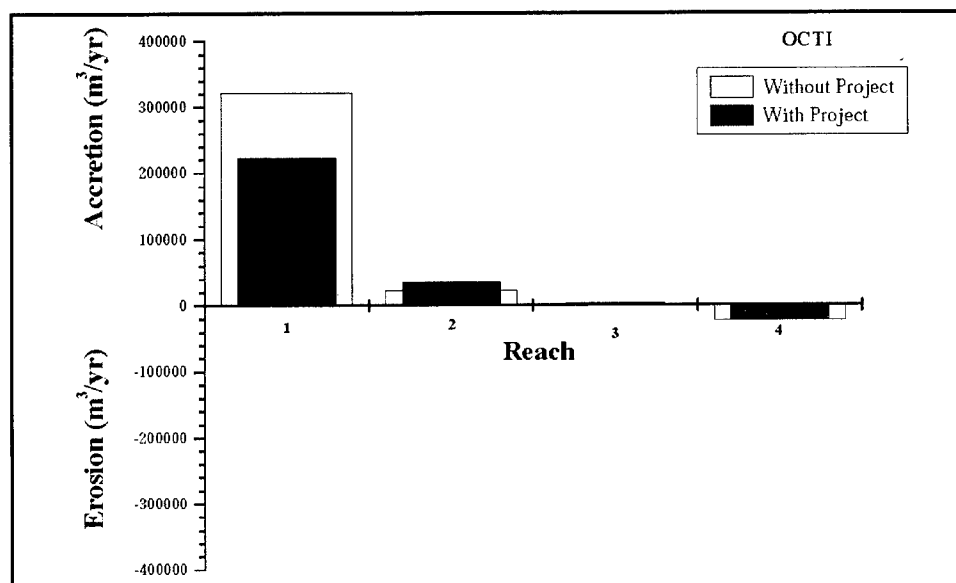


Figure 36. Erosion and accretion for Grid 2 using OCTI wave climatology

Table 11
Erosion and Accretion Potential for Grid 2 (WIS)

Reach	Erosion/Accretion without Project, m ³ /year				Erosion/Accretion with Project, m ³ /year			
	1	2	3	Avg	1	2	3	Avg
1	281,600	207,300	243,200	244,000	173,500	159,100	198,500	177,000
2	0	23,100	80,000	34,400	12,500	27,200	80,900	40,200
3	29,800	29,300	43,500	34,300	30,600	30,200	44,300	35,100
4	-24,900	-44,900	-12,100	-27,300	-24,400	-44,700	-11,900	-27,000

Table 12
Erosion and Accretion Potential for Grid 2 (OCTI)

Reach	Erosion/Accretion without Project, m ³ /year				Erosion/Accretion with Project, m ³ /year			
	1	2	3	Avg	1	2	3	Avg
1	321,700	267,700	365,700	318,400	223,900	230,200	323,700	259,200
2	22,900	28,100	74,700	41,900	36,500	32,800	75,800	48,400
3	2,100	9,700	26,900	12,900	2,900	10,700	27,600	13,700
4	-22,800	-59,000	-32,800	-38,200	-22,100	-58,500	-32,300	-37,700

less accretion in Reach 1, more accretion in Reach 2, and minimal change to Reaches 3 and 4.

Grid 2 Renourishment Requirements

Areas with potential for erosion were considered areas needing periodic renourishment. Reach 4 requires approximately 25,000-40,000 m³/year. (Figures 37 and 38 correspond to Method 1.) Impacts on Reach 4 for with-project conditions are minimal. Computation with the OCTI and WIS data show the same trends.

Grid 2 Shoreline Retreat Rate

The potential for shoreline erosion for Grid 2 was computed from the renourishment quantities as explained previously (Tables 13 and 14, Figures 39 and 40—Method 1 only).

Tables 13 and 14 show that the only potential for shoreline retreat for Grid 2 is in Loveladies (Reach 4). The predictions show a shoreline retreat rate of approximately 2-3 m/year. The impact of with-project conditions on the shoreline retreat rate is minimal.

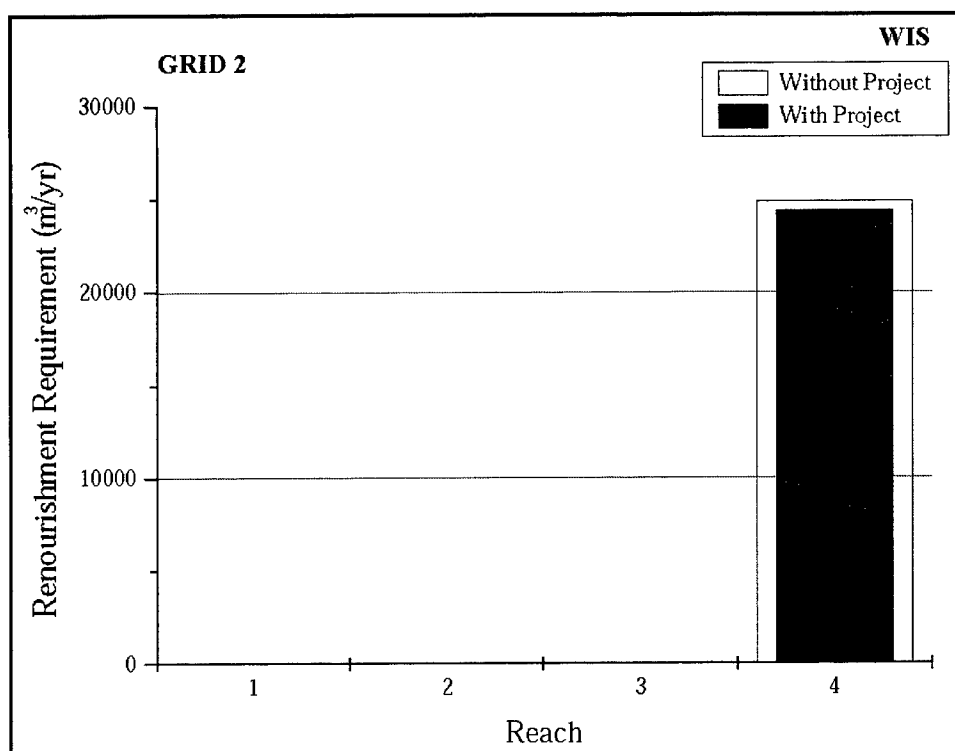


Figure 37. Renourishment requirements with WIS climatology

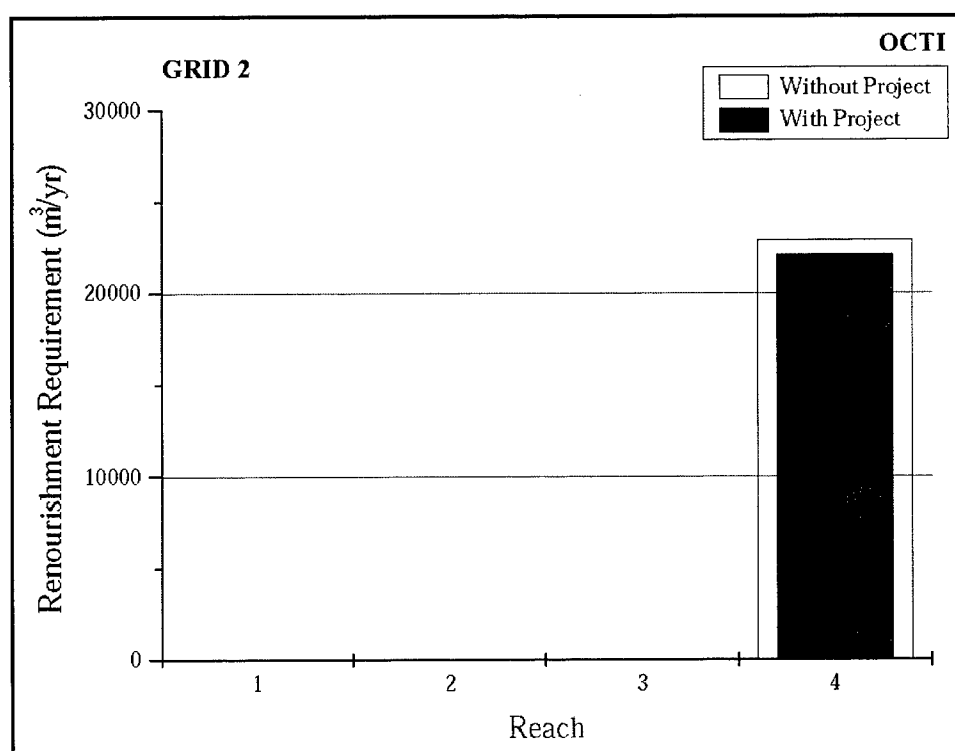


Figure 38. Renourishment requirements with OCTI climatology

Table 13
Shoreline Retreat Rate for Grid 2 (WIS)

Reach	Shoreline Retreat without Project, m/year				Shoreline Retreat with Project, m/year			
	1	2	3	Avg	1	2	3	Avg
1	–	–	–	–	–	–	–	–
2	–	–	–	–	–	–	–	–
3	–	–	–	–	–	–	–	–
4	2.0	3.6	1.0	2.2	2.0	3.6	1.0	2.2

Table 14
Shoreline Retreat Rate for Grid 2 (OCTI)

Reach	Shoreline Retreat without Project, m/year				Shoreline Retreat with Project, m/year			
	1	2	3	Avg	1	2	3	Avg
1	–	–	–	–	–	–	–	–
2	–	–	–	–	–	–	–	–
3	–	–	–	–	–	–	–	–
4	1.9	4.8	2.7	3.1	1.8	4.8	2.6	3.1

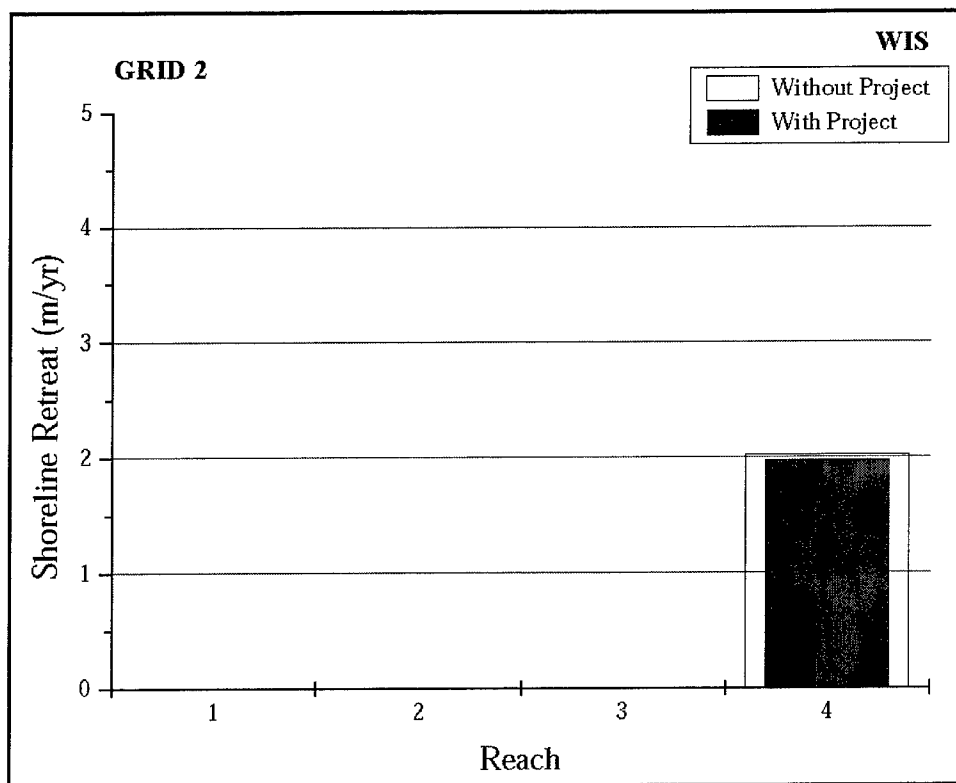


Figure 39. Shoreline retreat for Grid 2 using WIS wave climatology

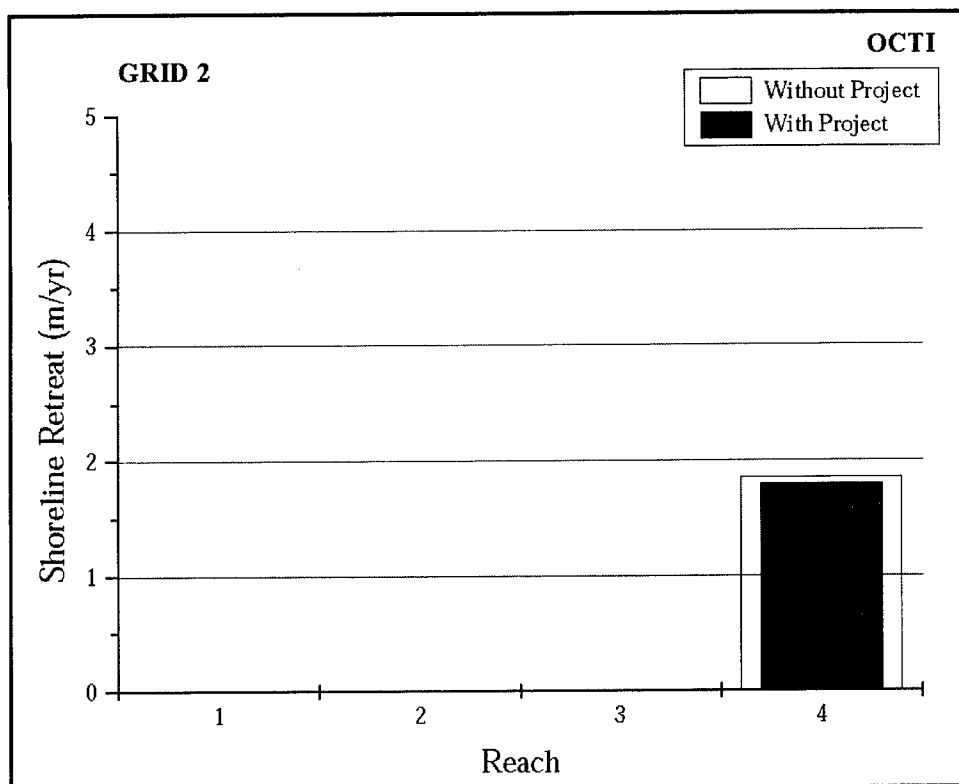


Figure 40. Shoreline retreat for Grid 2 using OCTI wave climatology

5 Conclusions

A numerical model study has provided information to assist the Philadelphia District in evaluating the impact of potential borrow sites on the Long Beach Island shoreline. Wave transformation and nearshore bathymetry were modeled with the spectral wave model STWAVE. The offshore wave climate was evaluated, and a 20-year WIS hindcast (1976-95) and a 10-year OCTI hindcast (1987-96) were used as the incident wave climate for model simulations. Wave climate was estimated for without-project and with-project bathymetric conditions.

Analysis of the WIS and OCTI climatology shows that the hindcast statistics differ somewhat. The WIS data show a better correspondence to the NDBC buoy data, both in directional distribution and frequency distribution. The OCTI statistics show a broader distribution of directions and a higher percentage of short period waves than the WIS and NDBC statistics. However, both the WIS and OCTI hindcasts were used in all analyses for comparison purposes.

An STWAVE grid (Grid 1) was developed to include coastal bathymetry extending from WIS Station AU2070 west to the Long Beach Island shoreline and from north of Barnegat Inlet to Beach Haven and encompassed all four potential borrow areas. Wave transformation between offshore and the Long Beach Island shoreline was modeled with this 100-m resolution grid. A finer grid (Grid 2), with 50-m resolution, was developed for the Borrow Area A Barnegat Inlet area. This grid was needed for investigation of sediment transport potential along beaches to the south of Barnegat Inlet, outside the immediate influence of Borrow Area A. For each grid and bathymetric configuration, STWAVE simulations for 756 incident wave conditions were made. For each simulation, the nearshore wave conditions were saved for use in littoral transport computations. Changes in wave height in the vicinity of the borrow areas induced by the changes in bathymetric configuration were observed.

Net potential longshore transport rates for Long Beach Island using the WIS and OCTI wave climatology were computed using an adapted version of the GENESIS shoreline modeling system program NSTRAN. A nodal zone in the vicinity of Barnegat Inlet, where the general shoreline orientation of New Jersey changes was observed. The potential net transport

shows a notable change from net northerly transport to net southerly transport in this region. The position of Long Island, NY affects the wave climate which in turn affects transport rates. The sheltering effect created by Long Island, NY limits waves from the north from impinging on northern New Jersey. South of Barnegat Inlet, the sheltering effect is not as apparent and net transport along Long Beach Island, NJ, is generally to the south. There is a local reversal (transport to the north) about 6-7 km south of Barnegat Inlet, probably due to the influence of Barnegat Inlet and its ebb shoal complex on the downdrift beaches.

An important point to note is that regardless of the value of the K coefficient in the transport computations, the general trends and reversals in transport mentioned above, are preserved. However, the magnitude of net potential transport computed for this study is strictly controlled by the calibration coefficient K. The selection of this coefficient is therefore critical. It was the intent of this study to compute "reasonable" transport values along Long Beach Island, with the ultimate goal being the comparison of these values for with- and without-project conditions. A reasonable transport value for Long Beach Island is on the order of 75,000 to 150,000 m³/year. The K coefficient was calibrated to bring the WIS transport results into this acceptable range.

The average of net potential transport for grid Cells 135 through 305 was used to estimate the net potential transport along Long Beach Island. Using OCTI hindcast wave climatology, the net potential transport for Long Beach Island was approximately 76,000 m³/year and using the WIS hindcast wave climatology, the net potential transport was approximately 114,000 m³/year. By comparing the with- and without-project conditions it is observed that there are changes in the net transport potential induced by the project. The greatest changes are in the vicinity of Borrow Area A (affecting Cells 50-70) and Borrow Area E (affecting Cells 230-280).

Computations of erosion and accretion along Long Beach Island (by three methods) show that the WIS and OCTI data produce the same trends of erosion and accretion. Reaches 1 and 2 are highly accretional and Reach 3 is accretional. For the with-project condition, these areas show less accretion. Since the reaches would remain accretional, this is not considered an adverse impact of the project. Reaches 4 through 6, and 8 through 12 have erosion potential for with- and/or without-project construction. Considering the length of each reach, Reaches 4 and 5 (both corresponding to Harvey Cedars) appear to have the greatest potential for erosion. The project mitigates erosion in Reaches 5 and 6, but increases the erosion potential in Reach 4. The with-project condition decreases erosion in Reaches 8, 9, and 12, but increases erosion potential in Reaches 10 and 11. It should be noted that the degree of adverse impacts in Reach 4, and Reaches 10 and 11 are different. The with-project condition causes more erosion potential in these reaches, however, considering the amount of increased erosion (volume) and the length of each reach, the impact to Reaches 10 and 11 is two to three times greater than the impact to Reach 4. Reach 4 is a highly erosive area and will change slightly with the project in place. Reaches 10

and 11 show large increases in the erosion volumes directly due to the project (Borrow Area E).

Using three methods and two wave data sets to compute erosion/accretion potential, results in a range of responses. The range of results varies from reach to reach. Reaches 1 and 2 have the greatest variability in response. The most consistent response is observed in Reaches 3, 4, 5, and 8. Neglecting Reaches 1 and 2, volumes can be considered to be within $\pm 30,000 \text{ m}^3$ of the average erosion/accretion volumes. From these statements one can identify Reaches 1, 2, and 7 as accretional and Reaches 4, 5, 8, 9, and 12 as erosional. Reach 3 shows fairly consistent responses from method to method, but the OCTI data set indicates less accretion than the WIS data set. Considering the standard deviation of $\pm 30,000 \text{ m}^3$, this reach could be erosional or accretional. The variability of results in Reaches 6, 10, and 11 and the average standard deviation of $\pm 30,000 \text{ m}^3$ makes it more difficult to classify these regions as erosional or accretional. However, it can be reiterated that a comparison of with- and without-project conditions in these reaches shows a slight gain of material in Reach 6, and a large decrease in volumes (strong negative impact) in Reaches 10 and 11 due to the project (Borrow Area E).

Note that these erosion and accretion values are based on potential transport rates. Actual erosion and accretion may be limited by the presence of functioning coastal structures and/or other engineering activities. It is recommended that historical accretion and erosion analysis (based on an analyses of historical shoreline position data) be done for comparison with these potential transport calculations. To the other extreme, if the project is constructed and the groins are not refurbished, then their functionality is further reduced. Potential transport rates may then be realized.

Areas with potential for erosion for with- and/or without-project conditions were considered areas needing periodic renourishment. Reaches 5, 9, and 12 each require 65,000-121,000 m^3/year . However, Reaches 9 and 12 cover longer stretches of shoreline and are therefore less of an erosional problem than Reach 5. Reaches 4, 10, and 11 would require additional placement of material with the project in place. Reaches 5, 6, 8, 9, and 12 would require less material with the project in place. Computation with the OCTI and WIS data show the same trends. However, the OCTI computations predict greater renourishment requirements in Reaches 9, 10, and 12 and smaller renourishment requirements in Reaches 4, 5, 6, and 8 as compared to the WIS computations. It should be reiterated that coastal structures or engineering activities could influence the renourishment requirements.

The greatest potential for shoreline retreat is in Harvey Cedars (Reaches 4 and 5) where the predictions show a shoreline retreat rate of 4-8 m/year. This area has historically had beach erosion problems and has had recent nourishment projects to maintain the beaches. The predictions show a shoreline retreat rate of 1-4 m/year in Ship Bottom (Reach 8), Brant Beach (Reach 9), and Spray Beach (Reach 12). The with-project conditions tend

to balance out the erosion in Harvey Cedars so that the southern portion erodes slightly less, and the northern portion erodes slightly more. The with-project conditions decrease the shoreline retreat rate in Reaches 6, 8, 9, and 12. The with-project conditions increase the shoreline retreat rate in Reaches 10 and 11.

The largest potential negative impact of the project is in Reach 11 (Haven Beach to Beach Haven Gardens), where the shoreline retreat rate increases 1-1.5 m/year. This change is directly related to bathymetric changes in Borrow Area E (removal of the nearshore shoal). Note that the presence of functioning coastal structures may prevent these rates from being realized. Harvey Cedars and Loveladies appear to be particularly susceptible to erosion, with or without the project constructed.

For Grid 2, the WIS and OCTI data show the same trends of erosion and accretion. Reach 4, corresponding to Loveladies, has erosion potential for with- and without-project construction. Areas with potential for erosion were considered areas needing periodic renourishment. Reach 4 requires 25,000-40,000 m³/year. Impacts on Reach 4 for with-project conditions would be minimal. Computations with the OCTI and WIS data show the same trends. Results show that the only potential for shoreline retreat for Grid 2 is in Loveladies (Reach 4) at a rate of 2-3 m/year.

Dredging the offshore borrow areas (B and D) has the least impact on the Long Beach Island shoreline. Removal of material from Borrow Area A reduces accretion rates at the northern end of Long Beach Island, which may or may not be considered troublesome. Removal of the nearshore shoal (Borrow Area E) has a strong negative impact on Reach 11 (Haven Beach to Beach Haven Gardens) and is not recommended.

References

- Bouws, E., Gunther, H., Rosenthal, W., and Vincent, C. L. (1985). "Similarity of the wind wave spectrum in finite depth water: 1. spectral form," *Journal of Geophysical Research*, 90(C1), 975-986.
- Brigham Young University. (1995). "Surface-water modeling system," Reference Manual, Version 5.0. Computer Graphics Laboratory, Provo, UT.
- Brooks, R. M., and Brandon, W. A. (1995). "A hindcast wave information for the U.S. Atlantic Coast: update 1976-1993 with hurricanes," Wave Information Study (WIS) Report 33, U.S. Army Engineer Waterways Experiment Station, Vicksburg, MS.
- Corson, W. D., Resio, D. T., Brooks, R. M., Ebersole, B. A., Jensen, R. E., Ragsdale, D. S., and Tracy, B. A. (1982). "Atlantic Coast hindcast, Phase II wave information," WIS Report 6, U.S. Army Engineer Waterways Experiment Station, Vicksburg, MS.
- Davis, J. E. (1992). "STWAVE theory and program documentation," Coastal Modeling System User's Manual, Instructional Report CERC-91-1, Supplement 1, M. A. Cialone, ed., U.S. Army Engineer Waterways Experiment Station, Vicksburg, MS.
- General Design Memorandum. (1984). Phase II, Barnegat Inlet, Ocean County, NJ.
- Gravens, M. B., Kraus, N. C., and Hanson, H. (1991). "GENESIS: Generalized model for simulating shoreline change, Report 2, workbook and system user's manual," Technical Report CERC-89-19, U.S. Army Engineer Waterways Experiment Station, Vicksburg, MS.
- Headquarters, U.S. Army Corps of Engineers. (1992). "Coastal littoral transport," Engineer Manual EM 1110-2-1502, Washington, DC.
- Leenknecht, D. A., and Tanner, W. W. (1997). "Grid generation and data analysis for wave transformation models," *Proceedings, 4th Congress on Computing in Civil Engineering*, Philadelphia, PA.

- Resio, D. T. (1987). "Shallow-water waves. I: theory," *Journal of Waterway, Port, Coastal, and Ocean Engineering*, 113(3), 264-281.
- Resio, D. T. (1988a). "Shallow-water waves. II: data comparisons," *Journal of Waterway, Port, Coastal, and Ocean Engineering*, 114(1), 50-65.
- Resio, D. T. (1988b). "A steady-state wave model for coastal applications," *Proceedings, 21st Coastal Engineering Conference*, American Society of Civil Engineers, 929-940.
- Smith, J. M., Resio, D. T., and Zundel, A. K. (1999). "STWAVE: Steady-State Spectral Wave model, Report 1, user's manual for STWAVE Version 2.0," Instruction Report CHL-99-1, U.S. Army Engineer Waterways Experiment Station, Vicksburg, MS.
- Thompson, E. F., Hadley, L. L., Brandon, W. A., McGehee, D. D., and Hubertz, J. M. (1996). "Wave response of Kahului Harbor, Maui, Hawaii," Technical Report CERC-96-11, U.S. Army Engineer Waterways Experiment Station, Vicksburg, MS.
- Thompson, E. F., Lin, L., and Jones, D. L. (1999). "Wave climate and littoral sediment transport potential, Cape Fear River Entrance and Smith Island to Ocean Isle Beach, North Carolina," Technical Report CHL-99-18, U.S. Army Engineer Research and Development Center, Vicksburg, MS.
- U.S. Army Engineer District, New York. (1954). "Atlantic Coast of New Jersey, Sandy Hook to Barnegat Inlet," Beach Erosion Control Report on Cooperative Study. New York, NY.
- U.S. Army Engineer District, Philadelphia. (1995). "New Jersey shore protection study, Barnegat Inlet to Little Egg Inlet reconnaissance study," Philadelphia, PA.
- U.S. Army Engineer District, Philadelphia. (1999). "Barnegat Inlet to Little Egg Inlet Draft Feasibility Report," Philadelphia, PA.

Appendix A

WIS Offshore Wave Climate

PERCENT OCCURRENCE (X1000) OF HEIGHT AND PERIOD BY DIRECTION
22.5 DEGREES ABOUT 0.0 DEGREES AZIMUTH

STATION: A2070 (39.8N, 74.0W / 18.0M)											NO. CASES: 3075
											% OF TOTAL: 5.4
HEIGHT	PEAK PERIOD (IN SECONDS)										TOTAL
IN	0.0-	5.0-	7.0-	9.0-	11.0-	13.0-	15.0-	17.0-	19.0-	21.0-	
METERS	4.9	6.9	8.9	10.9	12.9	14.9	16.9	18.9	20.9	LONGER	
0.00-0.74	1745	1745
0.75-1.24	1261	359	1620
1.25-1.74	11	1091	1102
1.75-2.24	.	520	5	525
2.25-2.74	.	160	11	171
2.75-3.24	.	11	63	74
3.25-3.74	.	.	13	13
3.75-4.24	.	.	5	5
4.25-4.74	0
4.75-5.24	0
5.25-5.74	0
5.75-6.24	0
6.25-6.74	0
6.8+	0
TOTAL	3017	2141	97	0	0	0	0	0	0	0	0

MEAN Hmo(M) = 1.1 LARGEST Hmo(M) = 4.2 MEAN TP(SEC) = 4.4
PERCENT OCCURRENCE (X1000) OF HEIGHT AND PERIOD BY DIRECTION
22.5 DEGREES ABOUT 22.5 DEGREES AZIMUTH

STATION: A2070 (39.8N, 74.0W / 18.0M)											NO. CASES: 1877
											% OF TOTAL: 3.3
HEIGHT	PEAK PERIOD (IN SECONDS)										TOTAL
IN	0.0-	5.0-	7.0-	9.0-	11.0-	13.0-	15.0-	17.0-	19.0-	21.0-	
METERS	4.9	6.9	8.9	10.9	12.9	14.9	16.9	18.9	20.9	LONGER	
0.00-0.74	1141	77	11	1229
0.75-1.24	515	438	953
1.25-1.74	1	544	545
1.75-2.24	.	268	8	276
2.25-2.74	.	59	59	118
2.75-3.24	.	3	58	1	62
3.25-3.74	.	.	11	11
3.75-4.24	.	.	6	3	9
4.25-4.74	0
4.75-5.24	0
5.25-5.74	0
5.75-6.24	0
6.25-6.74	0
6.8+	0
TOTAL	1657	1389	153	4	0	0	0	0	0	0	0

MEAN Hmo(M) = 1.1 LARGEST Hmo(M) = 4.2 MEAN TP(SEC) = 4.6
PERCENT OCCURRENCE (X1000) OF HEIGHT AND PERIOD BY DIRECTION
22.5 DEGREES ABOUT 45.0 DEGREES AZIMUTH

STATION: A2070 (39.8N, 74.0W / 18.0M)											NO. CASES: 2222
											% OF TOTAL: 3.9
HEIGHT	PEAK PERIOD (IN SECONDS)										TOTAL
IN	0.0-	5.0-	7.0-	9.0-	11.0-	13.0-	15.0-	17.0-	19.0-	21.0-	
METERS	4.9	6.9	8.9	10.9	12.9	14.9	16.9	18.9	20.9	LONGER	
0.00-0.74	1078	403	88	1569
0.75-1.24	225	605	106	936
1.25-1.74	1	515	32	548
1.75-2.24	.	229	95	3	327
2.25-2.74	.	32	184	216
2.75-3.24	.	.	143	143
3.25-3.74	.	.	29	8	37
3.75-4.24	.	.	6	6	12
4.25-4.74	.	.	.	3	3
4.75-5.24	0
5.25-5.74	0
5.75-6.24	0
6.25-6.74	0
6.8+	0
TOTAL	1304	1784	683	20	0	0	0	0	0	0	0

MEAN Hmo(M) = 1.1 LARGEST Hmo(M) = 4.5 MEAN TP(SEC) = 5.2
PERCENT OCCURRENCE (X1000) OF HEIGHT AND PERIOD BY DIRECTION
22.5 DEGREES ABOUT 67.5 DEGREES AZIMUTH

STATION: A2070 (39.8N, 74.0W / 18.0M)											NO. CASES: 2830
											% OF TOTAL: 5.0
HEIGHT	PEAK PERIOD (IN SECONDS)										TOTAL
IN	0.0-	5.0-	7.0-	9.0-	11.0-	13.0-	15.0-	17.0-	19.0-	21.0-	
METERS	4.9	6.9	8.9	10.9	12.9	14.9	16.9	18.9	20.9	LONGER	
0.00-0.74	850	617	533	172	2172
0.75-1.24	159	641	313	51	1164

1.25-1.74	1	354	210	27	592
1.75-2.24	.	155	220	27	402
2.25-2.74	.	13	224	8	245
2.75-3.24	.	.	121	8	129
3.25-3.74	.	.	87	6	93
3.75-4.24	.	.	10	8	18
4.25-4.74	.	.	.	8	8
4.75-5.24	.	.	.	1	1
5.25-5.74	.	.	.	5	5
5.75-6.24	0
6.25-6.74	0
6.8+	0
TOTAL	1010	1780	1718	321	0	0	0	0	0	0

MEAN Hmo(M) = 1.1 LARGEST Hmo(M) = 5.6 MEAN TP(SEC) = 6.1
PERCENT OCCURRENCE (X1000) OF HEIGHT AND PERIOD BY DIRECTION
22.5 DEGREES ABOUT 90.0 DEGREES AZIMUTH

STATION: A2070 (39.8N, 74.0W / 18.0M) NO. CASES: 13044
% OF TOTAL: 22.9

HEIGHT		PEAK PERIOD (IN SECONDS)										TOTAL
IN		0.0-	5.0-	7.0-	9.0-	11.0-	13.0-	15.0-	17.0-	19.0-	21.0-	
METERS		4.9	6.9	8.9	10.9	12.9	14.9	16.9	18.9	20.9	LONGER	
0.00-0.74	836	699	1632	3008	2890	1196	219	59	29	.	.	10568
0.75-1.24	189	915	1076	1452	1353	626	179	37	6	.	.	5833
1.25-1.74	1	420	605	811	677	263	82	17	.	.	.	2876
1.75-2.24	.	121	342	287	318	164	71	13	.	.	.	1316
2.25-2.74	.	25	210	160	138	118	39	10	.	.	.	700
2.75-3.24	.	1	109	191	70	54	22	6	.	.	.	453
3.25-3.74	.	.	41	99	53	20	10	13	.	.	.	236
3.75-4.24	.	.	3	70	44	15	1	6	.	.	.	139
4.25-4.74	.	.	1	35	35	8	.	3	.	.	.	82
4.75-5.24	.	.	.	17	13	17	5	52
5.25-5.74	11	15	26
5.75-6.24	3	1	4
6.25-6.74	0
6.8+	0
TOTAL	1026	2181	4019	6130	5605	2497	628	164	35	0	0	

MEAN Hmo(M) = 1.0 LARGEST Hmo(M) = 6.0 MEAN TP(SEC) = 9.7
PERCENT OCCURRENCE (X1000) OF HEIGHT AND PERIOD BY DIRECTION
22.5 DEGREES ABOUT 112.5 DEGREES AZIMUTH

STATION: A2070 (39.8N, 74.0W / 18.0M) NO. CASES: 12846
% OF TOTAL: 22.5

HEIGHT		PEAK PERIOD (IN SECONDS)										TOTAL
IN		0.0-	5.0-	7.0-	9.0-	11.0-	13.0-	15.0-	17.0-	19.0-	21.0-	
METERS		4.9	6.9	8.9	10.9	12.9	14.9	16.9	18.9	20.9	LONGER	
0.00-0.74	578	643	3641	4260	1943	355	75	18	13	.	.	11526
0.75-1.24	140	689	954	1692	1042	388	61	13	8	.	.	4987
1.25-1.74	1	376	429	799	542	361	58	13	5	.	.	2584
1.75-2.24	.	102	212	254	362	184	56	18	1	.	.	1189
2.25-2.74	.	17	148	130	213	80	51	10	.	.	.	649
2.75-3.24	.	1	77	133	85	53	30	1	.	.	.	380
3.25-3.74	.	.	25	77	59	25	22	1	.	.	.	209
3.75-4.24	.	.	8	39	73	15	8	143
4.25-4.74	.	.	1	20	51	23	3	3	.	.	.	101
4.75-5.24	.	.	.	11	27	18	1	57
5.25-5.74	.	.	.	1	17	30	8	6	.	.	.	62
5.75-6.24	11	15	.	1	.	.	.	27
6.25-6.74	3	1	4
6.8+	8	3	.	8	.	.	19
TOTAL	719	1828	5495	7416	4428	1556	376	84	35	0	0	

MEAN Hmo(M) = 1.0 LARGEST Hmo(M) = 8.4 MEAN TP(SEC) = 9.3
PERCENT OCCURRENCE (X1000) OF HEIGHT AND PERIOD BY DIRECTION
22.5 DEGREES ABOUT 135.0 DEGREES AZIMUTH

STATION: A2070 (39.8N, 74.0W / 18.0M) NO. CASES: 10229
% OF TOTAL: 17.9

HEIGHT		PEAK PERIOD (IN SECONDS)										TOTAL
IN		0.0-	5.0-	7.0-	9.0-	11.0-	13.0-	15.0-	17.0-	19.0-	21.0-	
METERS		4.9	6.9	8.9	10.9	12.9	14.9	16.9	18.9	20.9	LONGER	
0.00-0.74	746	947	4075	2715	650	124	17	15	11	.	.	9300
0.75-1.24	181	718	1228	1360	624	147	41	8	9	.	.	4316
1.25-1.74	.	284	335	480	342	94	27	13	5	.	.	1580
1.75-2.24	.	100	254	254	203	88	37	5	5	.	.	946
2.25-2.74	.	17	104	112	154	82	46	1	5	.	.	521
2.75-3.24	.	.	59	90	107	54	15	8	3	.	.	336
3.25-3.74	.	.	23	73	53	32	8	6	3	.	.	198
3.75-4.24	.	.	5	41	51	23	5	3	3	.	.	131
4.25-4.74	.	.	.	18	18	6	1	1	3	.	.	47
4.75-5.24	.	.	.	6	6	11	1	8	1	.	.	33
5.25-5.74	6	13	1	1	5	.	.	26
5.75-6.24	3	3	1	1	1	.	.	9

6.25-6.74	5	.	3	1	.	9
6.8+	1	.	1	.	.	2
TOTAL	927	2066	6083	5149	2217	683	200	74	55	0	

MEAN Hmo(M) = 1.0 LARGEST Hmo(M) = 7.5 MEAN TP(SEC) = 8.6
 PERCENT OCCURRENCE (X1000) OF HEIGHT AND PERIOD BY DIRECTION
 22.5 DEGREES ABOUT 157.5 DEGREES AZIMUTH

STATION: A2070 (39.8N, 74.0W / 18.0M) NO. CASES: 8150
 % OF TOTAL: 14.3

HEIGHT IN	PEAK PERIOD (IN SECONDS)										TOTAL
	0.0-	5.0-	7.0-	9.0-	11.0-	13.0-	15.0-	17.0-	19.0-	21.0-	
METERS	4.9	6.9	8.9	10.9	12.9	14.9	16.9	18.9	20.9	LONGER	
0.00-0.74	1257	1729	2881	1285	337	10	.	.	3	.	7502
0.75-1.24	260	1019	1095	1139	366	34	1	.	.	.	3919
1.25-1.74	.	415	362	412	186	30	5	.	.	.	1410
1.75-2.24	.	145	186	111	131	15	588
2.25-2.74	.	25	167	47	32	10	1	.	.	.	282
2.75-3.24	.	.	51	29	10	5	95
3.25-3.74	.	.	25	37	8	3	73
3.75-4.24	.	.	.	23	8	3	34
4.25-4.74	.	.	.	6	1	1	8
4.75-5.24	.	.	.	3	1	1	5
5.25-5.74	5	5
5.75-6.24	0
6.25-6.74	0
6.8+	0
TOTAL	1517	3333	4767	3092	1085	112	7	5	3	0	

MEAN Hmo(M) = 0.9 LARGEST Hmo(M) = 5.6 MEAN TP(SEC) = 7.4
 PERCENT OCCURRENCE (X1000) OF HEIGHT AND PERIOD BY DIRECTION
 22.5 DEGREES ABOUT 180.0 DEGREES AZIMUTH

STATION: A2070 (39.8N, 74.0W / 18.0M) NO. CASES: 8361
 % OF TOTAL: 14.6

HEIGHT IN	PEAK PERIOD (IN SECONDS)										TOTAL
	0.0-	5.0-	7.0-	9.0-	11.0-	13.0-	15.0-	17.0-	19.0-	21.0-	
METERS	4.9	6.9	8.9	10.9	12.9	14.9	16.9	18.9	20.9	LONGER	
0.00-0.74	2419	3531	2193	588	35	8766
0.75-1.24	530	1644	638	152	10	2974
1.25-1.74	1	985	263	56	8	1313
1.75-2.24	.	302	359	17	1	679
2.25-2.74	.	47	278	20	345
2.75-3.24	.	.	95	27	122
3.25-3.74	.	.	23	29	52
3.75-4.24	.	.	1	13	3	17
4.25-4.74	.	.	.	11	5	16
4.75-5.24	.	.	.	3	1	4
5.25-5.74	0
5.75-6.24	0
6.25-6.74	0
6.8+	0
TOTAL	2950	6509	3850	916	63	0	0	0	0	0	

MEAN Hmo(M) = 0.8 LARGEST Hmo(M) = 4.9 MEAN TP(SEC) = 5.9
 PERCENT OCCURRENCE (X1000) OF HEIGHT AND PERIOD BY DIRECTION
 22.5 DEGREES ABOUT 202.5 DEGREES AZIMUTH

STATION: A2070 (39.8N, 74.0W / 18.0M) NO. CASES: 5023
 % OF TOTAL: 8.8

HEIGHT IN	PEAK PERIOD (IN SECONDS)										TOTAL
	0.0-	5.0-	7.0-	9.0-	11.0-	13.0-	15.0-	17.0-	19.0-	21.0-	
METERS	4.9	6.9	8.9	10.9	12.9	14.9	16.9	18.9	20.9	LONGER	
0.00-0.74	2164	1160	318	3642
0.75-1.24	1125	1303	222	6	2656
1.25-1.74	46	876	357	1279
1.75-2.24	.	167	607	5	779
2.25-2.74	.	18	131	10	159
2.75-3.24	.	.	32	17	49
3.25-3.74	.	.	1	15	16
3.75-4.24	.	.	.	5	5
4.25-4.74	0
4.75-5.24	0
5.25-5.74	0
5.75-6.24	0
6.25-6.74	0
6.8+	0
TOTAL	3335	3524	1668	58	0	0	0	0	0	0	

MEAN Hmo(M) = 1.0 LARGEST Hmo(M) = 4.1 MEAN TP(SEC) = 5.2
 PERCENT OCCURRENCE (X1000) OF HEIGHT AND PERIOD BY DIRECTION
 22.5 DEGREES ABOUT 225.0 DEGREES AZIMUTH

STATION: A2070 (39.8N, 74.0W / 18.0M) NO. CASES: 2942
 % OF TOTAL: 5.2

HEIGHT IN METERS	PEAK PERIOD (IN SECONDS)										TOTAL
	0.0- 4.9	5.0- 6.9	7.0- 8.9	9.0- 10.9	11.0- 12.9	13.0- 14.9	15.0- 16.9	17.0- 18.9	19.0- 20.9	21.0- LONGER	
0.00-0.74	2311	248	5	2564
0.75-1.24	1656	260	51	1967
1.25-1.74	92	232	61	385
1.75-2.24	.	58	44	102
2.25-2.74	.	1	6	1	8
2.75-3.24	.	.	.	1	1
3.25-3.74	0
3.75-4.24	0
4.25-4.74	0
4.75-5.24	0
5.25-5.74	0
5.75-6.24	0
6.25-6.74	0
6.8+	0
TOTAL	4059	799	167	2	0	0	0	0	0	0	

MEAN Hmo(M) = 0.8 LARGEST Hmo(M) = 2.8 MEAN TP(SEC) = 4.0
 PERCENT OCCURRENCE (X1000) OF HEIGHT AND PERIOD BY DIRECTION
 22.5 DEGREES ABOUT 247.5 DEGREES AZIMUTH

STATION: A2070 (39.8N, 74.0W / 18.0M) NO. CASES: 2082
 % OF TOTAL: 3.6

HEIGHT IN METERS	PEAK PERIOD (IN SECONDS)										TOTAL
	0.0- 4.9	5.0- 6.9	7.0- 8.9	9.0- 10.9	11.0- 12.9	13.0- 14.9	15.0- 16.9	17.0- 18.9	19.0- 20.9	21.0- LONGER	
0.00-0.74	2368	13	1	2382
0.75-1.24	954	35	989
1.25-1.74	66	68	134
1.75-2.24	.	42	6	48
2.25-2.74	.	.	3	3
2.75-3.24	0
3.25-3.74	0
3.75-4.24	0
4.25-4.74	0
4.75-5.24	0
5.25-5.74	0
5.75-6.24	0
6.25-6.74	0
6.8+	0
TOTAL	3388	158	10	0	0	0	0	0	0	0	

MEAN Hmo(M) = 0.7 LARGEST Hmo(M) = 2.4 MEAN TP(SEC) = 3.5
 PERCENT OCCURRENCE (X1000) OF HEIGHT AND PERIOD BY DIRECTION
 22.5 DEGREES ABOUT 270.0 DEGREES AZIMUTH

STATION: A2070 (39.8N, 74.0W / 18.0M) NO. CASES: 2927
 % OF TOTAL: 5.1

HEIGHT IN METERS	PEAK PERIOD (IN SECONDS)										TOTAL
	0.0- 4.9	5.0- 6.9	7.0- 8.9	9.0- 10.9	11.0- 12.9	13.0- 14.9	15.0- 16.9	17.0- 18.9	19.0- 20.9	21.0- LONGER	
0.00-0.74	3458	11	3469
0.75-1.24	1079	22	1101
1.25-1.74	244	121	365
1.75-2.24	.	53	5	58
2.25-2.74	.	6	3	9
2.75-3.24	.	1	1
3.25-3.74	0
3.75-4.24	0
4.25-4.74	0
4.75-5.24	0
5.25-5.74	0
5.75-6.24	0
6.25-6.74	0
6.8+	0
TOTAL	4781	214	8	0	0	0	0	0	0	0	

MEAN Hmo(M) = 0.7 LARGEST Hmo(M) = 3.0 MEAN TP(SEC) = 3.4
 PERCENT OCCURRENCE (X1000) OF HEIGHT AND PERIOD BY DIRECTION
 22.5 DEGREES ABOUT 292.5 DEGREES AZIMUTH

STATION: A2070 (39.8N, 74.0W / 18.0M) NO. CASES: 3582
 % OF TOTAL: 6.3

HEIGHT IN METERS	PEAK PERIOD (IN SECONDS)										TOTAL
	0.0- 4.9	5.0- 6.9	7.0- 8.9	9.0- 10.9	11.0- 12.9	13.0- 14.9	15.0- 16.9	17.0- 18.9	19.0- 20.9	21.0- LONGER	
0.00-0.74	2917	5	2922
0.75-1.24	2008	73	2081
1.25-1.74	225	539	764
1.75-2.24	.	318	318
2.25-2.74	.	22	22
2.75-3.24	.	18	18
3.25-3.74	0

3.75-4.24	0
4.25-4.74	0
4.75-5.24	0
5.25-5.74	0
5.75-6.24	0
6.25-6.74	0
6.8+	0
TOTAL	5150	975	0	0	0	0	0	0	0	0	0

MEAN Hmo(M) = 0.9 LARGEST Hmo(M) = 3.1 MEAN TP(SEC) = 3.8
 PERCENT OCCURRENCE (X1000) OF HEIGHT AND PERIOD BY DIRECTION
 22.5 DEGREES ABOUT 315.0 DEGREES AZIMUTH

STATION: A2070 (39.8N, 74.0W / 18.0M) NO. CASES: 4141
 % OF TOTAL: 7.3

HEIGHT		PEAK PERIOD (IN SECONDS)										TOTAL
IN		0.0-	5.0-	7.0-	9.0-	11.0-	13.0-	15.0-	17.0-	19.0-	21.0-	
METERS		4.9	6.9	8.9	10.9	12.9	14.9	16.9	18.9	20.9	LONGER	
0.00-0.74		2330	1	2331
0.75-1.24		2631	171	2802
1.25-1.74		23	1096	1119
1.75-2.24		.	691	691
2.25-2.74		.	114	5	119
2.75-3.24		.	11	5	16
3.25-3.74		.	.	1	1
3.75-4.24		0
4.25-4.74		0
4.75-5.24		0
5.25-5.74		0
5.75-6.24		0
6.25-6.74		0
6.8+		0
TOTAL		4984	2084	11	0	0	0	0	0	0	0	0

MEAN Hmo(M) = 1.0 LARGEST Hmo(M) = 3.6 MEAN TP(SEC) = 4.1
 PERCENT OCCURRENCE (X1000) OF HEIGHT AND PERIOD BY DIRECTION
 22.5 DEGREES ABOUT 337.5 DEGREES AZIMUTH

STATION: A2070 (39.8N, 74.0W / 18.0M) NO. CASES: 3830
 % OF TOTAL: 6.7

HEIGHT		PEAK PERIOD (IN SECONDS)										TOTAL
IN		0.0-	5.0-	7.0-	9.0-	11.0-	13.0-	15.0-	17.0-	19.0-	21.0-	
METERS		4.9	6.9	8.9	10.9	12.9	14.9	16.9	18.9	20.9	LONGER	
0.00-0.74		2280	2280
0.75-1.24		2202	159	2361
1.25-1.74		42	1146	.	1	1189
1.75-2.24		.	475	475
2.25-2.74		.	205	3	208
2.75-3.24		.	8	17	25
3.25-3.74		.	.	10	10
3.75-4.24		0
4.25-4.74		0
4.75-5.24		0
5.25-5.74		0
5.75-6.24		0
6.25-6.74		0
6.8+		0
TOTAL		4524	1993	30	1	0	0	0	0	0	0	0

MEAN Hmo(M) = 1.0 LARGEST Hmo(M) = 3.7 MEAN TP(SEC) = 4.2
 PERCENT OCCURRENCE (X1000) OF HEIGHT AND PERIOD
 FOR ALL DIRECTIONS

STATION: A2070 (39.8N, 74.0W / 18.0M) NO. CASES: 57079
 % OF TOTAL: 152.7

HEIGHT		PEAK PERIOD (IN SECONDS)										TOTAL
IN		0.0-	5.0-	7.0-	9.0-	11.0-	13.0-	15.0-	17.0-	19.0-	21.0-	
METERS		4.9	6.9	8.9	10.9	12.9	14.9	16.9	18.9	20.9	LONGER	
0.00-0.74		28485	10092	15385	12031	5857	1687	311	94	57	.	73999
0.75-1.24		15123	9058	5686	5855	3396	1196	284	65	24	.	40687
1.25-1.74		764	9069	2659	2588	1757	749	172	44	10	.	17812
1.75-2.24		.	3754	2349	961	1018	453	165	37	6	.	8743
2.25-2.74		.	770	1545	492	539	290	138	22	5	.	3801
2.75-3.24		.	59	835	501	273	167	68	17	3	.	1923
3.25-3.74		.	.	296	347	174	82	41	22	3	.	965
3.75-4.24		.	.	47	212	181	58	15	10	3	.	526
4.25-4.74		.	.	3	106	112	41	5	8	3	.	278
4.75-5.24		.	.	.	44	51	49	8	8	1	.	161
5.25-5.74		.	.	.	6	41	59	10	8	5	.	129
5.75-6.24		18	20	1	3	1	.	43
6.25-6.74		3	6	.	3	1	.	13
6.8+		10	3	1	8	.	22
TOTAL		44372	32802	28805	23143	13420	4867	1221	342	130	0	0

MEAN Hmo(M) = 0.9 LARGEST Hmo(M) = 8.4 MEAN TP(SEC) = 6.4

Appendix B

OCTI Offshore Wave Climate

PERCENT OCCURRENCE (X1000) OF HEIGHT AND PERIOD BY DIRECTION
22.5 DEGREES ABOUT 0.0 DEGREES AZIMUTH

STATION: OCTI2 (0.0N, 0.0W / 0.0M)											NO. CASES: 538
											% OF TOTAL: 1.9
HEIGHT	PEAK PERIOD (IN SECONDS)										TOTAL
IN	0.0-	5.0-	7.0-	9.0-	11.0-	13.0-	15.0-	17.0-	19.0-	21.0-	
METERS	4.9	6.9	8.9	10.9	12.9	14.9	16.9	18.9	20.9	LONGER	
0.00-0.74	1375	1375
0.75-1.24	479	479
1.25-1.74	0
1.75-2.24	0
2.25-2.74	0
2.75-3.24	0
3.25-3.74	0
3.75-4.24	0
4.25-4.74	0
4.75-5.24	0
5.25-5.74	0
5.75-6.24	0
6.25-6.74	0
6.8+	0
TOTAL	1854	0	0	0	0	0	0	0	0	0	0

MEAN Hmo(M) = 0.7 LARGEST Hmo(M) = 1.2 MEAN TP(SEC) = 3.0
PERCENT OCCURRENCE (X1000) OF HEIGHT AND PERIOD BY DIRECTION
22.5 DEGREES ABOUT 22.5 DEGREES AZIMUTH

STATION: OCTI2 (0.0N, 0.0W / 0.0M)											NO. CASES: 1385
											% OF TOTAL: 4.8
HEIGHT	PEAK PERIOD (IN SECONDS)										TOTAL
IN	0.0-	5.0-	7.0-	9.0-	11.0-	13.0-	15.0-	17.0-	19.0-	21.0-	
METERS	4.9	6.9	8.9	10.9	12.9	14.9	16.9	18.9	20.9	LONGER	
0.00-0.74	2750	699	3449
0.75-1.24	358	837	1195
1.25-1.74	10	93	103
1.75-2.24	.	24	24
2.25-2.74	0
2.75-3.24	0
3.25-3.74	0
3.75-4.24	0
4.25-4.74	0
4.75-5.24	0
5.25-5.74	0
5.75-6.24	0
6.25-6.74	0
6.8+	0
TOTAL	3118	1653	0	0	0	0	0	0	0	0	0

MEAN Hmo(M) = 0.6 LARGEST Hmo(M) = 2.0 MEAN TP(SEC) = 4.1
PERCENT OCCURRENCE (X1000) OF HEIGHT AND PERIOD BY DIRECTION
22.5 DEGREES ABOUT 45.0 DEGREES AZIMUTH

STATION: OCTI2 (0.0N, 0.0W / 0.0M)											NO. CASES: 1414
											% OF TOTAL: 4.9
HEIGHT	PEAK PERIOD (IN SECONDS)										TOTAL
IN	0.0-	5.0-	7.0-	9.0-	11.0-	13.0-	15.0-	17.0-	19.0-	21.0-	
METERS	4.9	6.9	8.9	10.9	12.9	14.9	16.9	18.9	20.9	LONGER	
0.00-0.74	1130	282	13	1425
0.75-1.24	861	1357	2218
1.25-1.74	6	875	6	887
1.75-2.24	.	258	17	275
2.25-2.74	.	3	58	61
2.75-3.24	0
3.25-3.74	0
3.75-4.24	0
4.25-4.74	0
4.75-5.24	0
5.25-5.74	0
5.75-6.24	0
6.25-6.74	0
6.8+	0
TOTAL	1997	2775	94	0	0	0	0	0	0	0	0

MEAN Hmo(M) = 1.0 LARGEST Hmo(M) = 2.5 MEAN TP(SEC) = 4.6
PERCENT OCCURRENCE (X1000) OF HEIGHT AND PERIOD BY DIRECTION
22.5 DEGREES ABOUT 67.5 DEGREES AZIMUTH

STATION: OCTI2 (0.0N, 0.0W / 0.0M)											NO. CASES: 2832
											% OF TOTAL: 9.8
HEIGHT	PEAK PERIOD (IN SECONDS)										TOTAL
IN	0.0-	5.0-	7.0-	9.0-	11.0-	13.0-	15.0-	17.0-	19.0-	21.0-	
METERS	4.9	6.9	8.9	10.9	12.9	14.9	16.9	18.9	20.9	LONGER	
0.00-0.74	637	448	485	837	1420	213	4040
0.75-1.24	665	913	210	355	696	158	2997

1.25-1.74	3	1185	144	117	320	48	1817
1.75-2.24	.	220	127	65	144	72	628
2.25-2.74	.	6	48	58	44	24	180
2.75-3.24	.	.	3	6	10	17	36
3.25-3.74	6	6	12
3.75-4.24	6	6
4.25-4.74	10	10
4.75-5.24	13	13
5.25-5.74	3	3
5.75-6.24	0
6.25-6.74	0
6.8+	0
TOTAL	1305	2772	1017	1438	2640	570	0	0	0	0	

MEAN Hmo(M) = 1.0 LARGEST Hmo(M) = 5.3 MEAN TP(SEC) = 7.9
PERCENT OCCURRENCE (X1000) OF HEIGHT AND PERIOD BY DIRECTION
22.5 DEGREES ABOUT 90.0 DEGREES AZIMUTH

STATION: OCTI2 (0.0N, 0.0W / 0.0M) NO. CASES: 2859
% OF TOTAL: 9.9

HEIGHT		PEAK PERIOD (IN SECONDS)										TOTAL
IN		0.0-	5.0-	7.0-	9.0-	11.0-	13.0-	15.0-	17.0-	19.0-	21.0-	
METERS		4.9	6.9	8.9	10.9	12.9	14.9	16.9	18.9	20.9	LONGER	
0.00-0.74		696	230	417	568	792	193	2896
0.75-1.24		678	1089	541	506	668	124	3606
1.25-1.74		.	1061	244	399	279	110	2093
1.75-2.24		.	175	158	155	224	62	774
2.25-2.74		.	.	68	62	151	281
2.75-3.24		.	.	3	89	27	6	125
3.25-3.74		.	.	.	20	6	10	36
3.75-4.24		10	10
4.25-4.74		0
4.75-5.24		0
5.25-5.74		10	10
5.75-6.24		6	6
6.25-6.74		0
6.8+		0
TOTAL		1374	2555	1431	1799	2157	521	0	0	0	0	

MEAN Hmo(M) = 1.1 LARGEST Hmo(M) = 5.9 MEAN TP(SEC) = 7.7
PERCENT OCCURRENCE (X1000) OF HEIGHT AND PERIOD BY DIRECTION
22.5 DEGREES ABOUT 112.5 DEGREES AZIMUTH

STATION: OCTI2 (0.0N, 0.0W / 0.0M) NO. CASES: 1921
% OF TOTAL: 6.6

HEIGHT		PEAK PERIOD (IN SECONDS)										TOTAL
IN		0.0-	5.0-	7.0-	9.0-	11.0-	13.0-	15.0-	17.0-	19.0-	21.0-	
METERS		4.9	6.9	8.9	10.9	12.9	14.9	16.9	18.9	20.9	LONGER	
0.00-0.74		479	230	351	623	630	199	2512
0.75-1.24		596	885	251	282	286	103	2403
1.25-1.74		.	672	86	179	124	20	1081
1.75-2.24		.	79	72	86	93	330
2.25-2.74		.	.	79	41	58	178
2.75-3.24		.	.	6	13	24	43
3.25-3.74		.	.	.	6	17	23
3.75-4.24		10	10
4.25-4.74		10	10
4.75-5.24		6	6
5.25-5.74		10	10
5.75-6.24		0
6.25-6.74		0
6.8+		0
TOTAL		1075	1866	845	1230	1268	322	0	0	0	0	

MEAN Hmo(M) = 1.0 LARGEST Hmo(M) = 5.7 MEAN TP(SEC) = 7.5
PERCENT OCCURRENCE (X1000) OF HEIGHT AND PERIOD BY DIRECTION
22.5 DEGREES ABOUT 135.0 DEGREES AZIMUTH

STATION: OCTI2 (0.0N, 0.0W / 0.0M) NO. CASES: 1831
% OF TOTAL: 6.3

HEIGHT		PEAK PERIOD (IN SECONDS)										TOTAL
IN		0.0-	5.0-	7.0-	9.0-	11.0-	13.0-	15.0-	17.0-	19.0-	21.0-	
METERS		4.9	6.9	8.9	10.9	12.9	14.9	16.9	18.9	20.9	LONGER	
0.00-0.74		606	361	244	272	592	182	2257
0.75-1.24		692	865	193	227	313	44	2334
1.25-1.74		.	803	79	103	96	1081
1.75-2.24		.	151	41	48	68	308
2.25-2.74		.	.	75	44	65	184
2.75-3.24		.	.	10	51	27	88
3.25-3.74		.	.	.	3	3	3	9
3.75-4.24		.	.	.	3	6	10	19
4.25-4.74		6	6	12
4.75-5.24		0
5.25-5.74		0
5.75-6.24		0

6.25-6.74	0
6.8+	0
TOTAL	1298	2180	642	751	1176	245	0	0	0	0

MEAN Hmo(M) = 1.0 LARGEST Hmo(M) = 4.5 MEAN TP(SEC) = 7.0
 PERCENT OCCURRENCE (X1000) OF HEIGHT AND PERIOD BY DIRECTION
 22.5 DEGREES ABOUT 157.5 DEGREES AZIMUTH

STATION: OCTI2 (0.0N, 0.0W / 0.0M) NO. CASES: 1955
 % OF TOTAL: 6.7

HEIGHT	PEAK PERIOD (IN SECONDS)										TOTAL
IN	0.0-	5.0-	7.0-	9.0-	11.0-	13.0-	15.0-	17.0-	19.0-	21.0-	
METERS	4.9	6.9	8.9	10.9	12.9	14.9	16.9	18.9	20.9	LONGER	
0.00-0.74	658	461	206	613	382	10	2330
0.75-1.24	944	927	113	306	220	10	2520
1.25-1.74	.	1051	55	62	51	3	1222
1.75-2.24	.	151	86	37	31	3	308
2.25-2.74	.	10	75	44	37	3	169
2.75-3.24	.	.	10	75	10	95
3.25-3.74	.	.	.	27	27	3	57
3.75-4.24	13	3	16
4.25-4.74	3	3
4.75-5.24	0
5.25-5.74	0
5.75-6.24	0
6.25-6.74	0
6.8+	0
TOTAL	1602	2600	545	1164	774	35	0	0	0	0	

MEAN Hmo(M) = 1.1 LARGEST Hmo(M) = 4.6 MEAN TP(SEC) = 6.4
 PERCENT OCCURRENCE (X1000) OF HEIGHT AND PERIOD BY DIRECTION
 22.5 DEGREES ABOUT 180.0 DEGREES AZIMUTH

STATION: OCTI2 (0.0N, 0.0W / 0.0M) NO. CASES: 3920
 % OF TOTAL: 13.5

HEIGHT	PEAK PERIOD (IN SECONDS)										TOTAL
IN	0.0-	5.0-	7.0-	9.0-	11.0-	13.0-	15.0-	17.0-	19.0-	21.0-	
METERS	4.9	6.9	8.9	10.9	12.9	14.9	16.9	18.9	20.9	LONGER	
0.00-0.74	2071	1258	79	3408
0.75-1.24	2181	3481	279	55	5996
1.25-1.74	.	3129	124	75	3	3331
1.75-2.24	.	365	151	62	578
2.25-2.74	.	3	72	75	3	153
2.75-3.24	.	.	6	20	26
3.25-3.74	.	.	.	3	6	9
3.75-4.24	0
4.25-4.74	0
4.75-5.24	0
5.25-5.74	0
5.75-6.24	0
6.25-6.74	0
6.8+	0
TOTAL	4252	8236	711	290	12	0	0	0	0	0	

MEAN Hmo(M) = 1.1 LARGEST Hmo(M) = 3.6 MEAN TP(SEC) = 4.9
 PERCENT OCCURRENCE (X1000) OF HEIGHT AND PERIOD BY DIRECTION
 22.5 DEGREES ABOUT 202.5 DEGREES AZIMUTH

STATION: OCTI2 (0.0N, 0.0W / 0.0M) NO. CASES: 4278
 % OF TOTAL: 14.7

HEIGHT	PEAK PERIOD (IN SECONDS)										TOTAL
IN	0.0-	5.0-	7.0-	9.0-	11.0-	13.0-	15.0-	17.0-	19.0-	21.0-	
METERS	4.9	6.9	8.9	10.9	12.9	14.9	16.9	18.9	20.9	LONGER	
0.00-0.74	2908	3763	93	6764
0.75-1.24	2216	2295	158	4669
1.25-1.74	.	2964	2964
1.75-2.24	.	320	10	330
2.25-2.74	.	.	13	13
2.75-3.24	0
3.25-3.74	0
3.75-4.24	0
4.25-4.74	0
4.75-5.24	0
5.25-5.74	0
5.75-6.24	0
6.25-6.74	0
6.8+	0
TOTAL	5124	9342	274	0	0	0	0	0	0	0	

MEAN Hmo(M) = 0.9 LARGEST Hmo(M) = 2.4 MEAN TP(SEC) = 4.7
 PERCENT OCCURRENCE (X1000) OF HEIGHT AND PERIOD BY DIRECTION
 22.5 DEGREES ABOUT 225.0 DEGREES AZIMUTH

STATION: OCTI2 (0.0N, 0.0W / 0.0M) NO. CASES: 1809
 % OF TOTAL: 6.2

HEIGHT IN METERS	PEAK PERIOD (IN SECONDS)										TOTAL
	0.0- 4.9	5.0- 6.9	7.0- 8.9	9.0- 10.9	11.0- 12.9	13.0- 14.9	15.0- 16.9	17.0- 18.9	19.0- 20.9	21.0- LONGER	
0.00-0.74	3587	34	3621
0.75-1.24	1513	665	2178
1.25-1.74	6	417	423
1.75-2.24	.	10	10
2.25-2.74	0
2.75-3.24	0
3.25-3.74	0
3.75-4.24	0
4.25-4.74	0
4.75-5.24	0
5.25-5.74	0
5.75-6.24	0
6.25-6.74	0
6.8+	0
TOTAL	5106	1126	0	0	0	0	0	0	0	0	

MEAN Hmo(M) = 0.7 LARGEST Hmo(M) = 2.1 MEAN TP(SEC) = 3.7
 PERCENT OCCURRENCE (X1000) OF HEIGHT AND PERIOD BY DIRECTION
 22.5 DEGREES ABOUT 247.5 DEGREES AZIMUTH

STATION: OCTI2 (0.0N, 0.0W / 0.0M) NO. CASES: 303
 % OF TOTAL: 1.0

HEIGHT IN METERS	PEAK PERIOD (IN SECONDS)										TOTAL
	0.0- 4.9	5.0- 6.9	7.0- 8.9	9.0- 10.9	11.0- 12.9	13.0- 14.9	15.0- 16.9	17.0- 18.9	19.0- 20.9	21.0- LONGER	
0.00-0.74	965	3	968
0.75-1.24	75	75
1.25-1.74	0
1.75-2.24	0
2.25-2.74	0
2.75-3.24	0
3.25-3.74	0
3.75-4.24	0
4.25-4.74	0
4.75-5.24	0
5.25-5.74	0
5.75-6.24	0
6.25-6.74	0
6.8+	0
TOTAL	1040	3	0	0	0	0	0	0	0	0	

MEAN Hmo(M) = 0.5 LARGEST Hmo(M) = 1.1 MEAN TP(SEC) = 2.9
 PERCENT OCCURRENCE (X1000) OF HEIGHT AND PERIOD BY DIRECTION
 22.5 DEGREES ABOUT 270.0 DEGREES AZIMUTH

STATION: OCTI2 (0.0N, 0.0W / 0.0M) NO. CASES: 247
 % OF TOTAL: 0.9

HEIGHT IN METERS	PEAK PERIOD (IN SECONDS)										TOTAL
	0.0- 4.9	5.0- 6.9	7.0- 8.9	9.0- 10.9	11.0- 12.9	13.0- 14.9	15.0- 16.9	17.0- 18.9	19.0- 20.9	21.0- LONGER	
0.00-0.74	851	851
0.75-1.24	0
1.25-1.74	0
1.75-2.24	0
2.25-2.74	0
2.75-3.24	0
3.25-3.74	0
3.75-4.24	0
4.25-4.74	0
4.75-5.24	0
5.25-5.74	0
5.75-6.24	0
6.25-6.74	0
6.8+	0
TOTAL	851	0	0	0	0	0	0	0	0	0	

MEAN Hmo(M) = 0.3 LARGEST Hmo(M) = 0.7 MEAN TP(SEC) = 2.0
 PERCENT OCCURRENCE (X1000) OF HEIGHT AND PERIOD BY DIRECTION
 22.5 DEGREES ABOUT 292.5 DEGREES AZIMUTH

STATION: OCTI2 (0.0N, 0.0W / 0.0M) NO. CASES: 1231
 % OF TOTAL: 4.2

HEIGHT IN METERS	PEAK PERIOD (IN SECONDS)										TOTAL
	0.0- 4.9	5.0- 6.9	7.0- 8.9	9.0- 10.9	11.0- 12.9	13.0- 14.9	15.0- 16.9	17.0- 18.9	19.0- 20.9	21.0- LONGER	
0.00-0.74	4146	.	.	.	3	4149
0.75-1.24	93	93
1.25-1.74	0
1.75-2.24	0
2.25-2.74	0
2.75-3.24	0
3.25-3.74	0

3.75-4.24	0
4.25-4.74	0
4.75-5.24	0
5.25-5.74	0
5.75-6.24	0
6.25-6.74	0
6.8+	0
TOTAL	4239	0	0	0	3	0	0	0	0	0	0

MEAN Hmo(M) = 0.5 LARGEST Hmo(M) = 1.0 MEAN TP(SEC) = 2.9
 PERCENT OCCURRENCE (X1000) OF HEIGHT AND PERIOD BY DIRECTION
 22.5 DEGREES ABOUT 315.0 DEGREES AZIMUTH

STATION: OCTI2 (0.0N, 0.0W / 0.0M) NO. CASES: 1391
 % OF TOTAL: 4.8

HEIGHT IN	PEAK PERIOD (IN SECONDS)										TOTAL
METERS	0.0- 4.9	5.0- 6.9	7.0- 8.9	9.0- 10.9	11.0- 12.9	13.0- 14.9	15.0- 16.9	17.0- 18.9	19.0- 20.9	21.0- LONGER	
0.00-0.74	4663	4663
0.75-1.24	130	130
1.25-1.74	0
1.75-2.24	0
2.25-2.74	0
2.75-3.24	0
3.25-3.74	0
3.75-4.24	0
4.25-4.74	0
4.75-5.24	0
5.25-5.74	0
5.75-6.24	0
6.25-6.74	0
6.8+	0
TOTAL	4793	0	0	0	0	0	0	0	0	0	0

MEAN Hmo(M) = 0.5 LARGEST Hmo(M) = 1.0 MEAN TP(SEC) = 3.0
 PERCENT OCCURRENCE (X1000) OF HEIGHT AND PERIOD BY DIRECTION
 22.5 DEGREES ABOUT 337.5 DEGREES AZIMUTH

STATION: OCTI2 (0.0N, 0.0W / 0.0M) NO. CASES: 1100
 % OF TOTAL: 3.8

HEIGHT IN	PEAK PERIOD (IN SECONDS)										TOTAL
METERS	0.0- 4.9	5.0- 6.9	7.0- 8.9	9.0- 10.9	11.0- 12.9	13.0- 14.9	15.0- 16.9	17.0- 18.9	19.0- 20.9	21.0- LONGER	
0.00-0.74	3501	3501
0.75-1.24	279	279
1.25-1.74	10	10
1.75-2.24	0
2.25-2.74	0
2.75-3.24	0
3.25-3.74	0
3.75-4.24	0
4.25-4.74	0
4.75-5.24	0
5.25-5.74	0
5.75-6.24	0
6.25-6.74	0
6.8+	0
TOTAL	3790	0	0	0	0	0	0	0	0	0	0

MEAN Hmo(M) = 0.6 LARGEST Hmo(M) = 1.7 MEAN TP(SEC) = 3.0
 PERCENT OCCURRENCE (X1000) OF HEIGHT AND PERIOD
 FOR ALL DIRECTIONS

STATION: OCTI2 (0.0N, 0.0W / 0.0M) NO. CASES: 29014
 % OF TOTAL: 100.0

HEIGHT IN	PEAK PERIOD (IN SECONDS)										TOTAL
METERS	0.0- 4.9	5.0- 6.9	7.0- 8.9	9.0- 10.9	11.0- 12.9	13.0- 14.9	15.0- 16.9	17.0- 18.9	19.0- 20.9	21.0- LONGER	
0.00-0.74	31029	7775	1892	2915	3822	799	48232
0.75-1.24	11766	13317	1747	1733	2185	441	31189
1.25-1.74	37	12252	741	937	875	182	15024
1.75-2.24	.	1757	665	454	561	137	3574
2.25-2.74	.	24	492	327	361	27	1231
2.75-3.24	.	.	41	258	99	24	422
3.25-3.74	.	.	.	62	68	24	154
3.75-4.24	.	.	.	3	41	20	64
4.25-4.74	20	17	37
4.75-5.24	6	13	19
5.25-5.74	10	13	23
5.75-6.24	6	6
6.25-6.74	0
6.8+	0
TOTAL	42832	35125	5578	6689	8048	1703	0	0	0	0	0

MEAN Hmo(M) = 0.9 LARGEST Hmo(M) = 5.9 MEAN TP(SEC) = 5.4

Appendix C

Wave Model Description

The WES spectral wind-wave growth and propagation model STWAVE (Steady-state spectral WAVE) (Resio 1987, 1988a, 1988b; Davis 1992)¹ modified for wave-current interaction, was chosen for wave transformation modeling in the vicinity of Long Beach Island. STWAVE, which numerically solves the steady-state spectral energy-balance equation, was modified to solve the steady-state conservation of wave action:

$$\frac{\partial}{\partial x} \left(C_{ga_x} \frac{E(f, \theta)}{\omega_r} \right) + \frac{\partial}{\partial y} \left(C_{ga_y} \frac{E(f, \theta)}{\omega_r} \right) = \sum \frac{S}{\omega_r} \quad (1)$$

where

E = spectral energy density

f = frequency of spectral component

θ = propagation direction of spectral component

C_{ga} = absolute group velocity of spectral component

x, y = spatial coordinates

S = energy source/sink terms

ω_r = relative angular frequency (frequency relative to the current)

The source terms include wind input, nonlinear wave-wave interactions, dissipation within the wave field, and depth- and steepness-limited breaking. The terms on the left-hand side of Equation 1 represent wave propagation (refraction and shoaling) and the source terms on the right-hand side of the equation represent energy growth or decay in the spectrum. The assumptions made in STWAVE are:

- a. Mild bottom slopes.

¹ References cited in this appendix are listed in the References at the end of the main text.

- b. Negligible wave reflection.
- c. Spatially homogeneous offshore waves.
- d. Steady waves and winds.
- e. Linear refraction and shoaling.
- f. Linear wave-current interaction.
- g. Nonlinear wave-wave interaction.

STWAVE includes two breaking mechanisms: depth limited and steepness limited. The depth criterion limits the wave height-to-water depth ratio to 0.64. The steepness limit is expressed as:

$$H_{mo_{max}} = 0.1 L \tanh kd \quad (2)$$

where L is wavelength, k is wave number, and d is water depth (corrected for tide/surge).

STWAVE is a half-plane model, meaning that waves propagate only in directions headed from the seaward boundary into the grid interior. Typically waves propagate and/or winds blow toward a coast near the grid boundary opposite the seaward boundary. Waves reflected from the coast or waves generated by winds blowing offshore are neglected. Incident waves with dominant direction of more than about 60 deg from perpendicular to the seaward boundary are not accurately modeled because a significant fraction of the directionally spread energy is directed seaward and truncated by the model. For applications such as Long Beach Island, where a wide range of wave directions is important, more than one STWAVE grid must be developed.

STWAVE is a finite-difference model which calculates wave spectra on a rectangular grid with square grid cells using a backward ray-tracing scheme. The inputs needed to execute STWAVE are:

- a. Bathymetry and shoreline position.
- b. Size and resolution of the grid.
- c. 2-D wave spectrum on the offshore grid boundary (optional).
- d. Wind speed and direction (optional).
- e. Current field (optional).
- f. Water level.

The model outputs zero-moment wave height (H_{mo}), peak spectral period (T_p), and mean wave direction (θ_m) at all grid points, and the 2-D spectrum at selected grid points.

Directional wave spectra for model input are typically obtained from validated theoretical spectral forms or field measurements. If incident wave parameters significant height, peak period, and peak direction are specified, ACES 2.0 software (Leenknecht and Tanner 1997) can be helpful for creating the 2-D spectrum needed for STWAVE. The ACES 2.0 software generates a directional spectrum for given wave parameters and water depth, based on the TMA frequency spectrum (Bouws et al. 1985) with $\cos^n \theta_m$ form of directional spreading. Two parameters are specified regarding spectral shape: a spectral peak enhancement factor, γ , and the directional spreading parameter, n . Spectral shape parameters in this study were determined based on peak spectral period to give an approach equivalent to that described by Thompson et al. (1996) (Table C1). The ACES software requires that n be an even number.

Table C1
Spectral Shape Parameters Used In
ACES 2.0

T_p (sec)	γ	n
4-10	3.3	4
12	4	10
14	5	16
16	6	20
18	7	26
20	8	30

REPORT DOCUMENTATION PAGE

Form Approved
OMB No. 0704-0188

Public reporting burden for this collection of information is estimated to average 1 hour per response, including the time for reviewing instructions, searching existing data sources, gathering and maintaining the data needed, and completing and reviewing the collection of information. Send comments regarding this burden estimate or any other aspect of this collection of information, including suggestions for reducing this burden, to Washington Headquarters Services, Directorate for Information Operations and Reports, 1215 Jefferson Davis Highway, Suite 1204, Arlington, VA 22202-4302, and to the Office of Management and Budget, Paperwork Reduction Project (0704-0188), Washington, DC 20503.

1. AGENCY USE ONLY (Leave blank)		2. REPORT DATE September 2000	3. REPORT TYPE AND DATES COVERED Final report	
4. TITLE AND SUBTITLE Wave Climate and Littoral Sediment Transport Potential, Long Beach Island, New Jersey			5. FUNDING NUMBERS	
6. AUTHOR(S) Mary A. Cialone, Edward F. Thompson				
7. PERFORMING ORGANIZATION NAME(S) AND ADDRESS(ES) Coastal and Hydraulics Laboratory, U.S. Army Engineer Research and Development Center, 3909 Halls Ferry Road, Vicksburg, MS 39180-6199			8. PERFORMING ORGANIZATION REPORT NUMBER ERDC/CHL TR-00-21	
9. SPONSORING/MONITORING AGENCY NAME(S) AND ADDRESS(ES) U.S. Army Engineer District, Philadelphia Wanamaker Building, 100 Penn Square East Philadelphia, PA 19107-3390			10. SPONSORING/MONITORING AGENCY REPORT NUMBER	
11. SUPPLEMENTARY NOTES				
12a. DISTRIBUTION/AVAILABILITY STATEMENT Approved for public release; distribution is unlimited.			12b. DISTRIBUTION CODE	
13. ABSTRACT (Maximum 200 words) As part of a beach nourishment feasibility study for Long Beach Island, NJ, a study of the impacts of borrowing material from nearshore and offshore areas on regional coastal processes was examined. Specific analyses to determine the impacts of borrowing material from these sites are: (a) to examine the relative changes in wave climate due to bathymetric changes created at the borrow sites; (b) to determine the changes in potential longshore transport rates; (c) to examine the impacts on nourishment requirements for proposed beachfill areas; and (d) to look at the relative impacts on shoreline change rates.				
14. SUBJECT TERMS Littoral sediment transport Sediment transport Longshore transport Shoreline change Longshore transport potential Wave modeling			15. NUMBER OF PAGES 75	
			16. PRICE CODE	
17. SECURITY CLASSIFICATION OF REPORT UNCLASSIFIED	18. SECURITY CLASSIFICATION OF THIS PAGE UNCLASSIFIED	19. SECURITY CLASSIFICATION OF ABSTRACT	20. LIMITATION OF ABSTRACT	